

**USE OF  
POLYETHYLENE GRAFT MALEIC ANHYDRIDE FILM  
FOR BINDING EXTRACTABLE PROTEINS  
FROM NATURAL RUBBER**

**LADAWAN WATTHANACHOTE**

**A THESIS SUBMITTED IN PARTIAL FULFILLMENT  
OF THE REQUIREMENTS FOR  
THE DEGREE OF MASTER OF SCIENCE  
(POLYMER SCIENCE AND TECHNOLOGY)  
FACULTY OF GRADUATE STUDIES  
MAHIDOL UNIVERSITY**

**2007**

**COPYRIGHT OF MAHIDOL UNIVERSITY**

Thesis

Entitled

**USE OF  
POLYETHYLENE GRAFT MALEIC ANHYDRIDE FILM  
FOR BINDING EXTRACTABLE PROTEINS  
FROM NATURAL RUBBER**

.....  
Miss Ladawan Watthanachote  
Candidate

.....  
Lect. Thirawan Nipithakul,  
Doctorat de l'Université de Haute Alsace  
Major-Advisor

.....  
Assoc. Prof. Jitladda Sakdapipanich,  
Ph.D. (Material Systems Engineering)  
Co-Advisor

.....  
Assoc. Prof. Pranee Phinyocheep,  
Doctorat de l'Université du Maine  
Co-Advisor

.....  
Prof. M.R. Jisnuson Svasti, Ph.D.  
Dean  
Faculty of Graduate Studies

.....  
Assoc. Prof. Kalyanee Sirisinha,  
Ph.D. (Polymer Technology)  
Chair  
Master of Science Programme  
in Polymer Science and Technology  
Faculty of Science

Thesis

Entitled

**USE OF  
POLYETHYLENE GRAFT MALEIC ANHYDRIDE FILM  
FOR BINDING EXTRACTABLE PROTEINS  
FROM NATURAL RUBBER**

was submitted to the Faculty of Graduate Studies, Mahidol University  
for the degree of Master of Science (Polymer Science and Technology)

on

August 7, 2007

.....  
Miss Ladawan Watthanachote  
Candidate

.....  
Asst. Prof. Voravee P. Hoven,  
Ph.D. (Polymer Science and  
Engineering)  
Chair

.....  
Lect. Thirawan Nipithakul,  
Doctorat de l'Université de Haute Alsace  
Member

.....  
Assoc. Prof. Pranee Phinyocheep  
Doctorat de l'Université du Maine  
Member

.....  
Assoc. Prof. Jitladda Sakdapipanich,  
Ph.D. (Material Systems Engineering)  
Member

.....  
Prof. M.R. Jisnuson Svasti, Ph.D.  
Dean  
Faculty of Graduate Studies  
Mahidol University

.....  
Prof. Amaret Bhumiratana,  
Ph.D.  
Dean  
Faculty of Science  
Mahidol University

## ACKNOWLEDGMENTS

I would like to express my sincere gratitude and deepest appreciation to my advisor, Dr. Thirawan Nipithakul for her invaluable guidance, excellence and kind supervision, helpful discussion and encouragement throughout this thesis. This thesis research and related publications would be incomplete without her advice and guidance.

My appreciation also goes to Assoc. Prof. Dr. Pranee Phinyocheep, Assoc. Prof. Dr. Jitladda Sakdapipanich, Department of Chemistry, Faculty of Science, Mahidol University, and Asst. Prof. Dr. Voravee P. Hoven, Department of Chemistry, Faculty of Science, Chulalongkorn University for their valuable suggestions, comments and completion of this thesis.

I am very grateful to Asst. Prof. Dr. Nittaya Rattanasom for supporting dry skim NR used in this research.

I am very grateful to Innovation Co., Ltd., Bangkok, for supporting commercial PE-g-MAH granule used in this research.

Furthermore, I would like to thank all members of Jitladda laboratory, my friends at Mahidol University, and others, whose names are not mentioned here, for their kindnesses and helps in various ways. Finally, I would like to use this opportunity to express grateful thanks to my family for their love, care, encouragement and inspiration support during my study.

Ladawan Watthanachote

**USE OF POLYETHYLENE GRAFT MALEIC ANHYDRIDE FILM FOR BINDING EXTRACTABLE PROTEIN FROM NATURAL RUBBER**

LADAWAN WATTHANACHOTE 4736232 SCPO/M

M.Sc. (POLYMER SCIENCE AND TECHNOLOGY)

THESIS ADVISORS: THIRAWAN NIPITHAKUL, Doctorat de l'Université de Haute Alsace, JITLADDA SAKDAPIPANICH, Ph.D., PRANEE PHINYOCHEEP, Doctorat de l'Université du Maine

**ABSTRACT**

Two types of membrane material containing the maleic anhydride (MAH) group for protein binding were prepared by MAH photografting on LDPE film and compression of commercial PE-g-MAH granule into sheet form. Annealing the PE-g-MAH film induced efficient back formation of the anhydride groups. The surface properties of the film were analyzed by Attenuated Total Reflection Fourier Transforms Infrared Spectroscopy (ATR-FTIR) and water contact angle measurement. The obtained results indicated that PE-g-MAH obtained from UV photografting at distance between lamp and sample of 25 cm and under irradiation for 5 min showed higher anhydride content than that obtained from compression of commercial granule at 140°C. To obtain maximum anhydride content on the surface, the film was annealed at 120°C for 3 h.

Extractable proteins (EP) from dry skim natural rubber (NR) were selected to study protein binding ability of the PE-g-MAH film. The effects of extract solution types (i.e., Phosphate Buffer Saline; PBS and Sodium Dodecyl Sulfate; SDS), number of extractions and sample size on the extractable protein content were studied. The extractable proteins were analyzed by using Sodium Dodecyl Sulfate-Polyacrylamide Gel Electrophoresis (SDS-PAGE), CHN elemental analysis and FTIR technique. The results showed that the protein extraction by using small specimen in fresh SDS solution and repeating extraction to three times (12 h/time) gave a high extractable protein content.

In this work, Bovine Serum Albumin (BSA) was used as a model protein for determination of suitable immersion time. Quantitative analysis of the protein binding was investigated by the dye-binding assay of Bradford at wavelength 592 nm. The optimum immersion time of protein binding was 4 h. The anhydride group of PE-g-MAH film showed a high efficiency of protein immobilization (72.3  $\mu\text{g}/\text{cm}^2$ ). The amount of anhydride groups on the surface had a significant influence on the protein binding ability of the film. The spectroscopic results demonstrated that proteins can be successfully immobilized onto the film surface via covalent linkage.

**KEY WORDS:** POLYETHYLENE GRAFT MALEIC ANHYDRIDE/  
NATURAL RUBBER/ PROTEIN BINDING

162 PP.

การใช้แผ่นฟิล์มพอลิเอธิลีนกราฟท์มาเลอิกแอนไฮไดรด์สำหรับจับโปรตีนที่สกัดได้จากยางธรรมชาติ  
(USE OF POLYETHYLENE GRAFT MALEIC ANHYDRIDE FILM FOR BINDING  
EXTRACTABLE PROTEIN FROM NATURAL RUBBER)

ลดาวัลย์ วัฒนะ โชติ 4736232 SCPO/M

วท.ม. (วิทยาศาสตรจารย์และเทคโนโลยีพอลิเมอร์)

คณะกรรมการควบคุมวิทยานิพนธ์ : ถิรวรรณ นิพิฏฐกุล, Doctorat de l'Université de Haute Alsace,  
จิตต์ลัดดา สักดาภิพาณิชย์, Ph.D., ปราณี ภิญโญชีพ, Doctorat de l'Université du Maine

บทคัดย่อ

มาเลอิกแอนไฮไดรด์เมมเบรน 2 ชนิดที่นำมาใช้ศึกษาการจับโปรตีนคือ พอลิเอธิลีนกราฟท์มาเลอิกแอนไฮไดรด์ที่ได้จากการเตรียมโดยการฉายแสงยูวี และการทำเป็นฟิล์มโดยการอัดด้วยความร้อนของโคพอลิเมอร์เรซิน จากนั้นนำฟิล์มทั้งสองชนิดผ่านความร้อนเพื่อช่วยเพิ่มปริมาณหมู่แอนไฮไดรด์บนพื้นผิว สำหรับคุณสมบัติพื้นผิวของฟิล์มวิเคราะห์ได้โดยการใช้เทคนิคอินฟราเรดสเปกโทรสโกปีและการวัดมุมสัมผัส ผลการศึกษาพบว่าแผ่นฟิล์มที่ได้จากการเตรียมด้วยการฉายแสงยูวี ภายใต้สภาวะที่เหมาะสมคือ ระยะห่างระหว่างหลอดยูวีกับตัวอย่าง 25 เซนติเมตร และ เวลาในการฉายแสง 5 นาที มีปริมาณหมู่แอนไฮไดรด์บนพื้นผิวมากกว่าแผ่นฟิล์มที่เตรียมจากการอัดแผ่นของเรซินที่อุณหภูมิ 140 องศาเซลเซียส และการอบที่อุณหภูมิ 120 องศาเซลเซียส เป็นเวลา 3 ชั่วโมง เป็นวิธีที่เหมาะสมสำหรับการเพิ่มปริมาณหมู่แอนไฮไดรด์บนแผ่นฟิล์ม

ในส่วนของการสกัดโปรตีนจากยางสгимแห้ง ปริมาณโปรตีนที่สกัดได้ขึ้นอยู่กับชนิดของสารละลายที่ใช้สกัด จำนวนรอบที่สกัดและ ขนาดของชิ้นยาง โปรตีนที่สามารถสกัดได้นำมาวิเคราะห์ด้วย SDS-PAGE วิเคราะห์หาปริมาณธาตุ CHN ด้วย elemental analysis รวมถึงเทคนิคอินฟราเรดสเปกโทรสโกปีเพื่อวิเคราะห์ลักษณะเฉพาะของโปรตีน ซึ่งพบว่าสภาวะการสกัดที่ให้ปริมาณโปรตีนสูงคือการสกัดยางชิ้นขนาดเล็กในสารละลาย SDS ด้วยการสกัดซ้ำ 3 รอบ (12 ชั่วโมงต่อรอบ)

งานวิจัยนี้ได้เลือกโปรตีน BSA เพื่อศึกษาหาเวลาที่เหมาะสมในการจับโปรตีน ในการวิเคราะห์เชิงปริมาณของโปรตีน ได้ทำการตรวจวัดการดูดกลืนแสงยูวีที่ความยาวคลื่น 592 นาโนเมตร โดยอาศัยหลักการข้อมลิจของโปรตีนด้วยวิธี Bradford พบว่า ระยะเวลา 4 ชั่วโมง เป็นเวลาที่เหมาะสมสำหรับการจับโปรตีน หมู่แอนไฮไดรด์บนแผ่นฟิล์มแสดงการจับโปรตีนที่มีประสิทธิภาพสูง (72.3 ไมโครกรัมต่อตารางเซนติเมตร) ซึ่งปริมาณหมู่แอนไฮไดรด์บนพื้นผิวมีอิทธิพลสำคัญต่อความสามารถในการจับโปรตีน และจากผลทางสเปกโทรสโกปี สามารถยืนยันการจับโปรตีนผ่านพันธะโควาเลนต์กับหมู่แอนไฮไดรด์บนแผ่นฟิล์มได้เป็นอย่างดี

## CONTENTS

	<b>Page</b>
<b>ACKNOWLEDGMENTS</b>	iii
<b>ABSTRACT (in English)</b>	iv
<b>ABSTRACT (in Thai)</b>	v
<b>LIST OF TABLES</b>	xi
<b>LIST OF FIGURES</b>	xiii
<b>LIST OF ABBREVIATIONS</b>	xviii
<b>CHAPTER 1 INTRODUCTION</b>	1
<b>CHAPTER 2 OBJECTIVES</b>	3
<b>CHAPTER 3 LITERATURE REVIEW</b>	5
3.1 Natural Rubber Latex	5
3.2 Skim Natural Rubber	7
3.3 Proteins in Natural Rubber Latex	8
3.3.1 Protein Separation by Centrifugation	8
3.3.2 Proteins in Latex Fractions	9
3.3.3 Residual Extractable Proteins in Latex Products	11
3.4 Latex Protein Allergy	12
3.5 Reducibility of Extractable and Allergenic Proteins	14
3.5.1 Leaching	14
3.5.2 Enzyme Treatment	15
3.5.3 Fumed Silica	15
3.5.4 Ultrasonic Leaching	16
3.5.5 Chlorination	16
3.5.6 Irradiation	17
3.6 Functionalized Support for Protein Binding	17
3.6.1 Supports for Protein Covalent Coupling	20

## CONTENTS (continued)

	<b>Page</b>
3.6.1.1 Morphological Classification	20
3.6.1.2 Chemical Classification	21
3.6.2 Maleic Anhydride Copolymer	29
3.6.3 Polyethylene Graft Maleic Anhydride Film	31
3.6.3.1 Commercial Film (Fusabond® E MB226D)	31
3.6.3.2 UV Photografting	32
3.7 Protein	34
3.7.1 Amino Acid	34
3.7.2 Reactive Groups of Protein	36
3.7.3 Coupling Reaction	37
3.8 Protein Extraction and Characterization	39
3.8.1 Protein Extraction	39
3.8.2 Protein Precipitation	43
3.8.3 Lyophilization (Freeze-Drying) Process	45
3.8.4 Protein Characterization	45
3.8.4.1 Sodium Dodecyl Sulfate Polyacrylamide Gel Electrophoresis (SDS-PAGE)	45
3.8.4.2 Fourier Transform Infrared Spectroscopy (FTIR)	46
3.8.4.3 CHN Elemental Microanalysis	47
3.9 Protein Concentration Determination	47
3.9.1 The Absorbance Assay at 280 nm ( $A_{280}$ )	47
3.9.2 The Lowry Assay	47
3.9.3 The Bicinchoninic Acid (BCA)	48
3.9.4 The Bradford Assay	48
3.9.4.1 The Nature of the Change States of the Dye	48
3.9.4.2 Functional and Structural Requirements of Protein for Dye Binding	51
3.9.4.3 Interference	53

## CONTENTS (continued)

	<b>Page</b>
<b>CHAPTER 4 MATERIALS AND METHODS</b>	<b>55</b>
4.1 Materials	55
4.2 Apparatus	57
4.3 Preparation of Polyethylene grafted with Maleic Anhydride Film	60
4.3.1 MAH Photografting by UV Irradiation Technique	60
4.3.2 Compression of Commercial PE-g-MAH	60
4.3.2.1 Purification of PE-g-MAH Resin	61
4.3.2.2 Compression of Purified PE-g-MAH	61
4.3.3 Heat Treatment of PE-g-MAH Film	61
4.4 Characterization of the PE-g-MAH Film	61
4.4.1 Bulk Properties	61
4.4.2 Surface Properties	62
4.4.2.1 Attenuated Total Reflection Fourier Transform Infrared Spectroscopy (ATR-FTIR)	62
4.4.2.2 Contact Angle Measurement	63
4.5 Extraction of Proteins from Dry Skim NR	65
4.5.1 Protein Extraction	65
4.5.2 Protein Precipitation	65
4.6 Characterization of Extractable Proteins	66
4.6.1 Molecular weight of Extracted proteins by SDS-PAGE	66
4.6.1.1 Preparation of Reagents and Polyacrylamide Gel	66
4.6.1.2 Apparatus Setting and Procedure	69
4.6.2 Composition and Structure of Extractable Proteins	75
4.6.2.1 Freeze-Drying of Extracted Proteins	75
4.6.2.2 FTIR Analysis	76
4.6.2.3 CHN Analysis	76

## **CONTENTS (continued)**

	<b>Page</b>
4.6.3 Determination of Protein Content with Bradford Micro-Assay	76
4.6.3.1 Calibration Curve Preparation	76
4.6.3.2 Measurement of Protein Content in Extract Solution	77
4.7 Protein Binding Studies on the Films	79
4.7.1 Protein Binding on PE-g-MAH Film	79
4.7.2 Determination of Protein Binding	79
4.7.2.1 Characteristic of Protein-Immobilized Films	79
4.7.2.2 Determination of Immobilized Protein on the Films	80
 <b>CHAPTER 5 RESULTS AND DISCUSSION</b>	 <b>81</b>
5.1 Optimum Conditions for Preparation of PE-g-MAH Film	81
5.1.1 MAH Photografting by UV Irradiation Technique	82
5.1.2 Compression of Commercial PE-g-MAH	85
5.2 Study of Protein Extraction from Dry Skim NR	97
5.2.1 Effect of Solution Type on Protein Extraction	98
5.2.2 Effect of Multiple Extractions	101
5.2.3 Effect of Sample Size	102
5.3 Characterization of Extractable Protein	103
5.3.1 Molecular Weight of Extractable Protein	103
5.3.2 Composition and Structure of Extractable Protein	104
5.4 Protein Content Analysis	107
5.5 Study of Protein Binding on PE-g-MAH Film	117
5.5.1 Possibility of Protein Immobilization on the PE-g-MAH	117
5.5.2 Determination of Optimum Immersion Time	119
5.5.3 Study of Protein Binding with Extractable Protein	121
5.5.3.1 Determination of Coupling Condition	121

**CONTENTS (continued)**

	<b>Page</b>
5.5.3.2 Effect of MAH Content	125
5.5.3.3 Effect of Protein Concentration	128
5.5.3.4 Efficiency of Protein Immobilization	128
5.5.4 Modification of PE-g-MAH Film with 1,4-Butanediamine	131
<b>CHAPTER 6 CONCLUSIONS</b>	<b>136</b>
<b>REFERENCES</b>	<b>138</b>
<b>APPENDIX</b>	<b>148</b>
<b>BIOGRAPHY</b>	<b>162</b>

## LIST OF TABLES

<b>Table</b>	<b>Page</b>
3.1 Composition of fresh natural rubber latex	5
3.2 The 20 amino acids found in proteins	35
3.3 Reactive residues of protein	37
3.4 Buffer salts used in protein work	40
3.5 Detergents used for solubilization of proteins	41
3.6 Reducing agents	42
3.7 Precipitation agents	43
3.8 Dye-binding responses to polymeric L-amino acids	52
4.1 List of chemicals and reagent materials	55
4.2 List of Apparatus	57
4.3 List of the stock solutions	67
4.4 List of the components of separating gels (15% acrylamide)	68
4.5 List of Prestained standard on molecular weight for SDS-PAGE method	73
4.6 Preparation of calibration curve	77
5.1 Intensity ratio of PE-g-MAH under various conditions (Transmission mode)	83
5.2 Effect of grafting time and distance on contact angle of PE-g-MAH	84
5.3 Effect of annealing on contact angle	95
5.4 The assignments of characteristic absorption peaks of skim natural rubber	99
5.5 Effect of skim NR size on efficiency of protein extraction	102
5.6 CHN content of extractable proteins	105
5.7 Preparation of calibration curve in different assays	112
5.8 Compatible concentrations of possible interfering materials with Bradford assay	116
5.9 The components of protein in milk	117
5.10 Contact angles of annealed PE-g-MAH before and after BSA coupling and hydrolysis reaction	124

**LIST OF TABLES (continued)**

<b>Table</b>		<b>Page</b>
5.11	Intensity ratio of anhydride group on different PE-g-MAH films	125
5.12	The used conditions for BSA immobilization onto various supports	129
5.13	Comparison of the maximum binding capacities of the BSA protein onto various supports	130

## LIST OF FIGURES

Figure	Page
3.1 The components of natural rubber latex and their fractionation during centrifugation	9
3.2 Fresh latex centrifuged at 44,000 g in an angled rotor for 1 h shown in front and side perspectives of the centrifuge tube. The latex separates into three main fractions: the rubber cream (a, b), the C-serum (c), and the bottom fraction (d), which comprises mainly lutoids, the source of latex B-serum. Large rubber particles make up most of the rubber cream (a) while small rubber particles are found in Moir's zone (b) of the rubber cream	10
3.3 Allergenicity of latex gloves	12
3.4 The leaching process of latex gloves	14
3.5 Enzyme reactions on protein molecule	15
3.6 Proteins removal by functionalized support	18
3.7 Structure of cellulose	22
3.8 Structure of chitin	24
3.9 Structure of chitosan	24
3.10 Denaturation of Collagen	25
3.11 Protein coupling to maleic anhydride surface. Primary amino linkages (NH <sub>2</sub> ) on proteins attach the anhydride groups (left) forming covalent bond (right)	29
3.12 Coupling reaction between the BSA molecule and the Maleic Anhydride-alt-Methyl Vinyl Ether copolymer or P(MAMVE)	30
3.13 Immobilization of proteins by covalent coupling of lysine residues in BSA with retained maleic anhydride functional groups in polymer	30

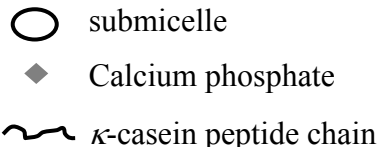
## LIST OF FIGURE (continued)

<b>Figure</b>	<b>Page</b>
3.14 Schematic reaction of MAH photografting	33
3.15 General structure of $\alpha$ -amino acid	34
3.16 The structure of a peptide	36
3.17 Aggregation of proteins by interactions in an aqueous-organic solvent mixture	44
3.18 Resonance forms of free ionic forms of CBBG. Red form, structure I; green form, structure II; blue forms, structure III and IV	49
4.1 The mini protean II cell	59
4.2 The power pac 300	59
4.3 Schematic diagram for grafting polymerization	60
4.4 ATR-FTIR Instrument: Gemanium crystal (a) and Zinc selenide crystal (b)	62
4.5 Contact angle goniometer	63
4.6 Water drop on solid surface	63
4.7 Drop shape analysis from contact angle measurement: (a) Poor surface wettability, Low surface energy and Contact angle $>90^\circ$ (b) Good surface wettability, High surface energy and Contact angle $<60^\circ$	64
4.8 View of gel plate assembly	69
4.9 Introducing the separating gel solution into the gel sandwich	70
4.10 Separation gel prior to polymerization	70
4.11 Introducing the stacking gel solution into the gel sandwich	71
4.12 Inserting the sample-well comb into the stacking gel	71
4.13 Stacking gel prior to polymerization	72
4.14 Introducing protein solution into sample well	73
4.15 The complete setting of electrophoresis apparatus	74
5.1 FTIR spectra of (a) PE film and (b) PE-g-MAH	82
5.2 Scheme of the hydrolysis of PE-g-MAH surface	84
5.3 ATR-FTIR spectrum (Ge) of PE-g-MAH granule	86

## LIST OF FIGURES (continued)

<b>Figure</b>	<b>Page</b>
5.4 ATR-FTIR spectra (Ge) of original and purified PE-g-MAH samples	87
5.5 DSC curves of original and purified PE-g-MAH	88
5.6 TGA curves of original and purified PE-g-MAH	89
5.7 Effect of compression temperature on intensity ratio of anhydride group	90
5.8 FTIR spectra of PE-g-MAH film (a) before and after annealing at (b) 110°C, 24 h and (c) 120°C, 3 h.	92
5.9 Effect of annealing conditions on the carbonyl index of purified PE-g-MAH sample	92
5.10 ATR-FTIR spectra (Ge) of PE-g-MAH film (a) before and after annealing at (b) 110°C, 24 h and (c) 120°C, 3 h.	94
5.11 Reaction of anhydride group conversion	94
5.12 DSC curves of purified PE-g-MAH before and after annealing	96
5.13 ATR-FTIR spectra (Ge) of (a) dry NR and (b) dry skim NR	97
5.14 FTIR spectra of skim natural rubber (a) before (b) after extraction with PBS and (c) after extraction with SDS	98
5.15 Effect of extract solvent on intensity ratio of protein in dry skim NR: (a) transmittance mode and (b) ATR mode	100
5.16 Protein content from extraction with SDS by using multiple extractions	101
5.17 SDS-PAGE images of standard protein (A) and extractable protein from dry skim NR (B)	103
5.18 ATR-FTIR spectra of (a) BSA standard protein and (b) extractable protein	106
5.19 Aromatic amino acids in proteins absorb light at 280 nm	107
5.20 UV-VIS spectra recorded for increasing BSA concentration in the range of 0-20 µg/ml (pH~ 6-7) and standard curve of 276 nm, absorbance versus protein concentrations	108
5.21 UV absorbance spectra for BSA and extractable proteins (EP)	109

## LIST OF FIGURES (continued)

<b>Figure</b>	<b>Page</b>
5.22 Structure of Coomassie brilliant blue (CBBG) G-250 dye	110
5.23 Colors of a typical standard curve	111
5.24 UV-VIS spectra of CBBG without protein (— · ·), with 20 µg/ml BSA (pH 0.4) (- - -) and blank subtraction (—)	111
5.25 Spectra of CBBG-protein complex of BSA under two different conditions Assay I) BSA 0-20 µg/ml, pH 0.2-0.4, Bradford concentration = 90.9%v/v Assay II) BSA 0-12 µg/ml, pH 0.4-1.0, Bradford concentration = 20.0%v/v	113
5.26 Calibration curves of BSA standard for (a) the spectrophotometric assay ( $\lambda_{\max} = 276 \text{ nm}$ ) (b) the Bradford assay ( $\lambda_{\max} = 592 \text{ nm}$ )	115
5.27 Casein Micelle <div style="margin-left: 40px;">  <ul style="list-style-type: none"> <li> submicelle</li> <li> Calcium phosphate</li> <li> <math>\kappa</math>-casein peptide chain</li> </ul> </div>	118
5.28 ATR-FTIR spectra of resin before (a) and after binding protein in milk (b) 5 h, (c) 7 h, (d) 9 h	119
5.29 Effect of binding time on the amount of immobilized protein (BSA) on commercial PE-g-MAH film.	120
5.30 The setup of protein binding testing	121
5.31 Coupling reaction between the protein molecule and the PE-g-MAH film (a) and the hydrolysis reaction of polymer (b)	122
5.32 ATR-FTIR spectra of PE-g-MAH (a) before (b) after protein binding and (c) after hydrolysis reaction.	123
5.33 Immobilization of extractable protein on commercial PE-g-MAH film ( $\square$ ) and UV photografted PE-g-MAH film ( $\text{▨}$ )	126
5.34 ATR-FTIR spectra of PE-g-MAH film (a) before and (b) after immersion in protein solution	127

**LIST OF FIGURES (continued)**

<b>Figure</b>	<b>Page</b>
5.35 Effect of extractable protein concentration on amount of protein immobilization	128
5.36 Principle of the modification	132
5.37 Preparation of polymer film bearing reactive amino groups	133
5.38 ATR-FTIR spectra of (a) PE-g-MAH (b) Annealed PE-g-MAH (c) BDA _PE-g-MAH (d) PEMI	134

## LIST OF ABBREVIATIONS

A <sub>280</sub>	= Absorbance Assay at 280 nm
APS	= Ammonium persulphate
ATR-FTIR	= Attenuated Total Reflection Fourier Transform Infrared spectrometer
AVG	= Average
BCA	= Bicinchoninic Acid
BDA	= 1,4-butanediamine
BPO	= Benzophenone
BSA	= Bovine serum albumin
CBBG	= Coomassie brilliant blue R-250
CHN	= Carbon Hydrogen Nitrogen
DSC	= Differential scanning calorimeter
DSC-TGA	= DSC–Thermal gravimetric analysis
EP	= Extractable protein
Ge	= Germanium
kDa	= kilo Dalton
MAH	= Maleic anhydride
NR	= Natural rubber
PBS	= Phosphate buffer saline
LDPE	= Low density polyethylene
PE-g-MAH	= Polyethylene grafted with maleic anhydride
SDS	= Sodium dodecyl sulphate
SDS-PAGE	= SDS-Polyacrylamide gel electrophoresis
STDEV	= Standard deviation
TCA	= Trichloroacetic acid
TEMED	= N,N,N',N'-Tetramethylenediamine
T <sub>m</sub>	= Melting temperature
Tris-HCl	= Tris (hydroxymethyl) aminomethane hydrochloride

**LIST OF ABBREVIATIONS (continued)**

UV	= Ultraviolet
UV-Vis	= UV-Visible spectrophotometer
ZnSe	= Zinc selenide
$\theta_c$	= Contact angle

## CHAPTER 1

### INTRODUCTION

Natural rubber latex (NRL) is extracted from *Hevea brasiliensis* tree and used to produce different kinds of rubber goods like gloves, condoms, balloons and some parts of medical and dental equipments. Natural rubber has been available commercially for more than a century. Its latex-dipped products, particularly gloves, have been used preferentially as effective barriers to transmitted diseases. However, the occurrence of Type I allergy has recently been reported by some hypersensitive users. The allergy caused by latex products has become a serious problem. The sweat can remove proteins and allow contact with skin, causing sensitization or allergic reactions.

Several methods for extractable and allergenic protein reducibility have been used in many works. These include the use of low protein lattices [1], suitable leaching protocols during processing [2] enzyme treatment [3], chlorination of the finished product, addition of fumed silica [4], and irradiation method [5]. These methods are difficult to process and need a long incubation time for processing. New technique of protein removal from natural rubber is developed. It is a simple and rapid technique by immersion of functionalized support into natural rubber latex under optimum condition. The proteins can be immobilized on support surface via covalent linkage.

The binding of proteins on solid supports is based on the covalent attachment of proteins to water-insoluble matrices. Proteins are heteropolymers built up from more than 20 types of monomer unit of amino acid residues that have  $-NH_2$  group in the side chain suitable for linking to a support matrices. The binding process involves mild reactions between amino group of the protein and several groups of functionalized carriers.

Many types of supports such as polystyrene [6], polyacrylamide [7], polyvinyl alcohol [8] and maleic anhydride copolymer [9-10] have been studied in protein

immobilization. Maleic anhydride (MAH) has interesting properties for protein coupling. The anhydride group is very reactive to primary amine group and slightly less reactive to alcohol. It was therefore selected as a reactive group on film surface for protein binding. Polymer bearing maleic anhydride could be directly prepared by UV photografting [11-13]. This method of surface modification shows significant advantages: low cost of operation, mild reaction conditions, selectivity to absorb UV light without affecting the bulk polymer and permanent alteration of the membrane surface chemistry.

Therefore, in this study, it is of interest to study the binding property of extractable protein from natural rubber with two types of polyethylene grafted with maleic anhydride (PE-g-MAH) films, prepared from UV photografting and compression of commercial granule. Initially, the protein extraction efficiency with various conditions was evaluated and the suitable time for protein immobilization was determined. The effects of MAH content and protein concentration were studied under optimal immersion time. After binding, the change of chemical structure on the film surface and the amount of immobilized protein were analyzed.

## CHAPTER 2

### OBJECTIVES

The present research describes the protein binding ability of maleic anhydride copolymer via covalent linkage under optimum condition, in order to remove allergenic and extractable protein from natural rubber. This will be very useful in improving the NR product.

In this work, it was divided into three parts:

#### ***Part I*** - Preparation of polyethylene grafted with maleic anhydride (PE-g-MAH)

The optimal condition for preparing PE-g-MAH film was investigated. Two types of MAH copolymers were used in the research; (1) PE-g-MAH obtained from MAH photografting on LDPE film and (2) commercial PE-g-MAH. In UV photografting process, the grafting polymerization was studied under some factors including reaction time and distance between UV lamp and sample. The anhydride group on the surface was converted from carboxylic acid under suitable annealing condition and the thermal behaviors of annealed film were analyzed.

#### ***Part II*** - Protein extraction and characterization

Extractable proteins from dry skim NR were selected to study protein binding ability of PE-g-MAH film. The effects of extract solution type, number of extractions and sample size on the extractable protein content were studied.

The molecular weight, composition and structure of extractable protein were analyzed by using SDS-PAGE, CHN analysis and FTIR technique, respectively.

#### ***Part III*** - Protein binding of PE-g-MAH film

The use of two PE-g-MAH films, prepared from UV photografting and compression of commercial granule, for protein binding was investigated. The Bovine

Serum Albumin (BSA) was used as a model protein to determine optimum immersion time for binding process. The amount of immobilized protein on the surface was quantified by Bradford assay. The evidence of covalent linkage between anhydride and amino groups was also examined.

## CHAPTER 3

### LITERATURE REVIEW

#### 3.1 Natural Rubber Latex

Fresh natural rubber latex is a cytoplasmic system consisting of particles of rubber hydrocarbon dispersed in aqueous serum phase. There are also numerous non-rubber particles called *lutoids* (The lutoids are often referred to as the  $\beta$ -fraction because they appear at the bottom of the centrifuge tube when fresh latex is centrifuged by ultracentrifugation.) The rubber particles are made up of rubber hydrocarbon surrounded by a protective membrane layer consisting of proteins and lipids. The composition of fresh latex [14] is shown in **Table 3.1**.

**Table 3.1** Composition of fresh natural rubber latex

Component	Percentage
Rubber hydrocarbon	25-45
Protein	1.0-1.8
Carbohydrates	1.0-2.0
Neutral lipids	0.4-1.1
Polar lipids	0.5-0.6
Inorganic constituents	0.4-0.6
Amino acids, amines etc.	0.4
Water	~ 50

### **a) Rubber Hydrocarbon**

The rubber hydrocarbon is cis-1,4-polyisoprene. Its number average molecular weight ranges from 200 to 600 kD and shows a clonal variation. The rubber content in latex may vary from 25% to 45%, depending on the clone, season, soil and environmental conditions, and the effects of tapping and yield stimulation.

### **b) Non-rubber Substances**

#### **Proteins**

Apart from rubber hydrocarbon and water, proteins and carbohydrates occur in the biggest concentration in latex. The protein content in latex can range from 1% to more than 1.8% in different samples of latex. About 25% to 30% of the proteins are found in the rubber phase, about 45% to 50% in the serum phase, and about 25% in the  $\beta$ -fraction in a typical latex sample containing about 1.4% protein. The amount of proteins in the rubber phase is less variable than the total amount of proteins in different sample of latex.

Earlier work showed that the serum proteins consist of 19 anionic and 5 cationic proteins [15]. The major protein is alpha-globulin with an isoelectric point of 4.8. There are 7 anionic and 6 cationic proteins in the  $\beta$ -fraction. The major proteins are Hevein (50%) and Hevamine (30%) with isoelectric points of 4 and 9, respectively.

#### **Lipids**

Of the total lipids, neutral lipids constitute about 50% to 60%. The rest is made up of glycolipids and phospholipids. These are found in the rubber phase and the  $\beta$ -fraction. The major phospholipid is phosphatidyl choline with smaller amounts of phosphatidyl ethanolamine and phosphatidyl inositol. The neutral lipids consist of carotenoids, sterol and fatty acid esters, triglycerides, tocotrienols, free fatty acid, beta-sitosterol, diglycerides, monoglycerides, and fatty alcohols.

### Carbohydrates

Quebrachitol or 1- methyl inositol is the most concentrated single component in the serum phase, amounting to about 1% of the whole latex. Smaller amounts of inositol isomers, sucrose, glucose, galactose, fructose and two pentoses have also been detected [16].

### Inorganic Constituents

Potassium is the most abundant element present in latex. Its concentration is of the order of a few thousand parts per million (ppm). Magnesium is the next most common element with a few hundred ppm being present. The other elements occurring in much smaller concentrations are calcium, sodium, rubidium, iron, zinc, copper and manganese.

## **3.2 Skim Natural Rubber**

Skim rubber is a material resulting from the concentration of natural rubber latex by centrifugation. After centrifugation process, about 5-10 % of total rubber, together with an enhanced proportion of the non-rubber constituents of the original latex, remains in the serum phase to form skim latex [17].

The skim latex consists of rubber particles with small size ranging from 0.04 to 0.4  $\mu\text{m}$  and contains about 3-10 % w/w of dry rubber content [18], 2-7 % w/w of water soluble materials and residual water [19].

In general, the skim latex is known as waste product in the factory producing the NR latex concentration. It contains large amounts of non-rubber materials and high dirt content. Moreover, the aqueous portion of skim NR latex contains proteins, sugars, nucleic acids and minerals and these minerals can produce the environmental problems in disposal water.

There are two basic causes for explanation of high impurities in skim rubber. First, the serum phase of the skim latex contains large amount of suspended proteins and dissolved matters. Second, the rubber particles remaining in the skim latex are

smaller than those in the ordinary NR latex particles and have a relatively larger surface for adsorption. A large proportion of the soluble non-rubber constituents of the initial latex tend to efflux with the skim rubber, resulting in a great amount of adsorbed substances per unit volume of rubber.

The residual rubber from skim latex is normally recovered by the addition of sulfuric acid [20]. This method can separate skim rubber out from skim latex as coagulum like crumb. Skim rubber contains 70-85% rubber component and a number of proteins.

### **3.3 Proteins in Natural Rubber Latex**

Proteins make up about 1-2% fresh weight of Hevea latex [21-23]. Because natural rubber latex is not a homogeneous fluid, latex proteins are not homogeneously dispersed. Latex proteins are found in the latex sera and also associated with latex organelles that can be separated by high-speed centrifugation. About 70 % of latex proteins are soluble, with the remaining being associated with membranes.

#### **3.3.1 Protein Separation by Centrifugation**

Centrifugation cleans and concentrates the latex by removing 50% of the water content and reducing the non-rubber solids (e.g., proteins, fatty-acid, soaps, salts, minerals). Rubber particles, coated with phospholipids, glycolipids and proteins, are hydrophobic particles and rise to the top of supernatant during centrifugation while proteins and other non-rubbers are mostly dissolved in the C-serum phase (see **Figure 3.1**).

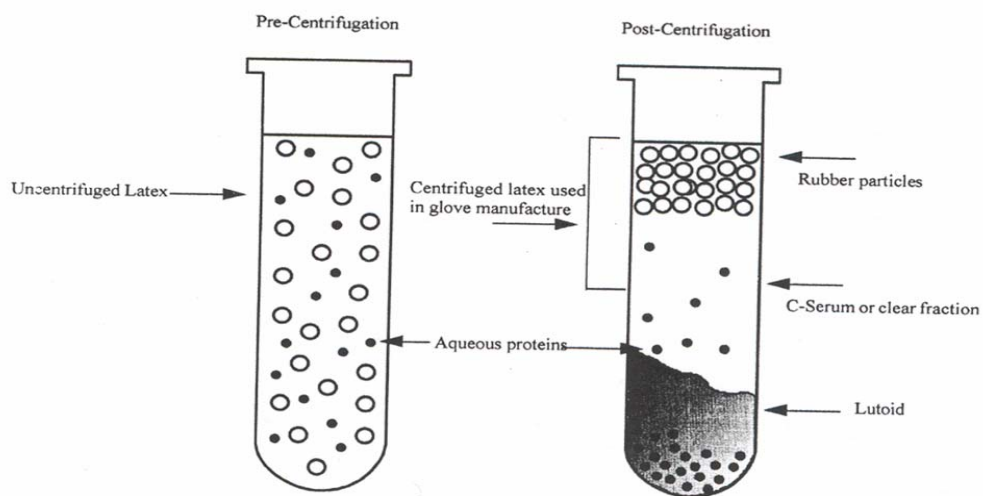


**Figure 3.1** The components of natural rubber latex and their fractionation during centrifugation.

### 3.3.2 Proteins in Latex Fractions

Although Moir [24], distinguished as many as nine fractions in Hevea latex following ultracentrifugation at 53,000g, there are basically three main fractions that are easily discerned [25]. These are the rubber phase, the C-serum, and the bottom fraction (in **Figure 3.2**).

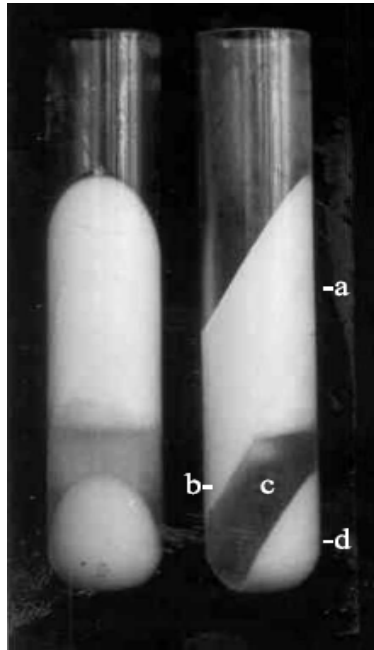


**Figure 3.2** Fresh latex centrifuged at 44,000 g in an angled rotor for 1 h shown in front and side perspectives of the centrifuge tube. The latex separates into three main fractions: the rubber cream (a, b), the C-serum (c), and the bottom fraction (d), which comprises mainly lutoids, the source of latex B-serum. Large rubber particles make up most of the rubber cream (a) while small rubber particles are found in Moir's zone (b) of the rubber cream.

The rubber phase comprises the rubber particles that are packed centripetally by centrifugation. With the C-serum in the interstices between rubber particles removed, two main proteins are extractable from the surface of the rubber particles. Whereas most of the C-serum and B-serum proteins are water-soluble, those of the rubber particles are generally insoluble. About 11 mg of proteins is bound to each gram of rubber.

The C-serum refers to the aqueous medium in which all the latex organelles are suspended. Latex C-serum contains a large variety of proteins associated with cellular metabolism. The C-serum proteins are therefore numerous, probably in the hundreds. A typical sample of C-serum contains about 12 mg proteins per milliliter.

While the latex bottom fraction comprises mainly the lutoids, other minors organelles (e.g., ribosomes, endoplasmic reticulum) are also present [26]. The latex B-serum is obtained by repeated freezing and thawing of the bottom fraction of centrifuged latex [27].

### 3.3.3 Residual Extractable Proteins in Latex Products

The starting material for all latex-dipped products, is derived from *Hevea brasiliensis* latex obtained from the tree on tapping. The fresh latex consists of about 35% rubber particles and 15% of non-rubber particles, all suspended in an ambient serum. Of the non-rubber substances present, proteins constitute approximately 1% - 1.5% (of total latex weight), of which about  $\frac{1}{4}$  is associated with surfaces of the dispersed latex particles, and the remaining present as soluble proteins in the serum phase. When converted into latex concentrate with a rubber content of 60%, some of the soluble proteins in the serum phase are removed. The proportion of the surface bound proteins is thus increased from  $\frac{1}{4}$  to about  $\frac{1}{2}$ , while that of the soluble proteins is decreased accordingly. Although there is still a certain quantity of proteins present, the amount extractable proteins when latex concentrate is processed into latex gloves or products is, however, only very small; it often does not exceed a few percent of the total. It is noteworthy that this small fraction constitutes the residual extractable proteins implicated in the Type I allergic reaction. Improvements of latex products, therefore, invariably involve the reduction or removal of this undesirable protein fraction, particularly the allergens. Removal of the latter alone is unfortunately not yet possible due to incomplete information regarding their identities-in spite of the very active research currently in progress in many laboratories.

### 3.4 Latex Protein Allergy

Latex allergy has a significant public health impact. Life threatening reactions to latex have been reported in latex sensitive customers. It can be serious enough to cause the severe allergic reaction, anaphylaxis, which can be fatal. **Figure 3.3** presents an allergy appearance after using latex gloves which have a residue protein in product.



**Figure 3.3** Allergenicity of latex gloves.

The adverse reactions associated with NR can be categorized in three types: irritant reactions, delayed-type allergic reactions and immediate-type allergic reactions.

#### ➤ **Irritant Reaction (Non-Allergic)**

This is skin irritation that does not involve the body's immune response. It is not an allergic response. Some causes include: frequent hand washing and inadequate drying, aggressive scrubbing technique or detergents, mechanical abrasive effect of glove powder, climatic irritation (cold climates can cause dry, chapped skin and hot weather can cause excessive sweating), and emotional stress. Even though this is not an allergic reaction, irritant hand dermatitis can cause breaks in the skin which can allow easier entry of the sensitizing latex protein or glove chemicals, and in turn lead to latex allergy [28] provides a review of irritant dermatitis and its management.

➤ **Delayed-Type Allergic Reaction (Type IV Hypersensitivity)**

Type IV Hypersensitivity is usually a sensitivity to chemicals used to make gloves, rather than to proteins from the natural rubber itself. Numerous chemicals are used in the manufacturing process, including antioxidants, emulsifiers, stabilizers, accelerators, stiffeners, colorants and fragrances. Any of these can cause a contact dermatitis 24-48 hours after exposure. Type IV Hypersensitivity is also called allergic contact dermatitis, T-cell-mediated allergy or chemical allergy. It is estimated that 80% of people who develop type I reactions experienced type IV reactions first. One route of sensitization, for example, is that latex proteins are more easily able to enter the body through the broken skin barrier.

➤ **Immediated-Type Allergic Reaction (Type I Hypersensitivity)**

These are systemic allergic reactions caused by circulating IgE antibodies to the proteins in natural latex. Symptoms include hives, rhinitis, conjunctivitis, asthma due to broncho constriction, and in severe cases anaphylaxis and hypotension. Symptoms occur soon after exposure to latex (within about 30 minutes). There are several routes of exposure that can lead to type I sensitivity: cutaneous, mucosal, parenteral, and aerosol (from inhaling latex glove powder).

However, the incidence of latex allergy associated with water extractable protein in gloves, of a type I hyper-sensitivity which can be potentially fatal, has posed a serious challenge to the latex glove manufactures [28-30]. Several reasons have been given for the desire to produce latex medical gloves with low protein contents. These are as follows: prevention of gloves of excessively high protein contents from getting into the market and thus sensitizing further individuals, gloves of low protein contents are likely to give low allergic response and to ensure that medical devices are safe for the users.

### 3.5 Reducibility of Extractable and Allergenic Proteins

Manufacturers of NR latex dipped products now have a range of established and novel methods available to reduce extractable and allergenic proteins.

#### 3.5.1 Leaching

Hot- and Cold-water washing (leaching) is now used extensively within the dipping industry. Leaching is the process of removal of hydrophilic materials from latex dipped products (i.e., gloves) by washing them in water (see **Figure 3.4**). The influence of glove thickness and the processing conditions have been studied by researchers. Their findings indicate the following:

- There is a need for the protein to migrate to the glove surface to facilitate extraction.
- The thinner the glove, the more effective is protein removal.
- Gloves produced from latex with lower rubber content had a higher level of extractable proteins (40%) than glove generated from latex with a higher rubber content (60%)



**Figure 3.4** The leaching process of latex gloves.

In general, wet gel leaching, i.e., leaching before curing the rubber, was found to be less effective than dry film leaching. This was thought to be due to the protein

having insufficient time to migrate to the film surface during the manufacturing process.

### 3.5.2 Enzyme Treatment

The use of proteolytic enzyme to digest latex proteins has been known for many years. However, it is only recently that the uses of these enzymes have been shown to reduce allergenic proteins in medical gloves. These enzymes break down proteins into smaller pieces which facilitates their removal, as can be seen in **Figure 3.5**.

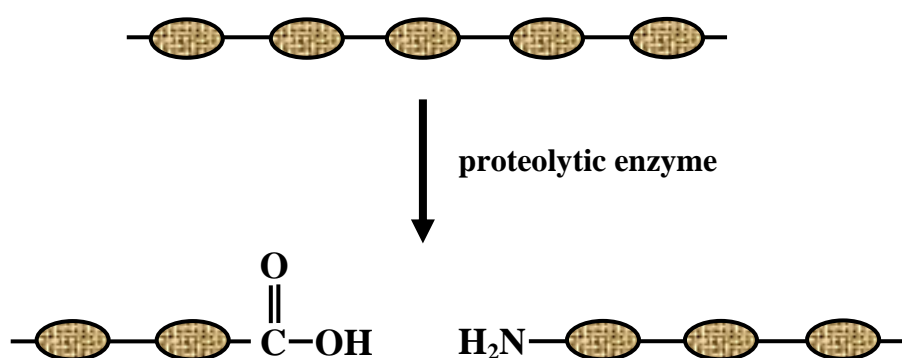


**Figure 3.5** Enzyme reactions on protein molecule.

Care must be taken to remove residual proteolytic enzymes, which may also give rise to an allergic response. The enzyme treatment was used in work of Klinklai et al. [31] to remove proteins from fresh NR latex. They found that the hyperdeproteinized NR is almost free from the protein after incubation of High-ammonia NR latex with a proteolytic enzyme followed by treatment with urea.

### 3.5.3 Fumed Silica

It has been theorized that fumed silica can be used both in straight and coagulant dipping to reduce extractable protein in surgical gloves. It is claimed that as little as 1-2 part per hundred of rubber may significantly reduce extractable protein from latex gloves without adversely affecting the dipping process. The mechanism by which dispersed fumed silica reduces proteins content in the latex is not known. The

practical significance of these findings remains to be demonstrated, however. The reduction of water-soluble protein content in rubber by using fumed silica was studied by Thiangchanya et al. [4]. They found that 3 phr of fumed silica with 0.17 phr of ZnO could reduce water-soluble protein content to less than 30  $\mu\text{g/g}$ . This may be due to the strongly combined effect of protein immobilization by silica/ZnO.

#### **3.5.4 Ultrasonic leaching**

There is some evidence that using ultrasonic in the leaching system can accelerate the removal of latex protein over leaching on its own. The effect seems to be more pronounced in pre-vulcanized films, i.e., those where the rubber is cured before formation of the rubber film, than in post-vulcanized films and there is apparently no detrimental effect on tensile properties.

#### **3.5.5 Chlorination**

The most effective method of reducing the extractable protein content in latex products is chlorination. It is a process where chlorine, ammonia, water and other chemicals are used in the manufacturing of gloves.

The primary aim of chlorinating medical gloves is to provide the end-user with a means of donning the glove in the absence of lubricating powder. Chlorination is also highly effective in lowering the level of extractable protein. This chlorination process removes powder and breaks down latex protein as well as chemical residue on or near the glove surface. Then through multiple washing and leaching processes, the protein and chemicals are further reduced to produce gloves that meet the lowest allowable protein claim of less than 50  $\text{mg/dm}^2$  of glove. This suggests that the reduction of extractable protein by chlorination is not just due to the extra leaching achieved in this process but the fact that the chlorine itself renders the proteins insoluble and/or forms a less penetrable layer for the proteins to migrate to the surface.

The process does, however, require tight controls as over-chlorination or inadequate neutralization of the powerful chemicals used can lead to discoloration and detrimental effects on the ageing properties of the glove.

Dalrymple and Audley [32] have shown that the effectiveness of the chlorination procedure in reducing extractable protein levels probably results from exposure of the latex to the water, salt, acid and ammonia associated with the process and not from the chlorination itself.

### 3.5.6 Irradiation

When field latex was irradiated with gamma rays, the water solubility of the proteins increases. The reduction of water-solution protein by irradiation was studied by Rogero et al [33]. In this study, field natural rubber latex was irradiated with different doses near a  $^{60}\text{Co}$  gamma source to reduce the water-soluble protein content in the final product. They found that the concentration of extractable proteins increased with increasing radiation dose. The similar result was also found by Parra et al. [34]. They studied the effect of combined treatment of water-soluble polymer addition and centrifugation of radiation vulcanization of natural rubber latex (RVNRL) on the removal of extractable proteins in RVNRL film.

## 3.6 Functionalized Support for Protein Binding

New technique for removal protein from natural rubber is the immersion of functionalized support into natural rubber latex under optimum condition. The support has a functional group which is reactive to amino group of protein. The protein can be immobilized on the support surface via covalent binding and protein-free NR latex is obtained, as shown in **Figure 3.6**. This technique is a simple and rapid process, no need for new equipment and it can completely remove protein from natural rubber latex.

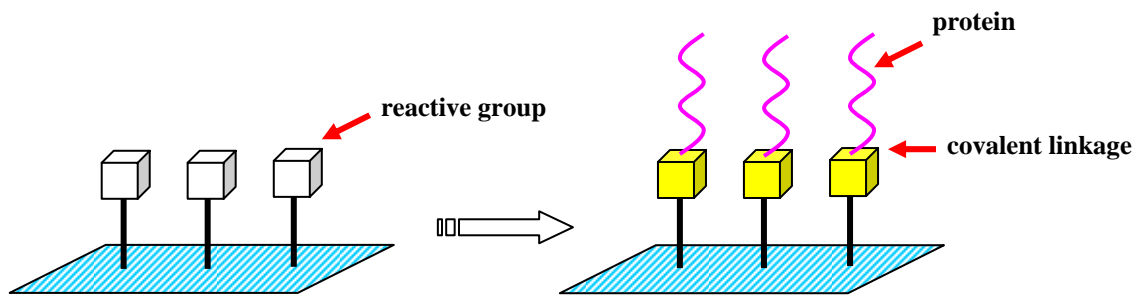


**Figure 3.6** Proteins removal by functionalized support.

Three common methods for the immobilization of protein can be identified, based on the interaction between the protein and the solid support: electrostatic interaction [35-36], entrapment [37], and covalent binding [38].

### *Electrostatic Interaction*

Immobilization via ionic interaction between the protein and solid support has been explored for many years. It has been shown to be sufficiently strong to minimize leaching [39]. Electrostatic interaction is the common law in bio-body activity. Protein adsorption under electrostatic condition can present not only the general information of life phenomenon but also the dynamic interaction of protein and target. Owing to these, considerable endeavors have been made in the adsorption of protein onto electrostatic microspheres over the last decades.

Hudson et al. [40] measured the adsorption properties of cytochrome C and xylanase on pure silica SBA-15, while weak hydrophobic forces provide the enzymes major interaction between the proteins and organofunctionalized SBA-15.

Greene et al. [41] quantified the adsorption of immunoglobulin G (IgG) protein onto several polyelectrolyte-modified sintered porous polyethylene (PPE) membranes. They were able to show that the observed improvement in the IgG binding is derived from electrostatic interactions between IgG and the polyelectrolyte surface. The greatest IgG adsorption occurred when the IgG and the surface possessed predominantly opposite charges, rather than when the surface possessed the greatest

electrostatic charge. And they found that the molecular weight of the terminating polyelectrolyte has a noticeable effect upon the electrostatic interaction.

### **Entrapment**

Entrapment refers to the physical confinement of protein in environment where the substrate is able to penetrate but the protein cannot escape. The entrapment method suffers from the following drawbacks:

- The difficulty in controlling the protein confining environment may impose large diffusion barriers on the transport of the substrate or product, resulting in reaction retardation and long response times.
- If the pore size distribution of the entrapment medium is not narrow, continuous loss of activity because of protein leaching can occur.
- Traditionally used polymers for protein entrapment often experience shrinkage and/or swelling during a reaction.

Various strategies have been developed for the entrapment of proteins into mesoporous materials. Blin et al. [42] demonstrated the entrapment of glucose oxidase in mesostructured silicas using a one-step sol-gel method. Under neutral pH conditions, the enzyme solution was added into a micellar solution of a nonionic fluorinated surfactant.

### **Covalent binding**

The most intensely studied immobilization technique is the formation of covalent bonds between the protein and the support matrix. The covalent binding method is based on the covalent attachment of proteins to water-insoluble matrices. The conditions for immobilization by covalent binding are much more complicated and less mild than in the cases of physical adsorption and ionic binding. The covalent binding is strong, so that stable immobilized protein preparations have been obtained that do not loss protein into the solution, even in the presence of high ionic strength solution. The covalent immobilization of proteins on the surfaces of polymer is

generally considered as a promising approach to enhance compatibility of biomaterials. Various procedures to covalently couple proteins to surfaces have already been described [43].

Three main factors have to be taken into account for covalent immobilization of proteins by a specific method: (1) the functional group of proteins soluble for covalent binding under mild conditions, (2) the coupling reaction between the proteins and the support and (3) the functionalized supports suitable for protein immobilization.

With the covalent binding, monomer unit of amino acid residues that have  $\text{NH}_2$  group in the side chain are suitable for linking to a support matrices. The binding of protein molecules to solid supports involves mild reactions between amino group of the protein and several groups of functionalized carriers.

### **3.6.1 Supports for Protein Covalent Coupling**

A variety of support properties, e.g., surface properties, morphology, configuration, composition and modification should be assessed with respect to the specific application prior to the selection for evaluation. Solid support can be classified according to their morphology (non-porous and porous matrices) and composition (organics and inorganics).

#### **3.6.1.1 Morphological classification**

##### **Non-porous supports**

Non-porous supports usually present a major disadvantage for protein immobilization. The surface area of non-porous carriers is extremely low, and therefore the available area of protein coupling is very limited. However, non-porous carriers can present some advantages due to their morphological characteristics. The diffusion constraints with respect to the soluble compounds can be eliminated or certainly reduced by decreasing the particle size or increasing the fluid linear velocity, since the protein is immobilized on the external surface of the carrier and is in immediate contact with the surrounding environment.

### **Porous supports**

Porous carriers have a high surface area per unit weight, which allows a high protein loading and thus makes them ideal for large industrial processes. A major disadvantage of porous carriers, however, is that most of the surface available for protein coupling is internal surface. Porous support must have an internal morphology that allows not only the protein coupling but also an easy accessibility to soluble molecules in order to minimize diffusional effects. On the other hand, proteins bound on the internal surface are protected from the turbulent and harsh external environment.

Synthetic porous polymers such as sintered porous polyethylene (PPE) can be cheaply manufactured with a higher degree of control over such properties as pore size, pore size distribution, pore volume, surface area and material density than is found in currently used porous material, specially nitrocellulose. The intrinsic chemical properties of polyethylene fail to provide any reactive functionality or surface hydrophilicity that is capable of binding proteins [44].

#### **3.6.1.2 Chemical classification**

Carriers can be classified according to their chemical composition as inorganic and organic supports.

### **Inorganic Supports**

A great variety of inorganic supports have been used as matrices for the immobilization of proteins. Their physical properties are suitable for industrial use and offer several advantages over their organic counterparts: high mechanical strength, thermal stability, resistance to organic solvents and microbial attack, excellent shelf life and easy handling. Moreover, inorganic materials do not change in structure over wide ranges of pH, pressure and temperature.

One of the most important prefabricated inorganic solid supports is controlled-pore glass (CPG). CPG is unsuitable for industrial purposes owing to its difficulty

preparing, high cost and unstable in alkaline environments. A method that permits the covalent binding of enzymes to porous glass has been developed by Stabel et al [45]. They found that rabbit anti-bovine IgG was covalently immobilized on thionyl chloride-activated succinamidopropyl controlled-pore glass (CPG) beads.

### Organic Supports

Most of the commercially available immobilized proteins are obtained with organic matrices. The reason for this is that there are a wide variety of functional reactive groups which can be put on organic supports. Organic carriers are classified as either natural macromolecules or synthetic polymers and having hydrophilic or hydrophobic characteristics.

#### a) Natural polymers

- **Cellulose** The polysaccharide cellulose (in **Figure 3.7**) was one of the first materials to be used as a matrix for the covalent binding of protein. Although the hydroxyl groups of polysaccharides are not reactive enough to form covalent bonds between the protein and the support without previous activation. Cellulose undergoes all the reactions associated with polyhydric alcohols so that a wide range of active cellulose can be prepared.

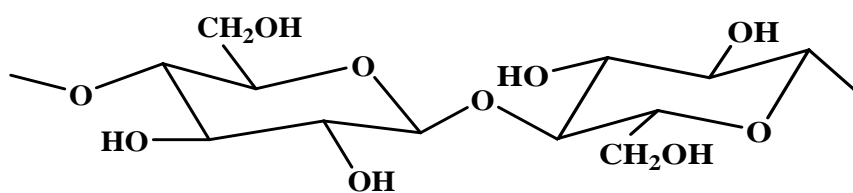


**Figure 3.7** Structure of cellulose.

Several types of chemically modified celluloses are commercially available and originally were used as ion-exchangers such as Diethylaminoethyl-cellulose (DEAE-cellulose). These modified celluloses were used to directly immobilize protein by

ionic binding and also have permitted a wide range of covalent binding methods in which the protein binds mainly through amino groups.

Varavinit et al. [46] studied the possibility of immobilization of glucoamylase on bagasse (a natural cellulosic material) after activation of the bagasse with periodic acid. They found that the aldehyde groups of the diacetyl cellulose were able to react with amino groups of a glucoamylase to form covalent bonds and result in a dialdehyde cellulose immobilized enzyme.

- **Dextran** Dextran is a basically linear, water soluble polysaccharide composed of (1 → 6)-linked  $\alpha$ -D-glucopyranosyl units (although dextrans are frequently branched). Insoluble and porous supports based on dextran (cross-linked) and possessing molecular sieving properties were originally developed as support for gel filtration chromatography and are commercially available in grades characterized by their water regain and molecular exclusion limits. Because of these properties, they have gained wide acceptance in protein immobilization.

Cross-linked dextrans have to be activated for use as support of immobilized proteins. Some other covalent coupling methods of immobilization of proteins that are used involve the use of cyanuric chloride [47], epichlorohydrin and benzoquinone for activation of hydroxyl groups (direct coupling), carbodimides for carboxyl derivatives, and 1-2-pyridine disulfide for thiol derivatives. Ionic derivatives of crosslinked dextran are also commercially available and used for protein coupling by ionic interactions.

New hydrogel microspheres based on crosslinked dextran containing N,N'- diethylaminoethyl (DEAE) groups with different chemical structures have been used in adsorption-desorption studies by Can and Güner [113]. The results indicated that bovine serum albumin attachment to the crosslinked DEAE dextran microbeads occurred rapidly at medium pH. Desorption occurred with NaCl but adsorption process was not fully reversible. These results support the interpretation that bovine serum albumin has a moderate affinity for crosslinked DEAE dextran.

- **Chitin and Chitosan** Chitosan is a natural source polymer prepared by N-deacetylation of chitin, which is the main structural component of crab and shrimp

shells. Chitin and chitosan are polysaccharide containing amino groups which have been used as inexpensive supports for protein immobilization. Chemically, chitin (**Figure 3.8**) is a polysaccharide composed of (1  $\rightarrow$ 4)-linked 2-acetamido-2-deoxy- $\beta$ -D-glucopyranosyl residues. About one of every six residues is not acetylated, whereas in chitosan (**Figure 3.9**) essentially all the residues are not acetylated (2-amino-2-deoxy-D-glucose). Water-soluble chitosan can be obtained from chitin by deacetylation in concentrated sodium hydroxide solution.

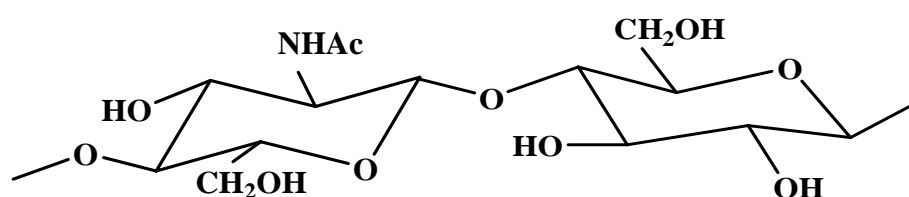


**Figure 3.8** Structure of chitin.

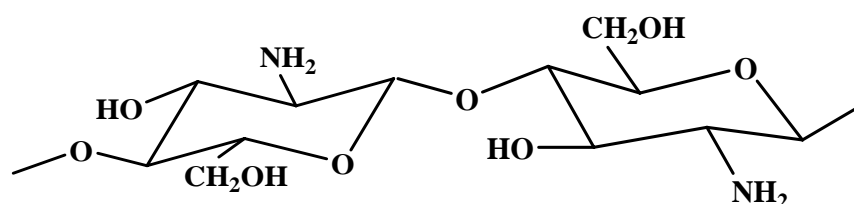


**Figure 3.9** Structure of chitosan.

Proteins can be bound to chitin by adsorption but this is usually followed by crosslinking with glutaraldehyde. Covalent linkage onto carbonyl derivatives, obtained by a previous treatment with glutaraldehyde, is also possible [48]. Chitin and chitosan derivatives have been reported to have favorable characteristics and have been qualified as attractive supports for protein immobilization. Some investigators reported the platelet adhesion on the surface of modified chitosan [49]. They found that chitosan has a better blood compatibility than polystyrene. All proteins on chitosan and on polystyrene materials represent a monolayer adsorption.

- **Collagen** Collagen has several advantages as an enzyme carrier. Its hydrophilicity facilitates the accessibility of enzymes to the binding sites. Its insoluble proteinaceous nature makes possible a strong physical adsorption of enzymes. Its open internal structure provides a high concentration of binding sites. Its fibrous structure and high swellability in aqueous solutions also contribute to its use as enzyme support matrix.

Protein can be immobilized on collagen by adsorption, complexation, entrapment and covalent coupling. Coulet and coworkers [50] described a covalent binding technique in which an acidic derivative of collagen was used for the preparation of several collagen-enzyme conjugates. Due to its biological origin, collagen may be particularly useful in biomedical applications.

- **Gelatin** The protein gelatin has several properties that make it attractive as a support for the immobilization of enzymes. It is easily obtained in solution from collagen by boiling with water (in **Figure 3.10**).

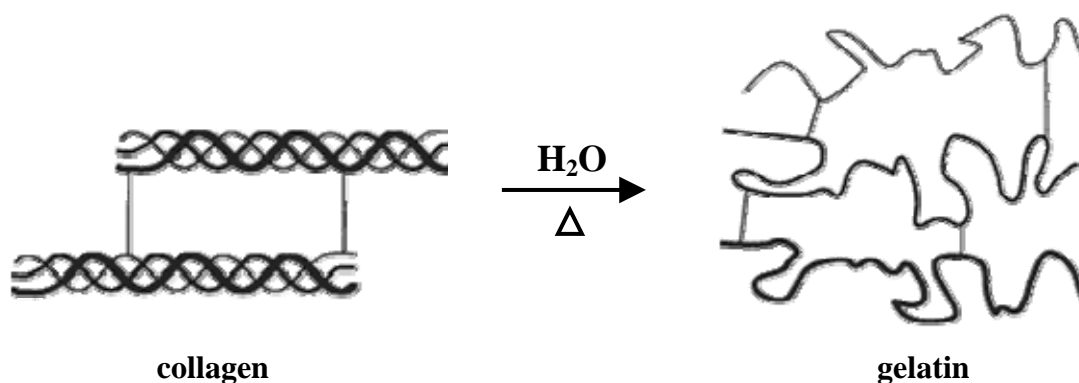


**Figure 3.10** Denaturation of Collagen.

Gelatin does not have the strength of collagen. Therefore, to use it as a water-insoluble enzyme carrier, it is necessary to crosslink the gel with multifunctional reagents (e.g., glutaraldehyde). The chemical, mechanical and thermal stabilities largely depend on the degree of crosslinking as well as the rigidity and the porosity of the gelatin support.

Enzymes can be immobilized on gelatin by gel entrapment followed by crosslinking [51] or by covalent coupling on the residual active groups of the multifunctional reagent (e.g., carbonyl groups of glutaraldehyde) at the surface of the gel.

Bajpai and Sharma [52] synthesized novel biocompatible hydrogel of binary polymeric blends of crosslinked poly(acrylic acid) grafted onto poly (vinyl alcohol) and gelatin by a redox polymerization technique. They found that the crosslinked polymer has resulted in a high water imbibing macromolecular matrix with remarkable blood compatibility.

- **Biodegradable materials** In recent years, protein or oligopeptide immobilization on biodegradable polymers such as poly-L-lactic acid (PLLA) has been used in tissue engineering. It is difficult to transplant isolated cell in PLLA scaffold because cell attachment on PLLA is rather low due to its hydrophobicity [53]. One approach to solve this problem is to immobilize a biocompatible layer on the surface of the polymer to improve cell-material interactions. To covalently immobilize protein molecules on a chemically inert polymer such as PLLA, it is necessary to introduce some reactive groups such as hydroxyl (-OH), carboxyl (-COOH) or amino groups on the polymer surface. Many methods like plasma treatment in ammonia [54], plasma induced grafting polymerization [55], photo-induced grafting polymerization [56], and ozone oxidization [57] have been used to introduce the above reactive groups on polymer surfaces. Protein molecules can be subsequently immobilized using chemical methods such as carbodiimide chemistry [58] or sulfonyl chloride chemistry [59].

Ma et al. [60] studied covalent immobilization of gelatin or collagen type I on poly-L-lactic acid (PLLA) film surfaces, which was grafted with poly (hydroxyethyl methacrylate) (PHEMA) or poly(methacrylic acid) (PMAA). The results showed an opportunity to adapt the grafting strategy to a chosen biomacromolecule therefore to potentially improve the cellular interaction on synthetic biomaterials.

## **b) Synthetic polymers**

Synthetic carriers are the largest number of supports available for protein immobilization. This is due to their physical and particular protein and application. Some advantages of this type of carriers are their inertness to microbial attack, the degree of porosity and their chemical composition which can be achieved by either copolymerization of very different available monomers or by chemical modification of preformed polymers. The most important synthetic carriers for protein immobilization are described in the following sections.

**- *Polystyrene*** This polymer was the first synthetic polymer to be used for the immobilization of proteins. The main derivative is the polyamino-styrene, obtained from polystyrene by nitration and reduction of polystyrene. Due to its relative inertness for chemical coupling of protein molecules, this derivative has been activated by carbonylation [61]. Despite the rather high concentration of reactive groups on this type of carriers, the bound protein and coupling yields are usually poor due to the inherent hydrophobicity of the polymer matrix. This shortcoming has been bypassed by copolymerization with hydrophilic monomers, acrylic and methacrylic acids. The major advantage of polystyrene as protein carrier is its low cost and availability.

Nita et al. [62] studied the possibilities for some biomaterials obtainment based on styrene polymers and copolymers, with acrylic and methacrylic acid, methacrylamide, acrylonitrile and maleic anhydride. The obtainment of biocompatible composites is realized through the adsorption of protein, the collagen, onto the prepared macromolecular surfaces. They found that styrene copolymers with polar groups and controlled dimension size ( $<3 \mu\text{m}$ ) exhibit a better absorption capacity of proteins and therefore, a better biocompatibility in respect with polystyrene.

**- *Polyacrylate*** Acrylic polymers are among the most acid synthetic polymers in the field of protein immobilization. They have been used in enzyme coupling methods as well as in entrapment. Some of them, such as polyacrylates,

poly(hydroxyl alkyl methacrylates) and derivatives are available from commercial sources, which lead to their broad use in protein immobilization.

**- Polyacrylamide** Polyacrylamides and their derivatives are among the synthetic matrices most often employed for the immobilization of proteins due to their chemical structure, with hydrophilic character.

Because of the solubility of the linear polymers in water these polymers have to be insolubilized by cross-linking with bifunctional compounds. One of the most popular methods is identical to that employed for the preparation of gel used for electrophoresis, based on the free-radical polymerization of acrylamide in an aqueous solution containing a crosslinking agent, usually, N,N'-methylene bisacrylamide. Furthermore, polyacrylamide can also be obtained by irradiating a frozen monomer solution using as irradiation sources  $^{60}\text{Co}$ .

Polyacrylamide matrices have been largely used as an entrapment technique for enzymes. However, they can be activated by several methods for chemical coupling of proteins.

**- Vinyl and allyl polymers** Polymers are carriers with neutral and hydrophilic characteristics that can be obtained by chemical modification of polyvinyl alcohol, polyallyl alcohol or vinyl ether copolymers. Reactive carriers based on polyvinyl alcohol are obtained by crosslinking the soluble polyvinyl alcohol with terephthaldehyde and by reaction of this crosslinked polymer with 2-3,-amino-phenyl-1, 3-dioxolane followed by diazotization or with 2, 4, 6- trichloro-sym-triazine.

Auramescu et al. [8] described the immobilization of BSA as model protein onto cellular poly(ethylene vinyl alcohol) (EVAL) microfiltration membranes. They found that immobilization of proteins can be performed via covalent binding of their amino or acid groups by modification of the secondary alcohol groups of the vinyl alcohol segments.

**- Maleic anhydride-based polymer** Copolymers of maleic anhydride and ethylene are common supports for the immobilization of proteins. They allow the direct coupling of proteins by adsorption due to their highly negatively charge groups.

Neutralization of the negative charge can be accomplished by the addition of diamines during the immobilization procedure, which also acts as a crosslinking agent to produce a highly water-insoluble protein preparation.

### 3.6.2 Maleic anhydride copolymer

Maleic anhydride copolymers have already been applied for covalent protein immobilization. They allow the direct coupling of proteins by adsorption due to their highly negatively charged groups.

Moreover, the anhydride group is very reactive to primary amine group and slightly less reactive to alcohol. Studies on protein removal have shown that amino groups of proteins spontaneously react in neutral and mildly alkaline media with the anhydride groups to form amide bonds. Reaction scheme for protein coupling to maleic anhydride group is presented in **Figure 3.11**.

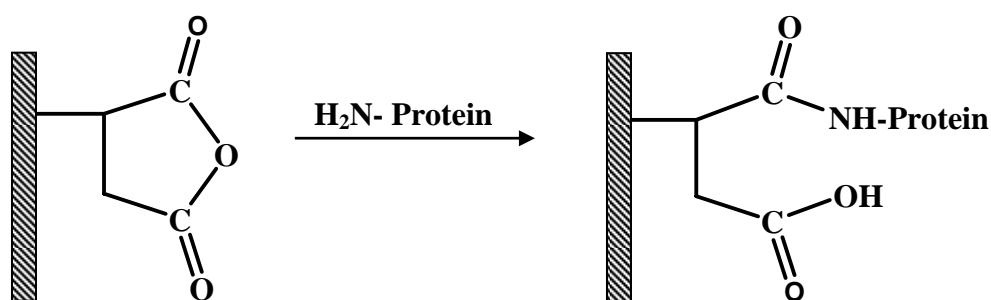


**Figure 3.11** Protein coupling to maleic anhydride surface. Primary amino linkages (NH<sub>2</sub>) on proteins attach the anhydride groups (left) forming covalent bond (right).

Furthermore, maleic anhydride (MAH) has properties that make it of particular interest for surface modification. It can be formed in such a way that anhydride group functionality is retained, which offers possibilities for subsequent chemical modification of the polymer.

The use of maleic anhydride as reactive group for protein binding study has appeared in many reports. Bovine Serum Albumin (BSA) is used as a model protein.

Ladaviere and coworkers [9] studied the covalent immobilization of BSA onto maleic anhydride-alt-methyl vinyl ether copolymers (MAMVE). The grafting reaction was shown in **Figure 3.12**.

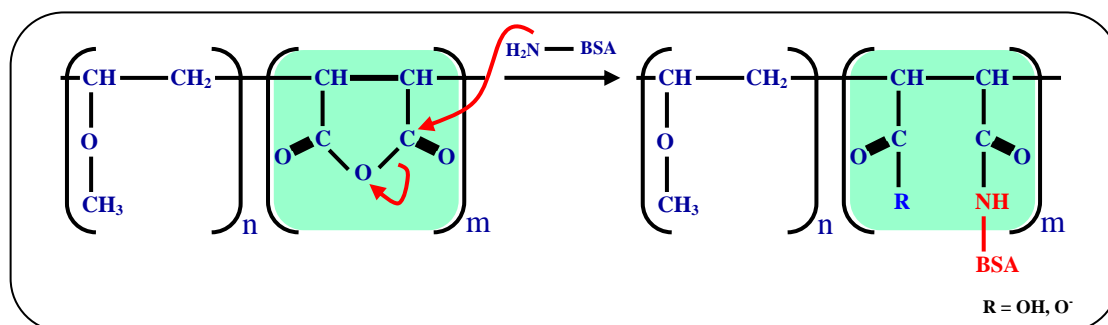


**Figure 3.12** Coupling reaction between the BSA molecule and the Maleic Anhydride-alt-Methyl Vinyl Ether copolymer or P(MAMVE).

From the result, it was found that the reaction was successfully achieved under aqueous conditions. The grafting reaction was shown to be controlled by attractive electrostatic interactions and so took place at a low salt concentration. Under these conditions, the covalent binding reaction was quite efficient, reproducible, and complete within 20 min. This study demonstrated that the immobilization of proteins in an aqueous medium could be an efficient process, despite the existing hydrolysis of the functional polymer by water molecule.

Liu and coworkers [10] studied the irreversible attachment of BSA to films of plasma-polymerized maleic anhydride.

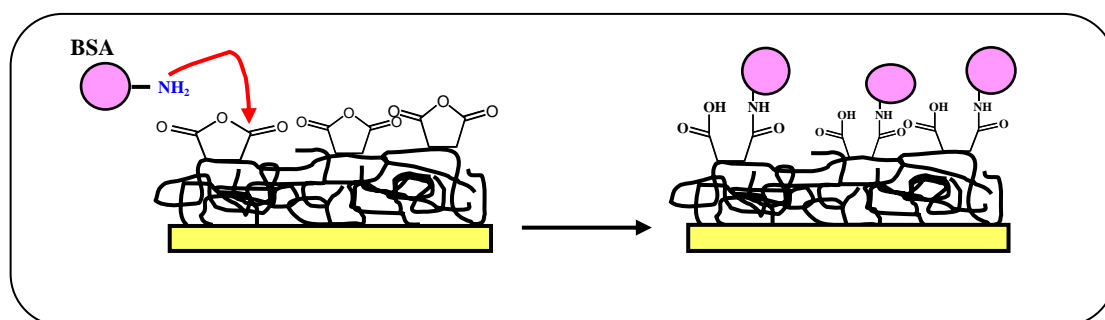


**Figure 3.13** Immobilization of proteins by covalent coupling of lysine residues in BSA with retained maleic anhydride functional groups in polymer.

They founded that BSA could be irreversibly bound to polymers made under pulse plasma conditions. And they speculated that BSA is being covalently bound to the polymer via the reaction of amino groups on lysine residues in BSA with the retained anhydride group functionality in the polymer, as can be seen in **Figure 3.13**.

Since the polyethylene-based support is resistant to solvents, this functionalized membrane offers an unlimited variety of organic synthesis routes for further modification.

### **3.6.3 Polyethylene graft Maleic Anhydride Film**

The modification of polyethylene through free-radical grafting maleic anhydride (MAH) in the presence of an initiator has received much attention over the past decades. The grafting of polyethylene has been successfully achieved using solution [63-64] and melt [65]. Surface grafting reactions induced by ultraviolet (UV) irradiation were also reported and concentrated mostly on modification of film [13, 66-69]. This method remains one of the fastest and most efficient methods for permanently modifying the surface properties. Moreover, the use of UV radiation offers an excellent alternative because of its simplicity and cleanness.

It was known that the amount of immobilized protein depends on the content of reactive groups on surface [70-73]. Therefore, two MAH-grafted PE copolymers, having different anhydride content on the surface, have been used in this thesis to evaluate comparatively the effectiveness of protein binding. They are a commercial MAH-grafted PE with 0.90 %wt MAH (Fusabond® E MB226D) and a home made PE-g-MAH sample, obtained by UV-photografting.

#### **3.6.3.1 Commercial Film (Fusabond® E MB226D)**

In the case of commercial sample, grafting of maleic anhydride onto olefin polymer was performed through reactive processing. It was found that purification was necessary for the removal of unreacted maleic anhydride in polymer mass [74]. Several purification methods have been proposed such as dissolution of sample in xylene followed by precipitation in acetone [75], soxhlet extraction with acetone [76]

and evaporation of the maleic anhydride in a vacuum oven at temperature above 100° C. In general, the hydrolysis of anhydride group could occur in the producing process. This led to the appearance of carboxylic acid on the graft copolymer film.

In earlier work, Bettini and Agnelli [74] reported that the PP-g-MAH sample, purified by dissolving in xylene and precipitation in acetone, was heat treated at 130° C for 24 h to convert the acid groups to anhydrides. Schmidt et al. [77] found that annealing of hydrolyzed polymer film at 120°C for 2 h led to a back-formation of the anhydride.

In the present work, in order to obtain the purified PE-g-MAH, Fusabond® E MB226D resin was refluxed in xylene and precipitated with acetone. After the purification, the film was prepared by using compression moulding. Then, the film was annealed in an oven to increase maleic anhydride content on the surface.

### 3.6.3.2 UV photografting

In this work, photografting technique was selected for preparing MAH-grafted PE film. It is known to be a useful technique for the modification and functionalization of polymeric materials due to its significant advantages: low cost of operation, mild reaction conditions, selectivity to absorb UV light without affecting the bulk polymer and permanent alteration of the membrane surface chemistry.

In classical method, photoinitiator and monomer are introduced at the same time onto PE surface. When the sample is irradiated, two mechanism can take place either abstraction of hydrogen atom from PE surface and then grafting or abstraction of hydrogen atom from monomer generating homopolymer.

Benzophenone (BP) is the most commonly used as photoinitiator. When BP is irradiated by UV, one electron in the highest occupied molecular orbital (HOMO) can absorb energy and excite to the lowest unoccupied molecular orbital (LUMO). This process therefore generates the semipinacol radicals by abstracting one hydrogen atom on PE surface and creates initiating sites on the film. Then the MAH monomer is grafted on the film. The reaction of MAH photografting is displayed in **Figure 3.14**. Although this technique has some advantages, for example, it is a continuous

production process and provides a uniform modification, there is a problem concerning the loss of monomer by formation of homopolymer.

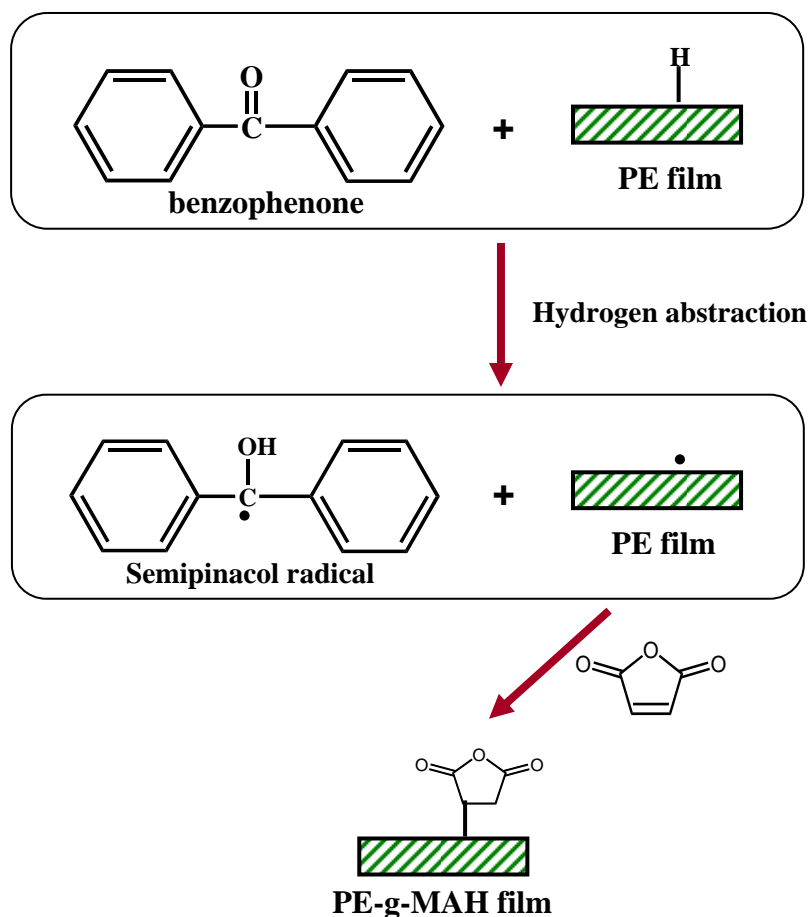


**Figure 3.14** Schematic reaction of MAH photografting.

Many previous works [11-13] showed that the degree of grafting depended on many factors in photografting process such as polymer substrates, monomer, concentration of photoinitiator, solvent, irradiation temperature, reaction time and the intensity of UV radiation. In this work, the effects of some principal factors including irradiation temperature, reaction time and the intensity of UV radiation were investigated. The intensity was varied by adjusting distance between UV lamp and sample under different radiation time. This led to a wide range of irradiation temperature.

## 3.7 Protein

### 3.7.1 Amino Acid

Proteins are composed of molecular building blocks called amino acids, an amino acid contains two functional groups, an amino group ( $-\text{NH}_2$ ) and a carboxylic acid group ( $-\text{COOH}$ ). In most of the amino acids found in proteins, the amino group, the carboxylic acid group and a hydrogen atom are bonded to a central carbon atom. Amino acids with this structure are called  $\alpha$ -(alpha)-amino acids (see **Figure 3.15**).

Different side groups (R) are attached to the center ( $\alpha$ ) carbon, giving each amino acid unique characteristics.

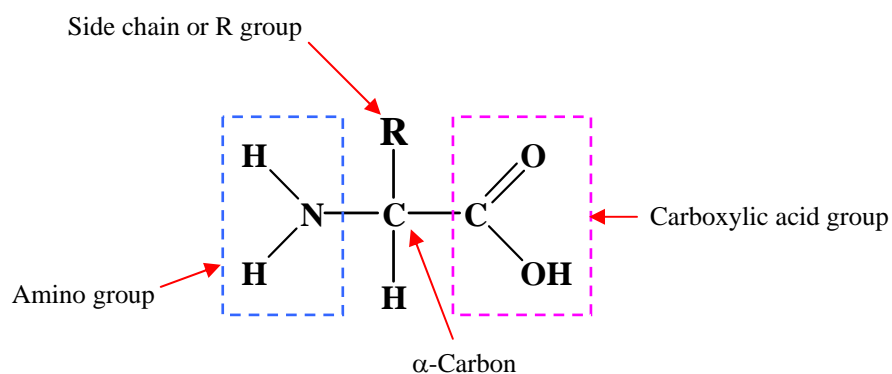


**Figure 3.15** General structure of  $\alpha$ -amino acid.

Amino acids are classified according to their side (R) groups. Nonpolar amino acids contain a hydrocarbon or aromatic side chain, which makes them hydrophobic. Polar amino acids are hydrophilic because their side (R) groups contain atoms such as  $-\text{OH}$  that are attracted to water. Some of the polar amino acids are acidic if the R contains a carboxylic acid group, and basic if the R group contains an amino group. The structures of the amino acids, their R side groups, common names, and their abbreviations (one or three letters) are listed in **Table 3.2**.

**Table 3.2** The 20 amino acids found in proteins

$\begin{array}{c} \text{H} \\   \\ \text{H}_3\text{N}^+ - \text{C} - \text{C} \begin{array}{l} \diagup \text{O} \\ \diagdown \text{O}^- \end{array} \\   \\ (\text{CH}_2)_3 \\   \\ \text{NH} \\   \\ \text{C}=\text{NH}_2 \\   \\ \text{NH}_2 \end{array}$ <p>Arginine (Arg / R)</p>	$\begin{array}{c} \text{H} \\   \\ \text{H}_3\text{N}^+ - \text{C} - \text{C} \begin{array}{l} \diagup \text{O} \\ \diagdown \text{O}^- \end{array} \\   \\ \text{CH}_2 \\   \\ \text{CH}_2 \\   \\ \text{C}=\text{O} \\   \\ \text{NH}_2 \end{array}$ <p>Glutamine (Gln / Q)</p>	$\begin{array}{c} \text{H} \\   \\ \text{H}_3\text{N}^+ - \text{C} - \text{C} \begin{array}{l} \diagup \text{O} \\ \diagdown \text{O}^- \end{array} \\   \\ \text{CH}_2 \\   \\ \text{C}_6\text{H}_5 \end{array}$ <p>Phenylalanine (Phe / F)</p>	$\begin{array}{c} \text{H} \\   \\ \text{H}_3\text{N}^+ - \text{C} - \text{C} \begin{array}{l} \diagup \text{O} \\ \diagdown \text{O}^- \end{array} \\   \\ \text{CH}_2 \\   \\ \text{C}_6\text{H}_4 \\   \\ \text{OH} \end{array}$ <p>Tyrosine (Tyr / Y)</p>	$\begin{array}{c} \text{H} \\   \\ \text{H}_3\text{N}^+ - \text{C} - \text{C} \begin{array}{l} \diagup \text{O} \\ \diagdown \text{O}^- \end{array} \\   \\ \text{CH}_2 \\   \\ \text{C}_8\text{H}_6\text{N} \\   \\ \text{H} \end{array}$ <p>Tryptophan (Trp / W)</p>
$\begin{array}{c} \text{H} \\   \\ \text{H}_3\text{N}^+ - \text{C} - \text{C} \begin{array}{l} \diagup \text{O} \\ \diagdown \text{O}^- \end{array} \\   \\ (\text{CH}_2)_4 \\   \\ \text{NH}_2 \end{array}$ <p>Lysine (Lys / L)</p>	$\begin{array}{c} \text{H} \\   \\ \text{H}_3\text{N}^+ - \text{C} - \text{C} \begin{array}{l} \diagup \text{O} \\ \diagdown \text{O}^- \end{array} \\   \\ \text{H} \end{array}$ <p>Glycine (Gly / G)</p>	$\begin{array}{c} \text{H} \\   \\ \text{H}_3\text{N}^+ - \text{C} - \text{C} \begin{array}{l} \diagup \text{O} \\ \diagdown \text{O}^- \end{array} \\   \\ \text{CH}_3 \end{array}$ <p>Alanine (Ala / A)</p>	$\begin{array}{c} \text{H} \\   \\ \text{H}_3\text{N}^+ - \text{C} - \text{C} \begin{array}{l} \diagup \text{O} \\ \diagdown \text{O}^- \end{array} \\   \\ \text{CH}_2 \\   \\ \text{C}_3\text{H}_3\text{N}_2 \end{array}$ <p>Histidine (His / H)</p>	$\begin{array}{c} \text{H} \\   \\ \text{H}_3\text{N}^+ - \text{C} - \text{C} \begin{array}{l} \diagup \text{O} \\ \diagdown \text{O}^- \end{array} \\   \\ \text{CH}_2 \\   \\ \text{OH} \end{array}$ <p>Serine (Ser / S)</p>
$\begin{array}{c} \text{H}_2 \\   \\ \text{C} \\ / \quad \backslash \\ \text{H}_2\text{C} \quad \text{CH}_2 \\   \quad \quad   \\ \text{H}_2\text{N}^+ - \text{C} - \text{C} \begin{array}{l} \diagup \text{O} \\ \diagdown \text{O}^- \end{array} \end{array}$ <p>Proline (Pro / P)</p>	$\begin{array}{c} \text{H} \\   \\ \text{H}_3\text{N}^+ - \text{C} - \text{C} \begin{array}{l} \diagup \text{O} \\ \diagdown \text{O}^- \end{array} \\   \\ \text{CH}_2 \\   \\ \text{CH}_2 \\   \\ \text{COOH} \end{array}$ <p>Glutamic Acid (Glu / E)</p>	$\begin{array}{c} \text{H} \\   \\ \text{H}_3\text{N}^+ - \text{C} - \text{C} \begin{array}{l} \diagup \text{O} \\ \diagdown \text{O}^- \end{array} \\   \\ \text{CH}_2 \\   \\ \text{COOH} \end{array}$ <p>Aspartic Acid (Asp / D)</p>	$\begin{array}{c} \text{H} \\   \\ \text{H}_3\text{N}^+ - \text{C} - \text{C} \begin{array}{l} \diagup \text{O} \\ \diagdown \text{O}^- \end{array} \\   \\ \text{H} - \text{C} - \text{OH} \\   \\ \text{CH}_3 \end{array}$ <p>Threonine (Thr / T)</p>	$\begin{array}{c} \text{H} \\   \\ \text{H}_3\text{N}^+ - \text{C} - \text{C} \begin{array}{l} \diagup \text{O} \\ \diagdown \text{O}^- \end{array} \\   \\ \text{CH}_2 \\   \\ \text{SH} \end{array}$ <p>Cysteine (Cys / C)</p>
$\begin{array}{c} \text{H} \\   \\ \text{H}_3\text{N}^+ - \text{C} - \text{C} \begin{array}{l} \diagup \text{O} \\ \diagdown \text{O}^- \end{array} \\   \\ \text{CH}_2 \\   \\ \text{CH}_2 \\   \\ \text{S} \\   \\ \text{CH}_3 \end{array}$ <p>Methionine (Met / M)</p>	$\begin{array}{c} \text{H} \\   \\ \text{H}_3\text{N}^+ - \text{C} - \text{C} \begin{array}{l} \diagup \text{O} \\ \diagdown \text{O}^- \end{array} \\   \\ \text{CH}_2 \\   \\ \text{CH} \\ / \quad \backslash \\ \text{CH}_3 \quad \text{CH}_3 \end{array}$ <p>Leucine (Leu / L)</p>	$\begin{array}{c} \text{H} \\   \\ \text{H}_3\text{N}^+ - \text{C} - \text{C} \begin{array}{l} \diagup \text{O} \\ \diagdown \text{O}^- \end{array} \\   \\ \text{CH}_2 \\   \\ \text{C}=\text{O} \\   \\ \text{NH}_2 \end{array}$ <p>Asparagine (Asn / N)</p>	$\begin{array}{c} \text{H} \\   \\ \text{H}_3\text{N}^+ - \text{C} - \text{C} \begin{array}{l} \diagup \text{O} \\ \diagdown \text{O}^- \end{array} \\   \\ \text{HC} - \text{CH}_3 \\   \\ \text{CH}_2 \\   \\ \text{CH}_3 \end{array}$ <p>Isoleucine (Ile / I)</p>	$\begin{array}{c} \text{H} \\   \\ \text{H}_3\text{N}^+ - \text{C} - \text{C} \begin{array}{l} \diagup \text{O} \\ \diagdown \text{O}^- \end{array} \\   \\ \text{CH} \\ / \quad \backslash \\ \text{CH}_3 \quad \text{CH}_3 \end{array}$ <p>Valine (Val / V)</p>

A peptide bond, the link between amino acids, is formed between the carboxylic group of one amino acid and the amino group of another. In the reaction, a molecule of water is released, as can be seen in **Figure 3.16**.

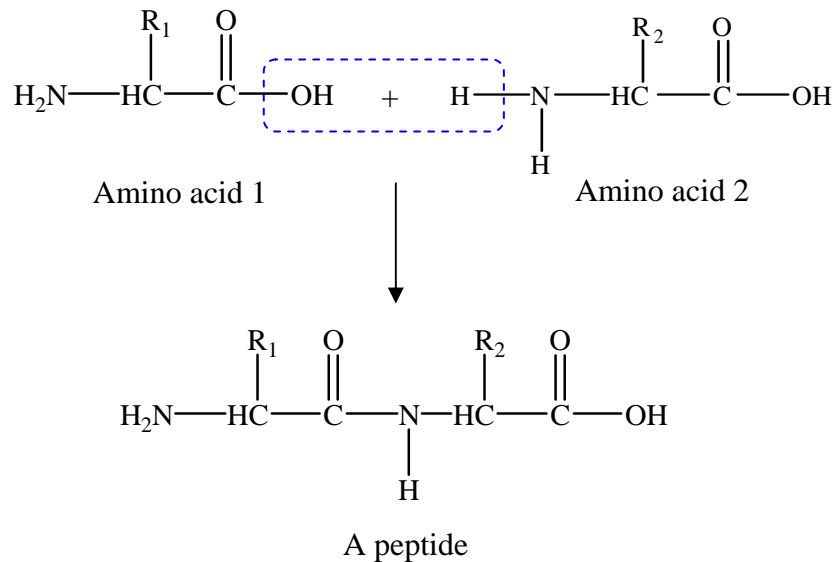


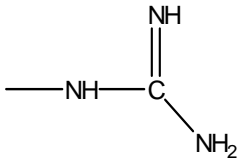
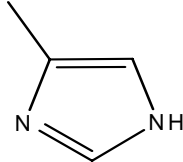
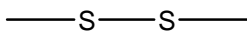
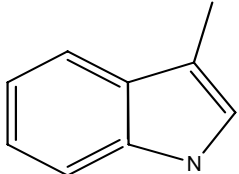
**Figure 3.16** The structure of a peptide.

The linking of two or more amino acids forms a peptide. Two amino acids are linked by a peptide bond in a dipeptide. In a tripeptide, there are three amino acids linked by peptide bonds. In any peptide, the amino acid on one end that has a free amino group (-NH<sub>2</sub>) is called the N-terminus. On the other end of the peptide, there is an amino acid with a free carboxylic group (-COOH) called the C-terminus.

### 3.7.2 Reactive Groups of Protein

Proteins are heteropolymers built up from more than 20 types of monomer units of amino acid residues. **Table 3.3** summarizes the residues of amino acids that have functional groups in the side chain suitable for linking to a support matrix.

**Table 3.3** Reactive residues of protein

-NH <sub>2</sub>	<i>t</i> -Amino of L-lysine (L-Lys) and N-terminus amino group
-SH	Thiol of L-cysteine (L-Cys)
-COOH	Carboxyl of L-aspartate (L-Aps) and L-glutamate (L-Glu) and C-terminus carboxyl group
	Phenolic of L-tyrosine (L-Tyr)
	Guanidino of L-arginine (L-Arg)
	Imidazole of L-histidine (L-His)
	Disulfide of L-cystine
	Indole of L-tryptophan (L-Trp)
-CH <sub>3</sub> -S-	Thioether of L-methionine (L-Met)
-CH <sub>2</sub> OH	Hydroxyl of L-serine (L-Ser) and L-threonine (L-Thr)

### 3.7.3 Coupling Reaction

The coupling of protein molecules to solid supports involves mild reactions between amino acid residues of the protein and several groups of functionalized support.

Several types of coupling reactions can be used, and most of the common covalent coupling reactions involve coupling through protein amino groups, thiol groups, carboxylic groups, or aromatic rings of L-tyrosine and L-histidine. The major classes of coupling reactions used for the immobilization of proteins are:

1. Diazotization
2. Amide (peptide) bond formation
3. Alkylation and arylation
4. Schiff 's base formation
5. Ugi reaction
6. Amidination reaction
7. Thiol-disulfide interchange reaction
8. Mercury-enzyme interaction
9.  $\gamma$ -Irradiation induced coupling

### *Amide (peptide) bond formation*

The amide bond method is based on the formation of amide (peptide) bonds, or similar bonds, between the protein and a water-insoluble support by the application of the peptide synthesis technique. Several procedures are available, depending on the different derivatized solid matrices.

The common mechanism feature in the peptide bond formation method is the attack of the nucleophilic group (amino, hydroxyl, thiol) of protein at an activated functional group on the support. These nucleophile are most effective in their unprotonated forms ( $-\text{NH}_2$ , ,  $-\text{S}^-$ ) at pH value above their pKa values. Owing to the irreversible denaturation of the protein at high pH, however, these reactions are commonly carried out at intermediate pH values (7.5-8.5) and at low temperature (4°C)

In this work, the acid anhydride derivative was selected to react with amino groups of protein (see **Figure 3.11**). Carboxylic acid groups are formed (in addition to the amide linkages) by cleavage of anhydride rings; these do not react with functional groups of protein but are ionized in the aqueous solutions spontaneously by  $\text{OH}^-$  ion, that is, at higher pH values, generating free carboxy groups with a highly negative

charge. The negative charge gives undesirable ionogenic properties to the preparation and may unfavorably affect the protein structure. To overcome this disadvantage it is usual to neutralize some of the negatively charged species by the addition of diamine during the immobilization procedure [78].

## 3.8 Protein Extraction and Characterization

### 3.8.1 Protein Extraction

For protein isolation and purification in general, the materials including protein are fractionated mainly by extraction method. The extraction of protein from a solid source often involves a compromise between recovery and purity. Optimization of extraction conditions should favor the release of the desired protein and leave difficult-to-remove contaminants behind.

To arrive at a suitable composition for the extraction medium, the conditions in which the protein of interest is suitable must first be studied. The final choice is usually a compromise between maximum recovery and maximum purity. The following factors have to be taken into consideration:

***pH*** Normally the pH value chosen is that of maximum activity of the protein. However, it should be noted that this is not always the pH that gives the most efficient extraction is necessarily the pH of maximum stability.

***Buffer salts*** Most proteins are maximally soluble at moderate ionic strength, 0.05 to 0.1, and these values are chosen if the buffer capacity is sufficient. Suitable buffer salts are given in **Table 3.4**. An acceptable buffer capacity is obtained within one pH unit from the pKa values given. The proteins as such also act as buffers, and the pH should be checked after the addition of large amounts of proteins to a weakly buffered solution. Some extraction doses not give rise to acids and bases and thus do not need a high buffer capacity. In other cases, this might be necessary and occasional control of the pH value of an extract is recommended.

**Table 3.4** Buffer salts used in protein work

Buffer	pK <sub>a</sub> -values	Properties
Sodium acetate	4.75	
Sodium bicarbonate	6.50; 10.25	
Sodium citrate	3.09; 4.75; 5.41	Binds Ca <sup>2+</sup>
Ammonium acetate	4.75; 9.25	Volatile
Ammonium bicarbonate	6.50; 9.25; 10.25	Volatile
Tris-chloride	8.21	
Sodium phosphate	1.5; 7.5; 12.0	
Tris-phosphate	7.5; 8.21	

The buffer solution was commonly used in biochemistry such as phosphate buffer saline (PBS). It is a salty solution containing sodium chloride, sodium phosphate and potassium phosphate. PBS has many uses because it is isotonic and non toxic to cell. It is used as a cellular cleaning solution. Furthermore, the protein solubility was adversely affected by the addition of sodium chloride (NaCl). It seems reasonable to suggest that the shift in isoelectric point as a result of salt addition may be one of the factors affecting protein solubility. Proteins with a lower isoelectric point would not experience the degree of electrostatic repulsion as higher isoelectric point proteins. Less electrostatic repulsion would mean less solubility.

**Detergents** In many extractions, the desired protein is bound to membranes or particles or is aggregated due to its hydrophobic character. In this case, the hydrophobic interactions should be reduced by using detergent. Some of the commonly used detergents are listed in **Table 3.5**. Several of them do not denature globular proteins or interfere with their biological activity. Others, such as sodium dodecyl sulfate (SDS), will do that. Quite often it is not necessary to continue using a detergent in the buffer after the first step in the purification, so its use is restricted to the extraction medium.

**Table 3.5** Detergents used for solubilization of proteins

Detergent	Ionic Character	Effect on protein	Critical micelle Concentration (%w/v)
Triton X-100	Nonionic	Mild, nondenaturing	0.02
Nonidet P-40	Nonionic		
Lubrol PX	Nonionic		0.006
Octyl glucoside	Nonionic		0.73
Tween 80	Nonionic		0.002
Sodium deoxycholate	Anionic		0.21
Sodium dodecyl sulfate	Anionic	Strongly denaturing	0.23
3-[(3-Cholamidopropyl) dimethyl amino] propanesulfonic acid	Zwitterionic		1.4

Except sodium dodecyl sulfate (SDS), most surfactants are used for protein stabilization, including polymers, polyols, nonionic and anionic surfactants. The mechanisms include: binding to the proteins and reducing the proteins' available hydrophobic surface areas, therefore decreasing the proteins' self-association and any deleterious interactions with non-specific hydrophobic surfaces; preventing surface-induced deactivation of proteins; inhibiting aggregation and precipitation [79].

**Reducing agents** The redox potential of the cytosol is lower than that of the surrounding medium where atmospheric oxygen is present. Intracellular proteins often have exposed thiol groups, and these might become oxidized in the purification process. Thiol groups can be protected by reducing agents such as 1,4-dithioerythritol (DTE), 1,4-dithiothreitol (DTT), or mercaptoethanol (see **Table 3.6**). Normally 10 to 25 mM concentrations are sufficient to protect thiols without reducing internal disulfides. In other cases, a higher concentration might be need [80].

**Table 3.6** Reducing agents

Agent	Structure
Mercaptoethanol	HS-CH <sub>2</sub> -CH <sub>2</sub> -OH
1,4-Dithioerythritol	$  \begin{array}{c}  \text{CH}_2\text{SH} \\    \\  \text{H} - \text{C} - \text{OH} \\    \\  \text{H} - \text{C} - \text{OH} \\    \\  \text{CH}_2\text{SH}  \end{array}  $
1,4-Dithiotreitol	$  \begin{array}{c}  \text{CH}_2\text{SH} \\    \\  \text{H} - \text{C} - \text{OH} \\    \\  \text{HO} - \text{C} - \text{H} \\    \\  \text{CH}_2\text{SH}  \end{array}  $

Many studies showed that the water-soluble proteins in dry NR were extracted by eluting pieces of dry NR in PBS or SDS solution.

In 1994, Alenius et al. [81] extracted latex proteins with PBS in continuous shaking condition at room temperature overnight. The eluates were then decanted and added another latex pieces. The mixtures were incubated in continuous shaking condition overnight. After centrifugation, the supernatants were collected and filtered through a 0.45  $\mu\text{m}$  membrane. The extracts were dialyzed and then subsequently freeze dried and stored at 4°C for protein determination.

Hasma H. [82] extracted protein from rubber particles. Rubber particles (RP) were isolated from fresh latex or high ammonia latex concentrate by ultracentrifugation. The isolated RP were rinsed with water two to three times before dispersing them in water, followed by dispersing them in 2% SDS. The dispersed RP were stirred for some time and left to stand in the cold overnight.

From the results, it was found that a SDS solution could extract some membrane components amounting to about 0.3% of the rubber which contained 10% nitrogen.

In the study of Rogero et al. [83], the protein content of the NR films obtained by casting method was made using 1g of small pieces (0.5x0.5 cm) and extracted with phosphate buffer solution (pH 7) in shaking water bath at 37°C for 2 h.

### 3.8.2 Protein Precipitation

Precipitation of a protein in an extract is required to concentrate proteins and also to separate protein from water soluble substances which may interfere with the determination. This process may be achieved by adding salts, organic solvents, or organic polymers, or by varying the pH or temperature of the solution. The most commonly used precipitation agents are listed in **Table 3.7**.

**Table 3.7** Precipitation agents

Agent	Type	Properties
Ammonium sulfate	Salt	Easily soluble, stabilizing
Sodium sulfate	Salt	
Ethanol	Solvent	Flammable, risk of denaturation
Acetone	Solvent	Flammable, risk of denaturation
Polyethylene glycol	Polymer	Uncharge, unflammable

Assay to quantitate proteins are susceptible to interference by nonproteinaceous substances present in the test sample [84-87]. To minimize interference to the assay, a purification step prior to the protein assay could be carried out. Many interfering substances can be precipitating proteins with trichloroacetic acid (TCA) 5-10% in cooled acetone and led to a large number of samples precipitation of the proteins [84]. The protein precipitation is frequently preferred because of its simplicity and rapidity. By this approach, the precipitated proteins are recovered by centrifugation while most of the soluble nonproteins that might interfere with the assay are discarded with the supernatant. In addition, the acid precipitation of proteins is useful to concentrate proteins. Organic solvents promote the precipitation of proteins due to the decrease in

water activity in the solution as the water is replaced by organic solvent. They have been widely used as precipitation agents, especially in the fractionation of serum proteins.

The principle causes of aggregation are likely to be electrostatic and dipolar van der Waals forces, similar to those occurring in the salting-in range in the absence of organic solvent. Hydrophobic attractions are less involved because of the solubilizing influence of the organic solvent on these areas. It has been found that precipitation occurs at lower organic solvent concentration at around the isoelectric points of the proteins, which supports the suggestion that the aggregation is similar to that occurring in isoelectric precipitation. A two dimensional representation of proteins in a water/ organic solvent mixture is shown in **Figure 3.17**. Here aggregation is occurring by interactions between opposite-charged areas on the protein surface.

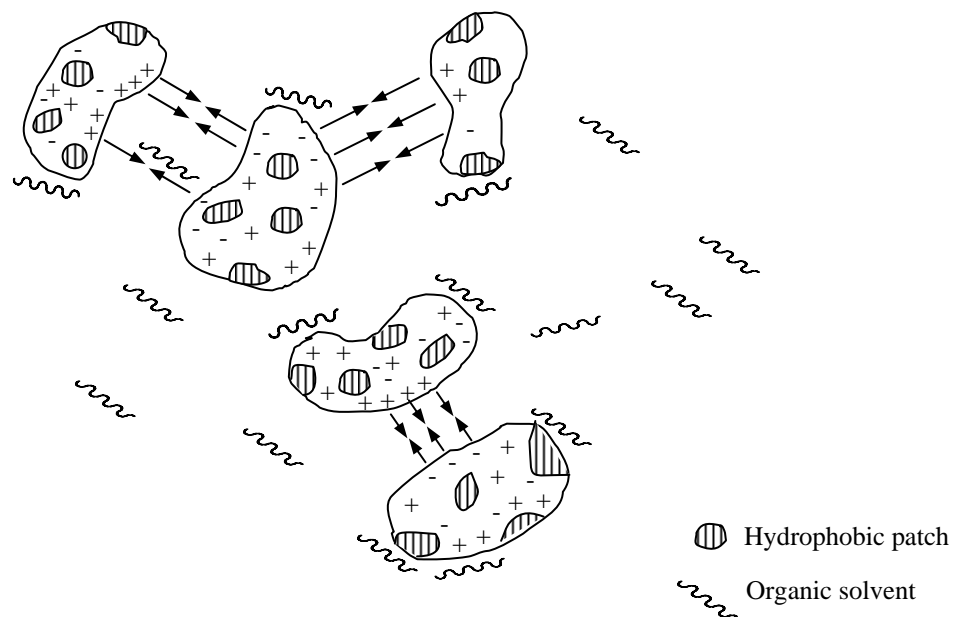


**Figure 3.17** Aggregation of proteins by interactions in an aqueous-organic solvent mixture.

Low temperature during the precipitation operations is often necessary to avoid protein denaturation. The addition of an organic solvent decreases the freezing point of the solution and temperatures below 0°C can be used. By redissolving the precipitated proteins in a smaller volume of solvent than that of the original sample, a

concentration effect is achieved. Concentrating protein in this manner is certainly more convenient than freeze-drying or centrifugal evaporation. In the alternative situation where protein concentration is too high, the precipitate can be dissolved in a larger volume of Lysis solution (mixture of urea, Triton<sup>®</sup> X-100 and 2-mercaptoethanol) to dilute it to a concentration that falls within the calibrated range of the protein assay.

### **3.8.3 Lyophilization (Freeze-Drying) Process**

The residual water in protein precipitate can be removed by Lyophilization or freeze drying. Freeze drying can be defined as the drying of a substance by freezing it and removing a proportion of any associated solvent by direct sublimation from the solid. Water can be transited through three phases. During lyophilization, the temperature and pressure are controlled to make sublimation instead fusion or vaporization occur. In principle, lyophilization is split into three separate stages: freezing, primary drying, and secondary drying. Freezing is to immobilize the product being freeze dried. The product structure, size and shape are fixed after freezing. Primary drying is to remove the free moisture that has been frozen. Secondary drying is to desorpt the bound moisture.

### **3.8.4 Protein Characterization**

Various techniques are used to characterize protein in terms of their molecular mass, chemical structure and composition.

#### **3.8.4.1 Sodium Dodecyl Sulfate Polyacrylamide Gel Electrophoresis (SDS-PAGE)**

SDS-PAGE is the most often used electrophoresis. First, SDS and a reducing agent such as 2-mercaptoethanol are added on a weight ratio basis, and temperature is elevated to over 100°C to denature the proteins. The denatured proteins are wrapped by SDS molecules. With the discontinuous buffer system, the proteins are mainly separated

according to sizes of proteins regardless of the charges. It can separate proteins from around 10000 to 300000 molecular weights by varying pore sizes of the gels. The pore sizes of the gels can be changed by changing the acrylamide gel, cross-linker and bisacrylamide concentration.

SDS-PAGE is commonly used for assessing purity and as a tool to determine the molecular weight by comparing the unknown sample with the known protein standards. SDS-PAGE can be used as a routine analysis of proteins over time during stability studies, because of the simple interpretation of the results in terms of the apparent molecular weights. This allows the detection of proteolytic degradation and the development of covalent aggregates, either reducible or non-reducible. Because the protein samples in SDS-PAGE are denatured, its application in detecting conformational change is limited until the proteolytic samples are used. SDS-PAGE has also limited resolving power unless a two-dimensional gel is used.

#### **3.8.4.2 Fourier Transform Infrared Spectroscopy (FTIR)**

The most informative IR bands for protein analysis are amide I (1620-1700  $\text{cm}^{-1}$ ), amide II (1520-1580  $\text{cm}^{-1}$ ) and amide III (1220-1350  $\text{cm}^{-1}$ ). Amide I is the most intense absorption band in proteins. It consists of stretching vibration of the C=O (70-85%) and C-N groups (10-20%). The exact band position is dictated by the backbone conformation and the hydrogen bonding pattern. Amide II is more complex than Amide I. Amide II is governed by in-plane N-H bending (40-60%), C-N (18-40%) and C-C (10%) stretching vibrations. Amide III bands are not very useful [88].

FTIR only need small amounts of proteins (1mM). It can detect the secondary structure ( $\alpha$  helix,  $\beta$  sheet,  $\beta$  turn and disordered structure) in a variety of physical states (solid, vapor, liquid, semi-solid). It's easy to operate. And IR are sensitive enough to detect conformational changes in proteins induced by freeze-drying, pressure, moisture and heat. In total, the KBr compression technique, the baseline subtraction and the distortion of peak intensity and area confer inaccuracy to the exact percentage of  $\alpha$ -helix and  $\beta$ -sheet [89].

### **3.8.4.3 CHN Elemental Microanalysis**

The technique used for the determination of CHN is based on the quantitative “dynamic flash combustion” method. Under optimum conditions even thermally resistant substances are completely oxidized. The resulting mixture is directed to the chromatographic column where the individual components are separated and eluted as Nitrogen (N<sub>2</sub>), Carbondioxide (CO<sub>2</sub>) and Water (H<sub>2</sub>O). All results for elemental analyses are calculated based on a known value of a standard by using the K value factors calculation. This K value is determined by analyzing an organic standard of a known elemental composition. The determination of the mass percentage of CHN elements in sample is based upon the direct weight of the material sample. Therefore, it is very important that samples are dry and free of foreign substances.

## **3.9 Protein Concentration Determination**

The methods used in protein quantification could be cause of variation of protein level. Several spectroscopic methods are commonly used in protein determination such as the absorbance assay at 280 nm, the Lowry assay, the Bicinchoninic acid (BCA) and the Bradford assay.

### **3.9.1 Absorbance Assay at 280 nm ( $A_{280}$ )**

The  $A_{280}$  is a rapid method of protein content analysis in a solution. This assay is based on the absorbance at 280 nm of tyrosine, phenylalanine, and tryptophan residues in sample solution. If sample solution has no these residues, it will be undetectable. This assay is adequate for crude protein mixture [90].

### **3.9.2 Lowry Assay**

The Lowry assay is a widely used quantitative assay of protein in solution. This assay uses the Folin-Ciocalteu phenol reagent as a reagent for protein determination. This assay has broad absorption peaks in red portion of visible spectrum (600 to 800

nm). The absorbance of unknown sample is read by comparison with a protein standard curve [84, 90-91].

### 3.9.3 Bicinchoninic Acid (BCA)

The BCA is a new protein measurement method based upon an alternative detection reagent. The reagent is bicinchoninic acid, a weak acid composed of two carboxylated quinoline rings. The BCA assay relies on two reactions. First, the peptide bonds in protein reduce  $\text{Cu}^{2+}$  ions from the cupric sulfate to  $\text{Cu}^{1+}$ . The amount of  $\text{Cu}^{2+}$  reduced is proportional to the amount of protein present in the solution. Next, two molecules of bicinchoninic acid chelate with each  $\text{Cu}^{1+}$  ion, forming a purple-colored product that strongly absorbs light at a wavelength of 562 nm [92].

### 3.9.4 Bradford Assay

The Bradford assay is a dye-binding method of protein determination in solution. This method uses the Coomassie Brilliant Blue G-250 for binding to proteins. The binding causes a shift in the absorption maximum of the dye from 465-595 nm and an increase in absorption at 595 nm. The absorbance of unknown sample is compared with a protein standard curve [85, 90]. This method has been utilized for quick and sensitive detection. The staining reaction completes within 1 min and the color is stable for 30 min. The protein detection range is from 10  $\mu\text{g/ml}$  to 2000  $\mu\text{g/ml}$  by standard method, and is from 0.1  $\mu\text{g/ml}$  to 50  $\mu\text{g/ml}$  by micro method.

#### 3.9.4.1 Nature of the Change States of the Dye

In order to understand the nature of the protein-dye interaction, knowledge of the molecular structure of the various dye species would be helpful, especially with regard to sites of protonation of the dye molecule, as shown in **Figure 3.18**.

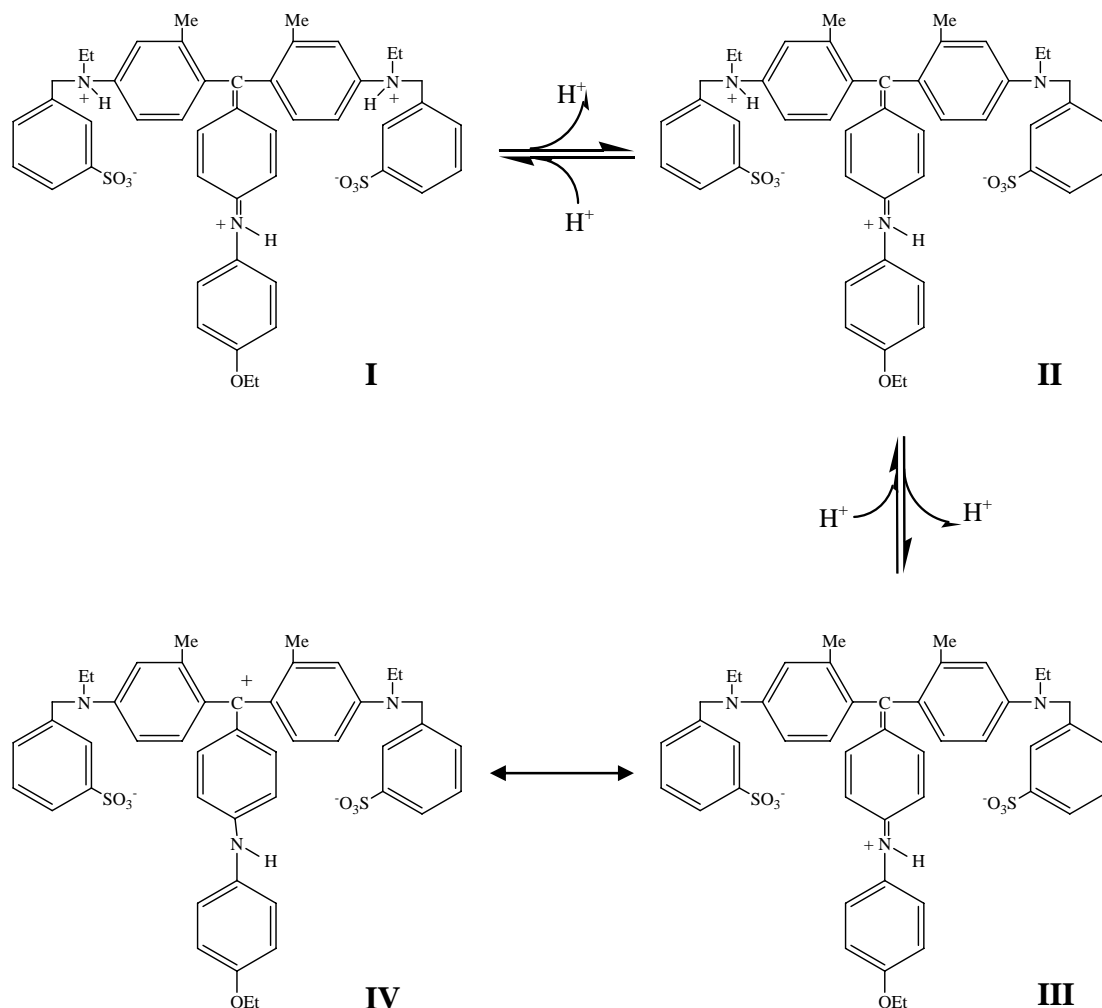


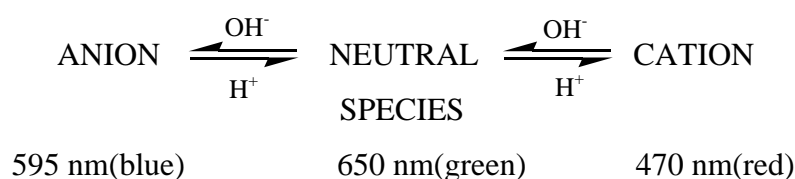
**Figure 3.18** Resonance forms of free ionic forms of CBBG. Red form, structure I; green form, structure II; blue forms, structure III and IV.

Beginning with the most protonated (red) form of the dye, it seems likely that neither of the sulfonate groups would be protonated (see **Figure 3.18**; structure I). Protonation or deprotonation of the dye molecule perturbs the conjugated double bond system, as observed from the spectral shifts of the absorbance maxima, but would not be the case with sulfonate protonation or deprotonation since the conjugated system would not be affected. It is also probable that the pKa of the sulfonic acid groups is too low for them to be involved in the protonations observed at low pH, given that the pKa of toluene sulfonic acid, for example, is about -1. The sulfonate groups will therefore be excluded from further consideration.

Because of the intrinsic structure of the dye, the fully protonated (red) form of the molecule must be that shown as structure I in **Figure 3.18**. Other resonance forms are also possible, but the main contributor is probably the form shown. Consideration of pKa (0.85) of diphenylamine [93] indicates that in the dye molecule the diphenylamine nitrogen is not likely to be doubly protonated positive charge at low pH. Successive protons are therefore probably lost from the two identical N, N-disubstituted aniline groups as the pH is raised to yield the blue form of the molecule (structure III of **Figure 3.18**). This loss of protons produces successively the “green” form (structure II of **Figure 3.18**, wavelength maximum 650 nm) and then the blue form (wavelength maximum 595 nm).

The three different absorbance maxima (wavelength at 650, 470 and 595 nm) of dye reagent protein mixture correspond to the three species of dye present: the doubly protonated, positively charged species absorbing at 470 nm, the singly protonated neutral species at 650 nm and the dye-protein complex at 595 nm. These forms of the Coomassie brilliant blue dye are present in equilibrium at the usual acidic pH of the assay (its pH-dependent color changes). When increasing of pH value, the color changes were observed from red to blue [87, 94].

Based on the identical absorbance maxima of the dye-protein complex and the dye ion, it can be concluded that the bound dye species is in fact the dye anion. The equilibrium shown below is forced to the left as the anion is bound by protein [87]:



Chial and coworker studied the change forms of free dye present at the usual acidic pH of the assay [94]. They found that as the pH was raised a reddish ionic form of the dye ( $\lambda_{\text{max}} = 470 \text{ nm}$ ) is replaced by a greenish dye form ( $\lambda_{\text{max}} = 650 \text{ nm}$ ) in the vicinity of pH 1. Further pH elevation showed another shift to blue dye form ( $\lambda_{\text{max}} = 590 \text{ nm}$ ) at about pH 2. The blue species remains the predominant dye form present in the pH range from 3 to 11. It was also supposed that CBBG dye exists as

two species, usually described as red and blue forms [95]. However, the data of this study suggest that the bound dye species has an absorbance maximum almost exactly intermediate between the blue (590 nm) and green (650 nm) species. The shift in absorbance maximum of 30 nm can easily be accounted for by a conformational shift of the dye on protein binding with resulting change in the planarity of the conjugated ring systems [94].

#### **3.9.4.2 Functional and Structural Requirements of Protein for Dye Binding**

The assay's specificity for protein is demonstrated by its lack of response to a wide range of chemical classes, including a diversity of nitrogenous compounds. The greatest response (by eightfold) was given by poly-L-arginine, followed by the aromatic and other basic polyamino acids (**Table 3.8**). The low reactivity of poly-L-lysine [96] is not compatible with the model of Fazekas de St. Groth et al. [97]. Furthermore, dye response to the uncharged aromatic polyamino acids demonstrates that nonelectrostatic interactions must play a role in Coomassie blue dye binding.

**Table 3.8** Dye-binding responses to polymeric L-amino acids

Polymeric amino acid	Molecular weight	Mean blank corrected absorbance (595 nm)	Relative response <sup>a</sup>
poly(Arg) <sup>b</sup>	40,000	4.033	36.0
poly(Tyr) <sup>c</sup>	100,000	0.531	4.7
poly(Trp) <sup>c</sup>	5,000	0.491	4.4
poly(His)	11,000	0.472	4.2
poly(Phe)	15,000	0.215	1.9
poly(Lys, Ala)			
100, 0	35,000	0.112	1.0
80, 20 <sup>d</sup>	38,000	0.028	0.3
46, 54 <sup>d</sup>	37,000	0.001	0.0
0, 100 <sup>c</sup>	25,000	0.000	0.0
poly(Gly)	6,000	0.000	0.0
poly(Asn)	9,000	0.000	0.0
poly(Asp)	20,000	0.000	0.0

*Note.* Samples are aqueous, 1.0 mg/ml unless otherwise stated.

<sup>a</sup> Compared to poly(lysine)

<sup>b</sup> sample was diluted to 125 µg/ml to bring value in range. The value shown is dilution corrected.

<sup>c</sup> Dissolved in DMSO, 1.0 mg/ml.

<sup>d</sup> Random copolymers of L-alanine and L-lysine, by molar ratio.

Free L-amino acids (arginine, histidine, lysine, tryptophan, alanine, glycine, asparagines and aspartic acid) and functional group moieties corresponding to the reactive polypeptids were assayed. None of these compounds gave a significant color response at concentration equivalent to the polyamino acid functional group concentration (595 nm mean blank corrected absorbance  $\leq$  0.006 AU). A molecular weight threshold has been suggest for the binding of CBBG dye in both the Bradford

system [95] in staining electrophoretic gels [98-99] Since polyglycine produced no dye response, the peptide chain alone cannot be responsible for dye binding. It was concluded that a compound must have both a macromolecular form and an active basic or aromatic functional group in order to bind with the CBBG dye anion. Furthermore, the Bradford assay will be most responsive to arginine-rich proteins.

### 3.9.4.3 Interferences

An important drawback of the Bradford method stems from its variation in response to different proteins, as discussed elsewhere [100]. For any given protein, however, further discrepancies may arise from nonprotein interferences that produce protein overestimation, underestimation, and a reduction of the linear response range. These sources of interference are best explained from the knowledge of the ionic dye species involved.

Overestimation of protein will occur when a nonprotein produces a 595 nm absorption that is not compensated for dye the solvent-dye blank. Proteins appear to be the only compounds capable of generating the dye anion at the assay pH. However, a number of compounds are capable of favoring stabilization of the neutral species. Since the bandwidth of the 650 nm neutral species produces strong absorption at 595 nm, this stabilization does indirectly cause interference.

Underestimation may result from factor reducing dye binding. In addition to stabilizing the neutral dye species, some detergents are known to decrease assay response to a number of protein, most likely due to competition with the dye for protein. The net result of these opposing effects is difficult to predict. Competitive effects leading to protein underestimation have been demonstrated with guanidine hydrochloride and sodium ascorbate. Competition effects of known added reagents may generally be compensated through their inclusion in the standard calibration.

While the potential interference problems of over- and underestimation due to additives may generally be avoided using proper controls, an important side effect is a reduction in the assay's linear response range [101]. Assay response to protein is due to the equilibrium shift away from the undetected cation, through the neutral species, to the anion absorbing at 595 nm. Since the linear assay response must therefore be

due to the net conversion of dye cation to anion, the concentration of free cation in the reagent ultimately limits linear range. Compounds stabilizing the neutral species do so at the expense of the dye cation pool. Although the additional neutral absorption may be compensated for by using a dye blank, the overall result is a smaller pool of dye cation, and a reduction in the linear range of the assay.

While many workers consider the Bradford assay the method of choice due to its sensitivity, specificity, and speed, its limitations must also be considered. The assay's specificity for arginine residue is a probable cause of variability in response between proteins, and reagents affecting the dye equilibria can cause interference.

## CHAPTER 4

### MATERIALS AND METHODS

#### 4.1 Materials

The materials used in this study are listed in **Table 4.1**.

**Table 4.1** List of chemicals and reagent materials

Chemicals and Reagent materials	Supplier / Grade
Acetic acid (CH <sub>3</sub> COOH)	Fluka / AR grade
Acetone ((CH <sub>3</sub> ) <sub>2</sub> CO)	Labscan / AR grade
Acrylamide (C <sub>3</sub> H <sub>5</sub> NO)	Amersham / AR grade
Ammonium persulphate (APS)((NH <sub>4</sub> ) <sub>2</sub> S <sub>2</sub> O <sub>8</sub> )	Amersham / AR grade
Benzophenone (BPO) (C <sub>13</sub> H <sub>10</sub> O)	Fluka / AR grade
Bovine Serum Albumin (BSA)	Sigma / Standard
Bradford reagent	Sigma / AR grade
Bromophenol blue (C <sub>19</sub> H <sub>10</sub> Br <sub>4</sub> O <sub>5</sub> S)	Amersham / AR grade
1,4-Butanediamine (NH <sub>2</sub> (CH <sub>2</sub> ) <sub>4</sub> NH <sub>2</sub> )	Sigma / AR grade
Coomassie Brilliant Blue R-250	Amersham / AR grade
Dipotassium hydrogen phosphate (K <sub>2</sub> HPO <sub>4</sub> )	Sigma-Aldrich / AR grade
Ethyl acetate (CH <sub>3</sub> COOC <sub>2</sub> H <sub>5</sub> )	Amersham / AR grade
Glycerol (C <sub>3</sub> H <sub>8</sub> O <sub>3</sub> )	Fluka / AR grade

**Table 4.1** List of chemicals and reagent materials (cont)

<b>Chemicals and Reagent materials</b>	<b>Supplier / Grade</b>
Isopropanol (C <sub>3</sub> H <sub>8</sub> O)	Amersham / AR grade
Maleic anhydride (MAH) (C <sub>4</sub> H <sub>2</sub> O <sub>3</sub> )	Fluka / AR grade
Maleic anhydride-polyethylene copolymer (Fusabond® E MB226D; 0.90%MAH)	Innovation / Commercial grade
2-Mercaptoethanol (HSCH <sub>2</sub> CH <sub>2</sub> OH)	Sigma / AR grade
Methanol (CH <sub>3</sub> OH)	Labscan / AR grade
N, N, N', N' - Tetramethylethylenediamine (TEMED) ((CH <sub>3</sub> ) <sub>2</sub> N(CH <sub>2</sub> ) <sub>2</sub> N(CH <sub>3</sub> ) <sub>2</sub> )	Amersham / AR grade
Phosphate buffer saline (PBS)	Merck / AR grade
Polyethylene film (LDPE)	- / Commercial grade
Potassium dihydrogen phosphate (KH <sub>2</sub> PO <sub>4</sub> )	Sigma-Aldrich / AR grade
Prestained Standards	Bio Rad / Standard
Sodium dodecyl sulfate (SDS) (C <sub>12</sub> H <sub>25</sub> OSO <sub>3</sub> Na)	BDH / AR grade
Toluene (C <sub>6</sub> H <sub>5</sub> CH <sub>3</sub> )	BDH / AR grade
Trichloroacetic acid (CCl <sub>3</sub> COOH)	Fluka / AR grade
Tris(hydroxymethyl) aminomethane hydrochloride (Tris-HCl) (NH <sub>2</sub> C(CH <sub>2</sub> OH) <sub>3</sub> )	Amersham / AR grade
Triton® X-100 (t-oct-C <sub>6</sub> H <sub>4</sub> -(OCH <sub>2</sub> CH <sub>2</sub> ) <sub>n</sub> OH)	Fluka / AR grade
Urea (NH <sub>2</sub> CONH <sub>2</sub> )	BDH / AR grade
Xylene (C <sub>6</sub> H <sub>4</sub> (CH <sub>3</sub> ) <sub>2</sub> )	BDH / AR grade

## 4.2 Apparatus

The apparatus used in this study are listed in **Table 4.2**.

**Table 4.2** List of Apparatus

Apparatus	Model / Manufacturer
<p><b><i>I. Preparation of PE-g-MAH film</i></b></p> <ul style="list-style-type: none"> <li>- UV reactor</li> <li>- Compression molding machine</li> <li>- Cooling press machine</li> </ul>	<p>-</p> <p>3831.4 DIOA00 / Carver</p> <p>-</p>
<p><b><i>II. Protein extraction and concentration</i></b></p> <ul style="list-style-type: none"> <li>- Electric analytical balance <math>\pm 0.0001</math> g</li> <li>- Freeze dryer (Lyophilizer)</li> <li>- pH meter</li> <li>- Shaker</li> <li>- Centrifuge machine</li> <li>- Vortex mixer</li> </ul>	<p>CP 2245 / Sartorius</p> <p>SuperModulyo / Thermo electron</p> <p>CG / Schott</p> <p>VRN-360 / Gemmy Industries</p> <p>Himac CR 22G / Hitachi</p> <p>Genies 2 / Scientific Industries</p>
<p><b><i>III. Protein binding</i></b></p> <ul style="list-style-type: none"> <li>- UV-Vis Spectrophotometer</li> <li>- Incubator shaker</li> <li>- Quartz cuvettes with 1 cm of path length</li> </ul>	<p>JASCO V-530 / Perkin Elmer</p> <p>Memmert / -</p> <p>T660/H / Scientific Promotion</p>
<p><b><i>IV. SDS-PAGE (Electrophoresis)</i></b></p> <ul style="list-style-type: none"> <li>- Mini-Protean II cell (see <b>Figure 4.1</b>) <ul style="list-style-type: none"> <li>▪ Electrode assembly with gaskets</li> <li>▪ Lower buffer chamber</li> <li>▪ Glass plates; inner plate size 7.3x10 cm<sup>2</sup> and outer plate size 8.3x10 cm<sup>2</sup></li> <li>▪ Clamp assemblies</li> <li>▪ 10 wells combs</li> <li>▪ 0.75 mm thick spacers</li> </ul> </li> </ul>	<p>Bio-Rad Laboratories</p>

**Table 4.2** List of Apparatus (cont)

<b>Apparatus</b>	<b>Model / Manufactor</b>
<ul style="list-style-type: none"> <li>▪ Casting standard with gasket</li> <li>- Power Pac 300 (see <b>Figure 4.2</b>)</li> <li>- Cellophane</li> <li>- Hot plate</li> <li>- Shaker</li> </ul>	<ul style="list-style-type: none"> <li>Bio-Rad Laboratories</li> <li>Bio-Rad Laboratories</li> <li>HS-2 / PNP</li> <li>PSU 2T plus / Biosan</li> </ul>
<p><b><i>V. Characterization of film</i></b></p> <ul style="list-style-type: none"> <li>- Fourier Transform Infrared Spectrometer</li> <li>- Contact angle goniometer</li> <li>- Elemental microanalyzer</li> <li>- Differential Scanning Calorimeter (DSC)</li> <li>- DSC–Thermal Gravimetric Analysis (TGA)</li> </ul>	<ul style="list-style-type: none"> <li>Equinox 55 / Bruker</li> <li>G-1 / Kruss</li> <li>2400CHN / Perkin Elmer</li> <li>DSC7 / Perkin Elmer</li> <li>2960 SDTV3 / Universal</li> </ul>

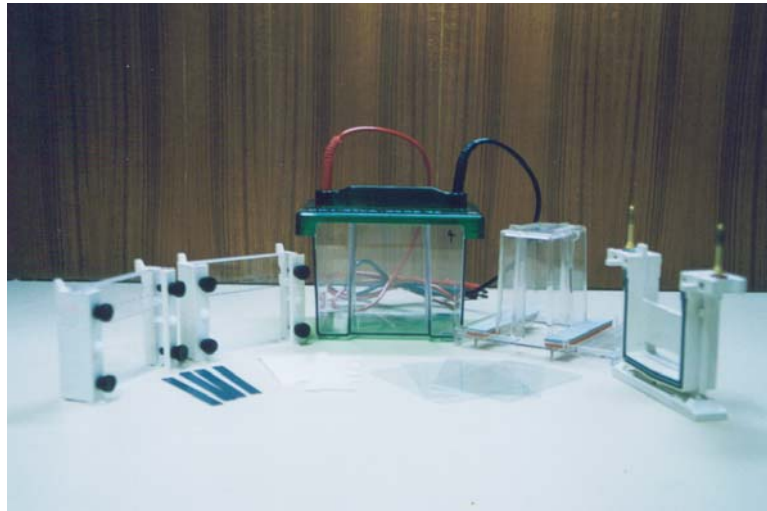


**Figure 4.1** The mini protean II cell

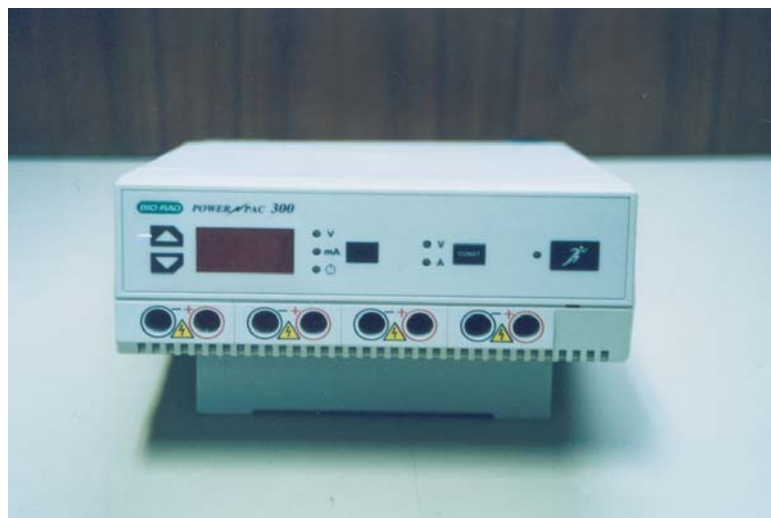


**Figure 4.2** The power pac 300

### 4.3 Preparation of Polyethylene Grafted with Maleic Anhydride Film

#### 4.3.1 MAH Photografting by UV Irradiation Technique

Low density polyethylene (LDPE) film was cut into circular samples (diameter ~ 5 cm) and then subjected to extraction in soxhlet with acetone to get rid of the additives and impurities before use.

Maleic anhydride (MAH) was grafted onto LDPE film by UV irradiation (UV lamp: high-pressure mercury lamp, 1000 w). The films containing MAH and BPO were laid on the holder of the irradiation equipment, as shown in **Figure 4.3**. The distance between the film and the UV lamp was compared at 25 and 50 cm. The irradiation times of 1, 5, 10 and 15 min were used in this work.

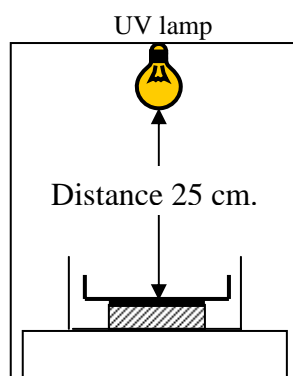


**Figure 4.3** Schematic diagram for grafting polymerization.

After irradiation, the grafted films were taken out, separated, and then washed in acetone for 5 min. Next, the films were sonicated in a large amount of toluene for 10 min for the removal of residual MAH and rinsed with acetone again. The grafted films were dried in an oven at temperature 50°C for 30 min. Finally, the PE-g-MAH films were obtained.

#### 4.3.2 Compression of Commercial PE-g-MAH

A commercial maleic anhydride grafted polyethylene with 0.90 wt% MAH (Fusabond® E MB226D) was used for the film preparation.

#### **4.3.2.1 Purification of PE-g-MAH Resin**

A total of 3 g PE-g-MAH resin was dissolved in 300 ml xylene under reflux at 130°C for 1 h. The temperature was lowered to 45°C with stirring and continuous stirring for 30 min. The precipitate was vacuum filtered and washed several times with acetone. The sample was then left in an oven for solvent removal.

#### **4.3.2.2 Compression of Purified PE-g-MAH**

The purified PE-g-MAH was prepared into a sheet sample by using a hydraulic hot press at 15 ton and under temperature 140°C. The open mold was placed between the heated platens of the molding press, filled with a given quantity of molding material and closed under pressure. After performing the compression molding for 5 min, the sample was cooled for 10 min before opening the mold.

#### **4.3.3 Heat Treatment of PE-g-MAH Films**

The PE-g-MAH film was placed in an oven under temperature 110°C for 24 h and 120°C for 3 h. A heating procedure provides high content of anhydride groups on the surface by re-cyclization.

### **4.4 Characterization of the PE-g-MAH Film**

#### **4.4.1 Bulk Properties**

The thermal behavior of PE-g-MAH sample after purification and annealing was measured by Thermo Gravimetric Analysis (TGA) and Differential Scanning Calorimeter (DSC).

The TGA is a testing procedure in which changes in weight of a specimen. The sample was heated from 25 to 500°C at a rate of 10°C/min under nitrogen purge. For DSC, The sample was heated to 200°C from room temperature at a rate of 20°C/min

under nitrogen. Then, it was cooled to room temperature and heated again. The sample weight was approximately 5 mg.

#### 4.4.2 Surface Properties

##### 4.4.2.1 Attenuated Total Reflection Fourier Transform Infrared Spectroscopy (ATR-FTIR)

The PE-g-MAH film was studied by attenuated total reflection fourier transform infrared spectroscopy (ATR-FTIR) to determine the chemical nature of the surface. ATR-FTIR spectra were taken using a 45° germanium crystal(Ge) for single reflection mode and zinc selenide crystal(ZnSe) for multiple reflection mode on an equinox 55 Infrared Fourier Transform Spectrometer (**Figure 4.4**). The measurements were performed with 125 scans at a resolution of 4  $\text{cm}^{-1}$  over range of 4000 to 600  $\text{cm}^{-1}$ .

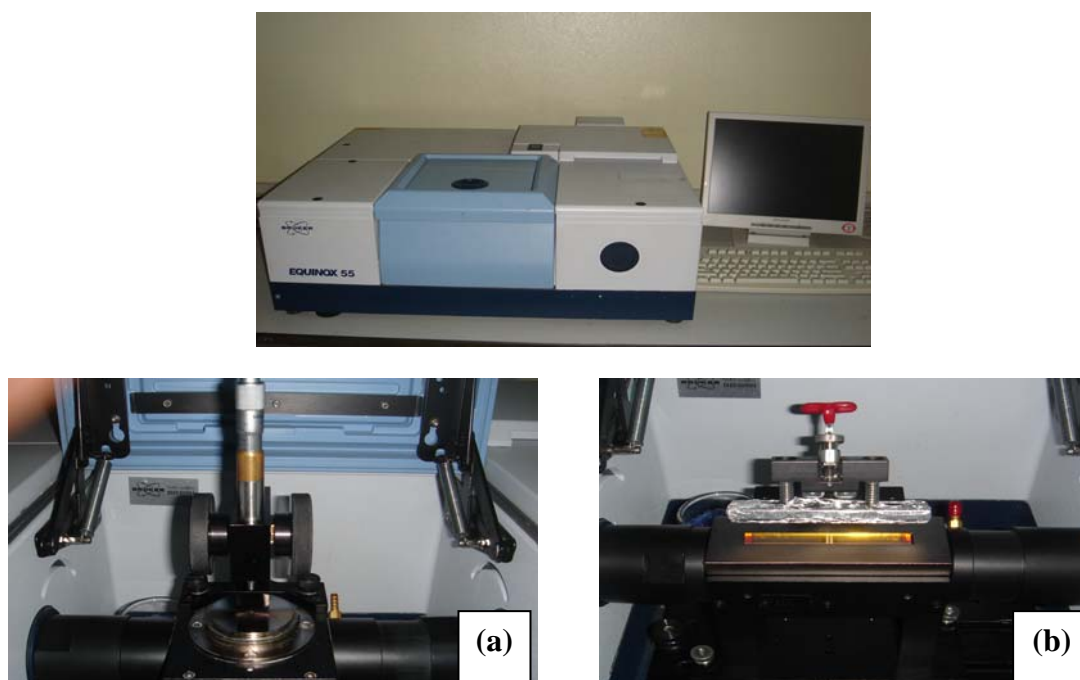


**Figure 4.4** ATR-FTIR Instrument: Germanium crystal (a) and Zinc selenide crystal (b)

#### 4.4.2.2 Contact Angle Measurement

The contact angles of the film surfaces were determined with a Kruss, G-1 contact-angle goniometer (**Figure 4.5**) at the ambient temperature. All measurements were performed with the sessile drop method and made with drops of 5  $\mu\text{l}$  of distilled water by syringe. This method is used to estimate wetting properties of a localized region on the film surface. Angle between the baseline of the drop and the tangent at the drop boundary is measured (**Figure 4.6**).



**Figure 4.5** Contact angle goniometer.

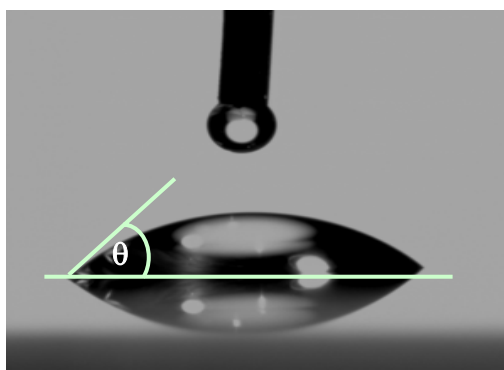


**Figure 4.6** Water drop on solid surface.

Experimentally, the wettability of the film surface can be adjusted to distinct values varying from poor surface wettability to good surface wettability depending on the functional group on the surface and surface contamination. The poor surface wettability has a low surface energy and a contact angle value is higher than  $90^\circ$  while

the good surface wettability has a high surface energy and a contact angle value is lower than  $60^\circ$ . In addition, the contact angle increases as the surface contamination increases because it is sensitive to hydrophobic interaction determined by surface organic contaminants that change the interface energy between the droplet and substrate. This leads to poor wettability condition as showed in **Figure 4.7(a)**). In other words, the clean surface (more hydrophilic) shows the lower contact angle, corresponding to good wettability condition as showed in **Figure 4.7(b)**). The reported values were the averages of eight measurements at different places on the same film sample. The accuracy of this technique is in the order of  $\pm 2^\circ$ .

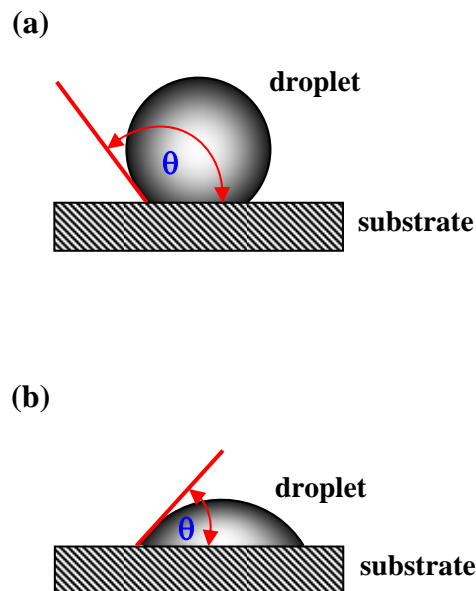


**Figure 4.7** Drop shape analysis from contact angle measurement:

- (a) Poor surface wettability, Low surface energy and Contact angle  $>90^\circ$
- (b) Good surface wettability, High surface energy and Contact angle  $<60^\circ$

## 4.5 Extraction of Proteins from Dry Skim NR

### 4.5.1 Protein Extraction

Dry skim NR was cut into small pieces. For a comparative test, two kinds of extract solution were chosen in this study. They are 0.01M phosphate buffered saline (PBS) at pH 7 and 2% sodium dodecyl sulphate (SDS).

First, 5 g of dry skim NR was immersed in 10 ml extract solution and then shaken at room temperature for 12 h. The mixture was filtered to remove any particular matters that might be present. The clear filtrate was then immediately subjected to protein precipitation.

In the study of sample size effect, the dry skim NR was dissolved by using toluene. The NR solution was poured into the plate and dried at room temperature. Finally, the rubber sheet with a thickness about 6 mm was obtained. The samples (~ 5 g) were prepared into two different surface area to volume ratios; small sheet (0.5x0.5 cm<sup>2</sup>) and rubber disc (diameter ~ 7 cm). They were then extracted in a defined solvent at the same extraction procedure.

The protein content of skim rubber is giving by:

$$\text{Extractable protein, EP (mg/g)} = \frac{\text{Total content of protein, C (mg)}}{\text{Weight of skim rubber (g)}} \dots\dots(1)$$

### 4.5.2 Protein Precipitation

1 ml of the filtrate was treated with 3 ml of 2-mercaptoethanol (0.07% v/v) and trichloroacetic acid (10 % w/v) in cooled acetone. The mixture was allowed to stand at -20°C for 24 h. The resulting precipitated proteins were sedimented by centrifugation of speed 10,000 rpm at 4°C for 10 min, and were rinsed with acetone to remove acid. Finally, the precipitated proteins were redissolved in Lysis buffer solution and were stored at -20°C.

Lysis buffer solution was prepared by dissolving ~24 g urea, 2 g Triton® X-100 and 0.035 ml 2-mercaptoethanol in distilled water and make up to 50 ml.

## **4.6 Characterization of Extractable Proteins**

### **4.6.1 Molecular Weight of Extracted Proteins by SDS-PAGE**

Sodium dodecyl sulfate- polyacrylamide gel electrophoresis (SDS-PAGE) is a low-cost, reproducible and rapid method for quantifying, comparing, and characterizing proteins. This method separates proteins based primarily on their molecular weights.

#### **4.6.1.1 Preparation of Reagents and Polyacrylamide Gel**

The stock solutions and gel formula for the electrophoresis system are described in **Tables 4.3 and 4.4**.

**Table 4.3** List of the stock solutions

<b>Solutions</b>	<b>Preparation</b>
1) 30% acrylamide mixture	Acrylamide, 29.2 g and N,N'-methylene bisacrylamide, 0.8 g in 100 ml; store at 4°C
2) Lower gel buffer, 0.75M Tris-HCl (pH 8.8)	Tris, 45.375 g. Bring to pH 8.8 with concentrated HCl and to 500 ml; store at 4°C
3) Upper gel buffer, 0.25M Tris-HCl (pH 6.8)	Tris, 15.125 g. Bring to pH 6.8 with concentrated HCl and to 500 ml; store at 4°C
4) 10%(w/v) SDS	SDS, 5 g in 50 ml
5) 25%(w/v) Ammonium persulphate (APS)	Ammonium persulphate, 0.25 g in 1 ml; make up fresh
6) Running buffer	Tris, 3.03 g, glycine, 14.4 g, and SDS, 1 g in 500 ml
7) Sample buffer	0.25M Tris-HCl (pH 6.8), 25 ml; 2-mercaptoethanol, 5 ml; SDS, 2 g; sucrose, 5 g; bromophenol blue 0.002 g. Bring to 50 ml
8) CBB-stain solution	Coomassie Brilliant Blue R-250, 0.5 g; Methanol, 50 ml; acetic acid 15 ml. Bring to 200 ml; stain for 15-30 min at room temperature
9) Destaining solution	Methanol, 125 ml and acetic acid 37.5 ml. Bring to 500 ml
10) Gel dry reagent	Glycerol, 15 ml; acetic acid, 5 ml; ethyl acetate, 0.25 ml; isopropanol, 25 ml; methanol, 225 ml. Bring to 500 ml

**Table 4.4** List of the components of separating gels (15% acrylamide)

Reagents	Separating gel ( $\mu$ l)
<p><b>A. Lower (separating) gel</b></p> <p><u>Mix first</u></p> <p>1) 30% acrylamide mixture</p> <p>2) 0.75M Tris-HCl (pH 8.8)</p> <p>3) 10% SDS</p> <p>4) Distilled water</p> <p><u>Add to polymerize</u></p> <p>5) 25% APS</p> <p>6) TEMED</p>	<p>7500</p> <p>7500</p> <p>150</p> <p>-</p> <p>50</p> <p>12</p>
<p><b>B. Upper (stacking) gel</b></p> <p><u>Mix first</u></p> <p>1) 30% acrylamide mixture</p> <p>2) 0.25M Tris-HCl (pH 6.8)</p> <p>3) 10% SDS</p> <p>4) Distilled water</p> <p><u>Add to polymerize</u></p> <p>5) 25% APS</p> <p>6) TEMED</p>	<p>750</p> <p>2900</p> <p>3750</p> <p>75</p> <p>25</p> <p>6</p>

### 4.6.1.2 Apparatus Setting and Procedure

#### *A. Pouring a Separating gel and Stacking gel*

The separating and stacking gels were successively poured between a molds formed by two glass plates, separated by spacers of 0.75 to 3 mm. with extremely clean. Assemble to plates with the spacers as shown in **Figure 4.8**.

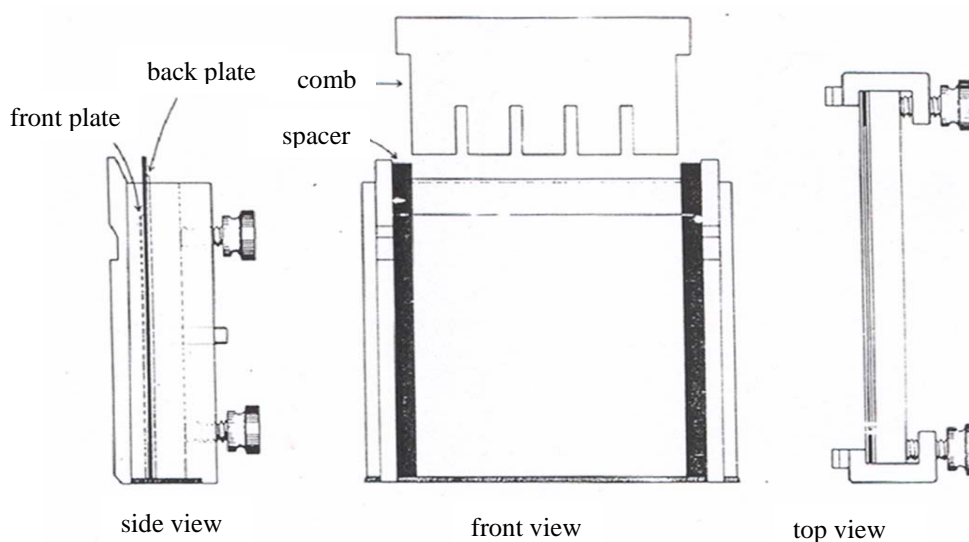


**Figure 4.8** View of gel plate assembly.

For Mini Gel, be sure that the bottom of both gel plates and spacer were perfectly flush against a flat surface before tightening clamp assembly. A slight misalignment will result in leak.

To prepare the separating gel (see **Table 4.4**), the appropriate components were mixed together in a small flask, swirled rapidly without causing bubble formation or aeration. And then pipette rapidly a suitable volume of the final solution into the mold formed by the glass plates. No bubbles or leaks should be present (**Figure 4.9**). To keep the gel surface flat, water was added on top of the separation gel solution (layer about 1 cm). The gel was allowed to polymerize (30-60 minutes) (**Figure 4.10**).

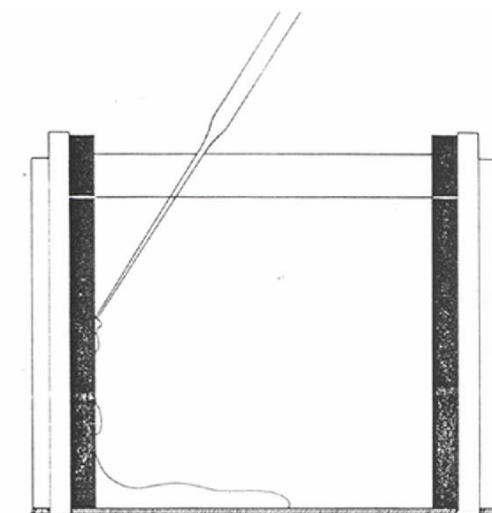


**Figure 4.9** Introducing the separating gel solution into the gel sandwich.

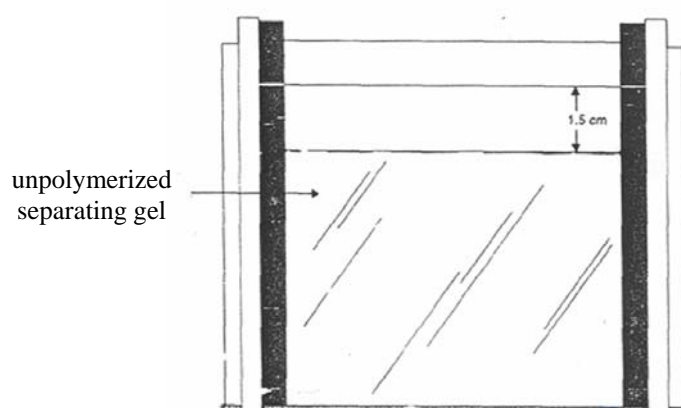


**Figure 4.10** Separation gel prior to polymerization.

After polymerization of the separating gel was completed, pour off water covering the separating gel. Next the stacking gel was prepared in a small flask. The mixture was pipetted into the mold (onto separating gel) until solution reaches top of front plate (**Figure 4.11**).

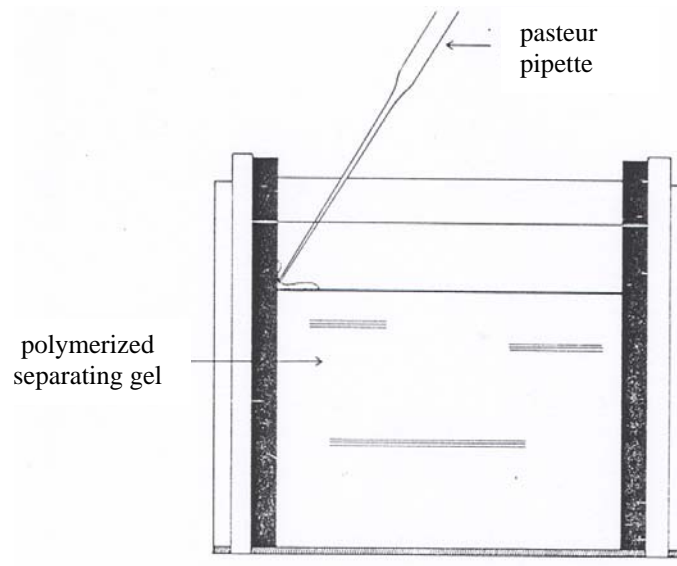


**Figure 4.11** Introducing the stacking gel solution into the gel sandwich.

The wells could be inserted into the liquid stacking gel solution before polymerization begins. The comb was carefully inserted into gel sandwich until bottom of teeth reach top of front plate (see **Figures 4.12 and 4.13**). Be sure no bubbles were trapped on ends of teeth. Tilting the comb at a slight angle was helpful for insertion without trapping air bubbles. And the stacking gel was allowed to polymerization (about 30 min).

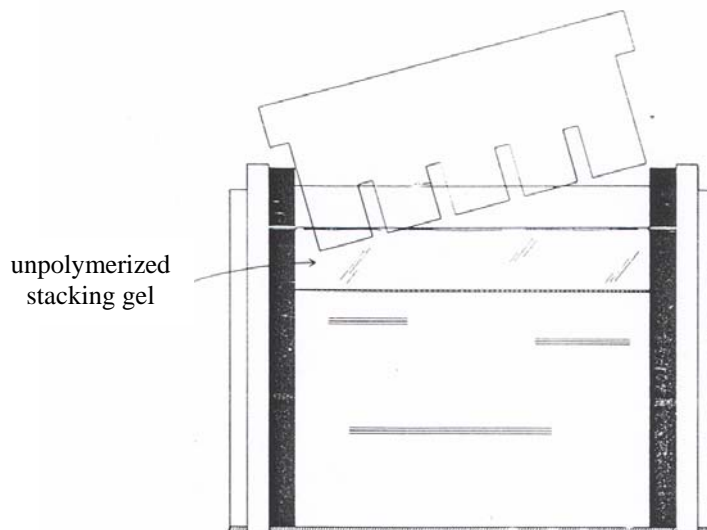


**Figure 4.12** Inserting the sample-well comb into the stacking gel.

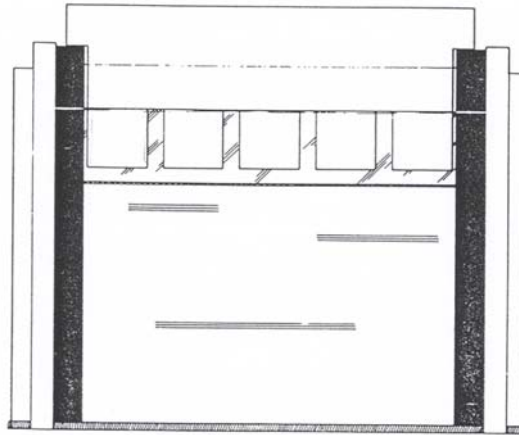


**Figure 4.13** Stacking gel prior to polymerization.

After stacking gel had polymerized, the comb was removed carefully and placed gel into electrophoresis chamber.

Electrophoresis buffer was added to inner and outer reservoir, making sure that both top and bottom of gel were immersed in buffer.

### ***B. Preparation of the Protein Solution and Sample Loading***

The 40  $\mu$ l of extracted protein solution was mixed with 40  $\mu$ l of buffer in a microtube and heated at 100°C for 5 min. The mixture was allowed to stand at room temperature for 10 min to cool down and spin down protein solution for 1 sec on vortex. The sample and standard solutions were gently loaded into each well using a syringe (**Figure 4.14**).

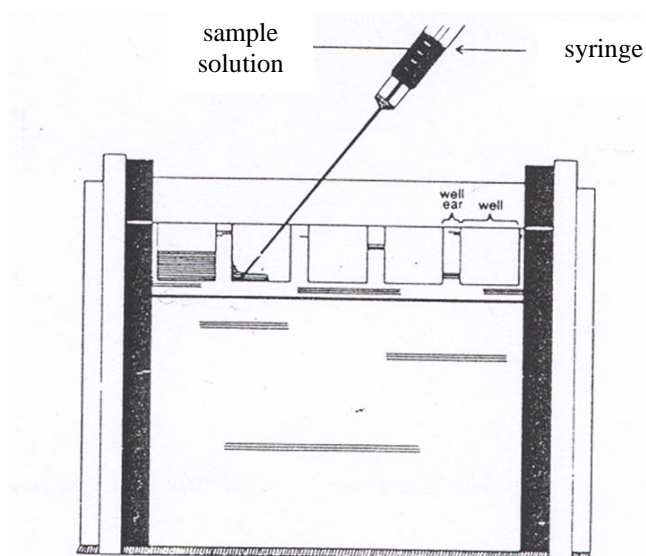


**Figure 4.14** Introducing protein solution into sample well.

The volume of sample should not exceed 20  $\mu\text{l}$  in each well of the electrophoresis gel. The 5  $\mu\text{l}$  of the standard solution was loaded into the well as molecular weight reference markers in all experiment (**Table 4.5**).

**Table 4.5** List of Prestained standard on molecular weight for SDS-PAGE method

Protein	Molecular weight (Daltons)
Myosin	200,000
$\beta$ -galactosidase	116,250
Phosphorylase b	97,400
Serum albumin	66,200
Ovalbumin	45,000
Carbonic anhydrase	31,000
Trypsin inhibitor	21,500
Lysozyme	14,400
Aprotinin	6,500

Layer protein solution on bottom of well and raise syringe tip as dye level rises. Be careful to avoid introducing air bubbles as this may allow some of sample to be carried to adjacent well.

### *C. Running a Gel*

After complete loading, the electrophoresis apparatus was assembled with the power supply (**Figure 4.15**)

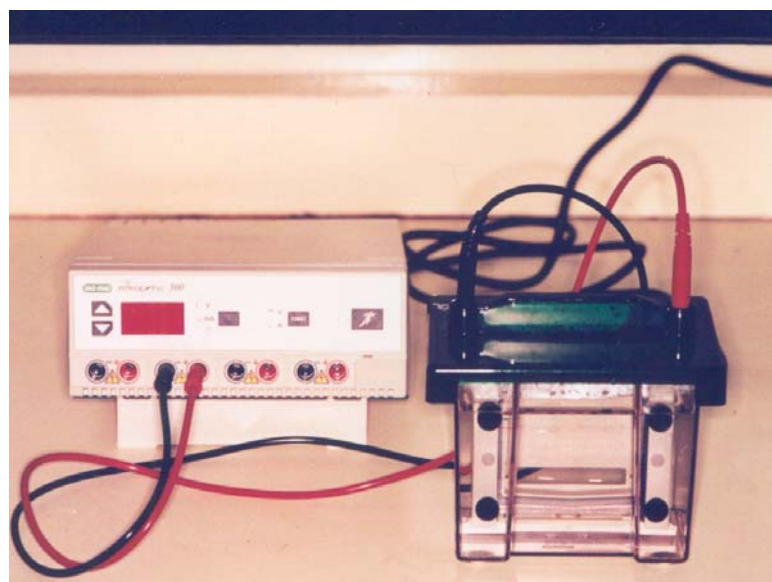


**Figure 4.15** The complete setting of electrophoresis apparatus.

The electrophoresis was carried out at a constant electrical current of 15 mA and turn on power supply to 200 V. When electrode plugs was attached to proper electrodes, the current should flow towards the anode. The dye front should migrate to 1 cm from the bottom of the gel in 30-40 min.

### *D. Staining a Gel with Coomassie Blue*

After electrophoresis, gel plate was removed from electrode assembly. A spacer was carefully removed and gently pried apart the gel plates. The gel will stick

to one of the plates. Next, pick up the gel and transfer it to a small container. Add 20 ml of Coomassie Stain solution and agitated for 5-10 min on slow shaker.

After staining, the solution was poured out. The gel was rinsed in a few water. And then the 50 ml Coomassie Destain was added into gel. It was found that strong band of protein is visible immediately and the gel is largely destained within an hour.

### ***E. Drying a Gel***

The gel was placed upside down on a clean surface (glass plate). Water was used as a lubricant and gel was covered with cellophane sheet. The gel should stick to the paper. It is useful to roll out air bubbles. Finally, the gel was dried at room temperature for 24 h.

## **4.6.2 Composition and Structure of Extractable Proteins**

### **4.6.2.1 Freeze-Drying of Extracted Proteins**

Lyophilization or Freeze-drying is a simple process that removes water (moisture) from frozen products. The protein precipitate was dried to constant weight before analysis.

The protein sample should not be redissolved with lysis solution to avoid contamination. After protein precipitation, the protein sample was stored at  $-20^{\circ}\text{C}$  in microtube. Next, the sample was frozen for 2 min in liquid nitrogen and then immediately placed in a chamber. A vacuum is established, to ensure that the chamber is devoid of air and operating at very low absolute pressure. When the inside of the drying chamber reached the proper pressure and temperature, the moisture in the frozen objects was converted to vapor. It was allowed for 3-5 h. Finally, the dried protein was obtained and closely sealed.

#### **4.6.2.2 FTIR Analysis**

The FTIR instrument was used to indicate the structure characteristic of extracted protein that compared with BSA standard protein. The spectrums were made in single mode (Germanium crystal) at 16 scan and a resolution of  $4\text{ cm}^{-1}$ .

#### **4.6.2.3 CHN Analysis**

Elemental analysis for carbon (C), hydrogen (H) and nitrogen (N) contents in the dried protein sample was carried out using a Perkin Elmer CHN analyzer. The CHN elemental analysis was very effective in quantitatively determining analysis the nitrogen content in the amino group of protein.

### **4.6.3 Determination of Protein Content with Bradford Micro-Assay**

#### **4.6.3.1 Calibration Curve Preparation**

The Bovine Serum Albumin (BSA) as the standard was carried out according to the Protocol of micro assay procedure.

The BSA standard solution was prepared in 0.2M potassium phosphate buffer solution (pH=7) of a concentration of 1.0 mg/ml. The solution was stored at  $-20^{\circ}\text{C}$  for further procedures.

1.0 mg/ml of BSA standard solution was used as stock solution for calibration curve preparation and the calibration curve remains linear only from 0-20  $\mu\text{g/ml}$ . The amount of reagent used to prepare the calibration curve was illustrated in **Table 4.6**.

**Table 4.6** Preparation of calibration curve

Tube No.	[BSA] protein standard ( $\mu\text{g/ml}$ )	Stock solution ( $\mu\text{l}$ )	Phosphate buffer ( $\mu\text{l}$ )	Bradford reagent (ml)
1	0(blank)	0	100.00	1
2	2.5	2.75	97.25	1
3	5.0	5.50	94.50	1
4	7.5	8.25	91.75	1
5	10.0	11.00	89.00	1
6	12.5	13.75	86.25	1
7	15.0	16.50	83.50	1
8	17.5	19.25	80.75	1
9	20.0	22.00	78.00	1

The phosphate buffer solution was pipetted into microtube. The BSA stock solution and Bradford reagent (brown solution) were added respectively.

The mixtures were mixed on vortex and allowed to stand at room temperature for 5 min. The solution color is developed into violet. Then the absorbance at 592 nm was measured by UV-VIS spectrophotometer.

#### 4.6.3.2 Measurement of Protein Content in Extract Solution

The extracted protein was stored in lysis solution at  $-20^{\circ}\text{C}$ . Bring the frozen protein out of the freezer for at least 30 min prior to using it. Then this lysis solution of concentration  $C_1$  was diluted with 0.1M PBS to give approximately final concentration of 1 mg/ml. The concentration of protein solution ( $C_2$ ) was measured by the same manner as BSA standard. The accuracy of protein content was obtained from using two volumes of extract sample. 10  $\mu\text{l}$  and 15  $\mu\text{l}$  of about 1 mg/ml protein solution were pipetted into a phosphate buffer solution to prepare solutions in the range of 0-20  $\mu\text{g/ml}$ . Add 1 ml of Bradford reagent to each tube, and mix well by vortex. The mixture concentration was fixed at  $C_3$   $\mu\text{g/ml}$ . The absorbance at

wavelength 592 nm was measured and then converted into protein content by using the BSA calibration curve.

From calibration curve, the concentrations of BSA ( $\mu\text{g/ml}$ ) (x-axis) were plotted versus absorbance at 592 (y-axis). Then a concentration equation was computed. Use the equation and the measured absorbance for unknown sample to determine the concentration of unknown sample in unit  $\mu\text{g/ml}$ .

The concentration of protein solution is calculated by the formula as shown below:

$$\text{Concentration of protein solution, } C_2 (\mu\text{g/ml}) = \frac{C_3 * V_3}{V_2} \dots\dots\dots (2)$$

Where;

- $C_3$  = concentration from measurement ( $\mu\text{g/ml}$ )
- $V_2$  = volume of protein solution for testing (10 or 15  $\mu\text{l}$ )
- $V_3$  = total volume of mixture (protein solution, phosphate buffer and Bradford reagent) ( $\mu\text{l}$ )

The exact protein concentration was obtained from the average value of calculated protein content of two volumes of protein solution for testing (10 and 15  $\mu\text{l}$ ).

To determine the total protein content in lysis solution, the calculation is followed by below equation:

$$\text{Total protein content, } C_1 (\mu\text{g/ml}) = \frac{C_2 * V_2}{V_1} \dots\dots\dots (3)$$

Where;

- $C_2$  = concentration of protein solution ( $\mu\text{g/ml}$ )
- $V_1$  = volume of lysis solution used to prepare protein solution ( $\mu\text{l}$ )
- $V_2$  = total volume of protein solution ( $\mu\text{l}$ )

## **4.7 Protein Binding Studies on the Films**

### **4.7.1 Protein Binding on PE-g-MAH Film**

Bovine Serum Albumin (BSA) as a model protein was used to study protein binding on the film. The protein concentration was fixed at 1 mg/ml. The extracted protein was measured initial concentration and then prepared to give approximately final concentration of 1 mg/ml.

The commercial PE-g-MAH film having approximately 2x2 cm<sup>2</sup> was used for BSA binding while circular samples of PE-g-MAH film (diameter of 0.6 cm) was used to bind extractable proteins. Before binding, sample was immersed in 0.1M PBS at pH 7 for 2 h.

The films were then placed into individual 1.5 ml microtube to which 0.5 ml of protein solution was added. The mixture was incubated at room temperature for defined time on shaker. After incubating, the films were removed from the protein solution and rinsed with 0.1M PBS. Finally, the films were sonicated in 2 ml of 1% SDS for 15 min to remove noncovalently bound BSA and dried in vacuum at room temperature.

### **4.7.2 Determination of Protein Binding**

#### **4.7.2.1 Characteristic of Protein-Immobilized Films**

Changes of chemical structure of film surface due to protein binding were followed by ATR-FTIR with the same condition. The sample was measured by using germanium (Ge) crystal and zinc selenide (ZnSe) crystal to determine protein information on the surface. The most informative IR bands for protein analysis are amide I (1620-1700 cm<sup>-1</sup>) and amide II (1520-1580 cm<sup>-1</sup>).

#### 4.7.2.2 Determination of Immobilized Protein on the Films

The amount of immobilized protein on the film was measured after certain immersion time. The binding capacity was determined by measuring the protein content in solution before and after binding. The reducing of protein content in solution could be converted into amount of immobilized protein on the film.

The amount of immobilized protein on the film surface in  $\mu\text{g protein/cm}^2$  surface area was calculated as follows:

$$\text{Amount of immobilized protein } (\mu\text{g/cm}^2) = \frac{P_i - P_f}{A} \quad \dots\dots\dots (4)$$

Where;

- $P_i$  = total content of protein before binding ( $\mu\text{g}$ )
- $P_f$  = total content of protein after binding ( $\mu\text{g}$ )
- $A$  = surface area of film;  $2\pi r^2$  ( $\text{cm}^2$ ) for commercial film and  $\pi r^2$  ( $\text{cm}^2$ ) for UV photografted film

The reported value is based on the average value of 5-10 samples.

## **CHAPTER 5**

### **RESULTS AND DISCUSSION**

In this work, extractable proteins from dry skim NR were selected to study protein binding ability of the PE-g-MAH film. Membrane materials containing maleic anhydride group were carried out using UV photografting and compression of commercial linear low density polyethylene graft maleic anhydride granule.

In this chapter, the results and discussion were described in four parts. Firstly, the optimal condition for preparing PE-g-MAH film was investigated. Two types of PE-g-MAH films were used in the research; (1) PE-g-MAH obtained from MAH photografting on LDPE film and (2) commercial PE-g-MAH. The second part involved the extraction of protein from dry skim NR, including determination of the effects of extract solution type, number of extraction and sample size on the extractable protein content. The molecular weight, composition and structure of extractable protein were analyzed by many techniques in the third part. In the last part, the protein binding was studied under optimum conditions. The characteristic of film after protein binding and the amount of immobilized protein on the film were determined and discussed.

#### **5.1 Optimum Conditions for Preparation of PE-g-MAH Film**

The bulk and surface properties of the PE-g-MAH film were analyzed by FTIR spectroscopy in transmission mode and reflection mode respectively. The contact angle measurement was employed to characterize the hydrophilicity of sample surface. DSC and TGA were also used to evaluate thermal behavior of samples. In this work, two preparation methods were used to obtain the PE film having MAH groups on the surface. They are grafting of MAH on PE film by using UV irradiation and compressing the commercial PE-g-MAH resin into sheet form.

### 5.1.1 MAH Photografting by UV Irradiation Technique

In this technique, the grafting polymerization was performed in acetone and studied under some factors including reaction time and distance between UV lamp and sample.

The FTIR spectra of original LDPE and PE-g-MAH obtained from MAH photografting on LDPE film are shown in **Figure 5.1**.

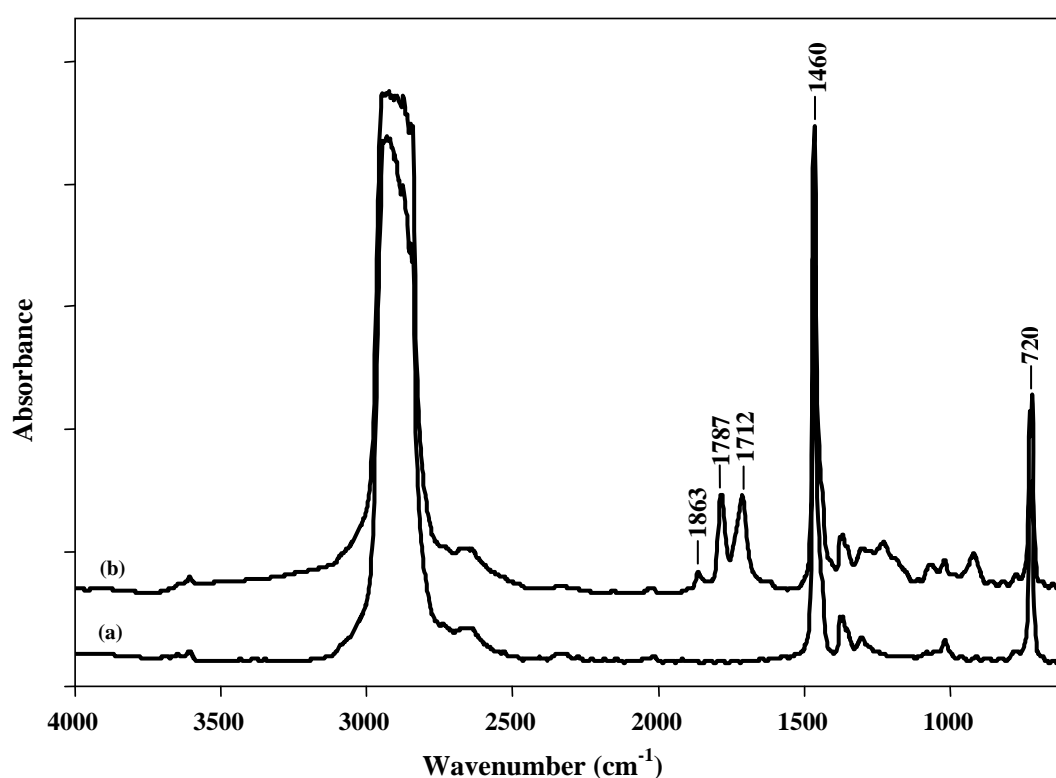


**Figure 5.1** FTIR spectra of (a) PE film and (b) PE-g-MAH.

The characteristic peaks of original LDPE were observed at 720 and 1460 cm<sup>-1</sup>, corresponding to CH<sub>2</sub> rocking and CH<sub>2</sub> bending respectively. And a broad peak of C-H stretching was also showed at 2800-3000 cm<sup>-1</sup>.

After MAH photografting, it is clearly seen that the spectrum of PE-g-MAH shows specific peaks at 1863 and 1787 cm<sup>-1</sup>, corresponding to the characteristic absorption of the carbonyl stretching in cyclic anhydride groups of MAH. Additionally, the sample also presented strong absorption peak which was assigned to

C=O stretching of carboxylic acid groups at  $1712\text{ cm}^{-1}$ . This was probably attributed to the surface transformation of anhydride from  $-(\text{CO})_2\text{-O-}$  to  $-(\text{COOH})_2\text{-}$  due to hydrolysis.

The intensity ratio of these peaks was used to determine the amount of surface grafting. The results are indicated in **Table 5.1**. It was derived from the intensity of anhydride peak at  $1787\text{ cm}^{-1}$  to that of reference peak at  $1460\text{ cm}^{-1}$ . The reference peak corresponds to  $\text{CH}_2$  bending of LDPE film. Furthermore, the intensity peak at  $1712\text{ cm}^{-1}$  was used to determine the amount of hydrolyzed anhydride group to acid group.

**Table 5.1** Intensity ratio of PE-g-MAH under various conditions (Transmission mode)

Distance(cm)	Time(min)	$I_{1787}/I_{1460}$	$I_{1787}/I_{1712}$	$I_{1712}/I_{1460}$
25	1	0.075	0.762	0.098
	5	0.226	1.110	0.204
50	10	0.093	0.550	0.114
	15	0.126	0.690	0.185

The infrared result clearly shows that the best condition required for the MAH photografting was 5 min of irradiation duration and 25 cm of distance between UV lamp and film, leading to the maximum degree of grafting. Furthermore, the intensity of the  $1787\text{ cm}^{-1}$  is stronger than that of the  $1712\text{ cm}^{-1}$  band, meaning that the majority of the anhydride functionality is maintained during irradiation treatment. It is noted that the amount of acid group increased with the UV treatment time.

The contact angle measurement was used to characterize the surface properties of modified film. The results are shown in **Table 5.2**.

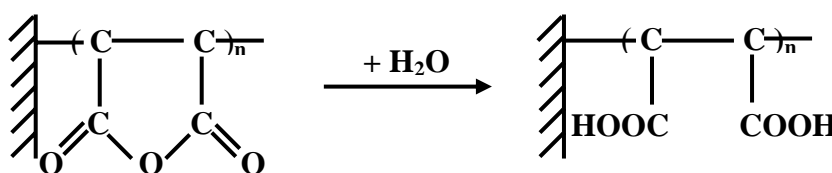
**Table 5.2** Effect of grafting time and distance on contact angle of PE-g-MAH

Distance(cm)	Power <sup>a</sup> (mJ/cm <sup>2</sup> )	Time(min)	Contact angle, $\theta$ (°)	
			$\theta_{\text{Left}}$	$\theta_{\text{Right}}$
25	324	1	$73.5 \pm 1.2$	$72.5 \pm 1.7$
	3240	5	$66.6 \pm 1.4$	$67.0 \pm 1.5$
50	3240	10	$77.7 \pm 0.9$	$77.6 \pm 1.0$
	4860	15	$71.9 \pm 1.1$	$71.3 \pm 0.9$

<sup>a</sup> The power of UV lamp 1000W is 2.7 mW/cm<sup>2</sup> of distance 100 cm.

From **Table 5.2**, it is obvious that the wettability of the LDPE film is improved greatly by grafting MAH onto it. Water contact angle decreased from 86° for the PE film to 67-78° for the grafted film. After UV grafting, it was found that at the same distance, the contact angles of PE-g-MAH films decreased with increasing UV irradiation time in all cases. This indicated the appearance of hydrophilic groups on the PE surface, leading to the improved wettability of grafted film.

The hydrophilic group observed in the grafting process corresponds to carboxylic acid (-COOH) which occurred through hydrolysis reaction with moisture in air because the process is performed under open system. Some anhydride groups change into carboxylic groups as clearly demonstrated in **Figure 5.2**.

**Figure 5.2** Scheme of the hydrolysis of PE-g-MAH surface [13].

From the data in this table, it can be seen that the lowest contact angle occurred at distance between lamp and sample of 25 cm and under irradiation for 5 min. It was expected that large amount of carboxylic group was obtained on the surface.

However, from FTIR result, it was found that the UV grafting with this condition gave the highest MAH content.

Furthermore, when the power of UV lamp was considered in all condition, it was observed that the power of UV light depends on lamp distance and radiation time. The UV radiation intensity of optimum condition (distance 25 cm and radiation time 5 min) equalizes  $3240 \text{ mJ/cm}^2$  which is as same as that of condition under distance 50 cm for 10 min. Although both conditions have a same power, they have a different efficiency of MAH grafting. This was due to the effect of irradiation temperature influenced on the grafting efficiency.

Deng et al. [69] reported that the grafting efficiency is affected greatly by temperature. The grafting efficiency was increased with increasing of temperature. However, after the temperature exceeds  $60^\circ\text{C}$ , the result shows a decreasing of the grafting efficiency, especially when the temperature is above  $80^\circ\text{C}$ . In our work, the irradiation temperature was measured about  $58\text{-}62^\circ\text{C}$  for distance 25 cm and irradiation time 5 min while irradiation temperature of distance 50 cm for 10 min was  $40\text{-}50^\circ\text{C}$ .

As the results, it can be concluded that the selected condition for the MAH photografting on PE film was at the distance between lamp and sample of 25 cm and under irradiation for 5 min.

### **5.1.2 Compression of Commercial PE-g-MAH**

Firstly, Granules of linear low density polyethylene grafted with maleic anhydride were analysed by using IR technique. Their spectra were recorded in **Figure 5.3**.

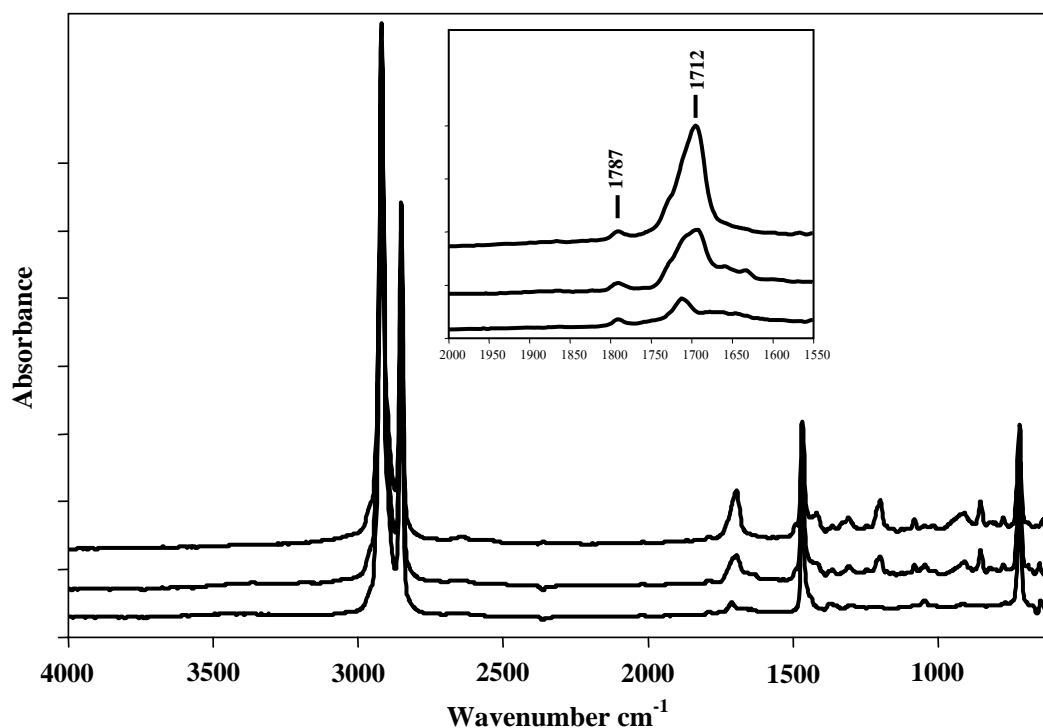


**Figure 5.3** ATR-FTIR spectra (Ge) of PE-g-MAH granules.

**Figure 5.3** shows clearly PE backbone having maleic anhydride groups. Generally, the characteristic peaks of maleic anhydride were observed at 1787 and 1863  $\text{cm}^{-1}$ , corresponding to symmetric and asymmetric carbonyl stretching respectively. And the absorbance at 1787  $\text{cm}^{-1}$  is much higher than the absorbance at 1863  $\text{cm}^{-1}$ . The characteristic of PE-g-MAH granules appeared only one specific peak at 1787  $\text{cm}^{-1}$  which was assigned to carbonyl stretching in cyclic anhydride group of maleic anhydride. This may be due to low maleic anhydride content on the surface (%grafting = 0.90 wt%). And the sample also presented strong absorption peak at 1712  $\text{cm}^{-1}$ , which was assigned to carbonyl stretching of carboxylic acid.

Furthermore, the ATR results show a variable intensity peak of carboxylic acid at 1712  $\text{cm}^{-1}$  and the impurity in range 600-1350  $\text{cm}^{-1}$ . This indicated the difference of chemical composition in each reactive extrusion granule. To obtain a uniform material before compression, it is necessary to purify the PE-g-MAH granules.

### (a) Purification

The commercial PE-g-MAH granules were purified by dissolving in xylene and precipitating in acetone. The sample was then dried to constant weight in an oven. After that, the chemical structure of purified sample in powder form was examined. The results are presented in **Figure 5.4**.

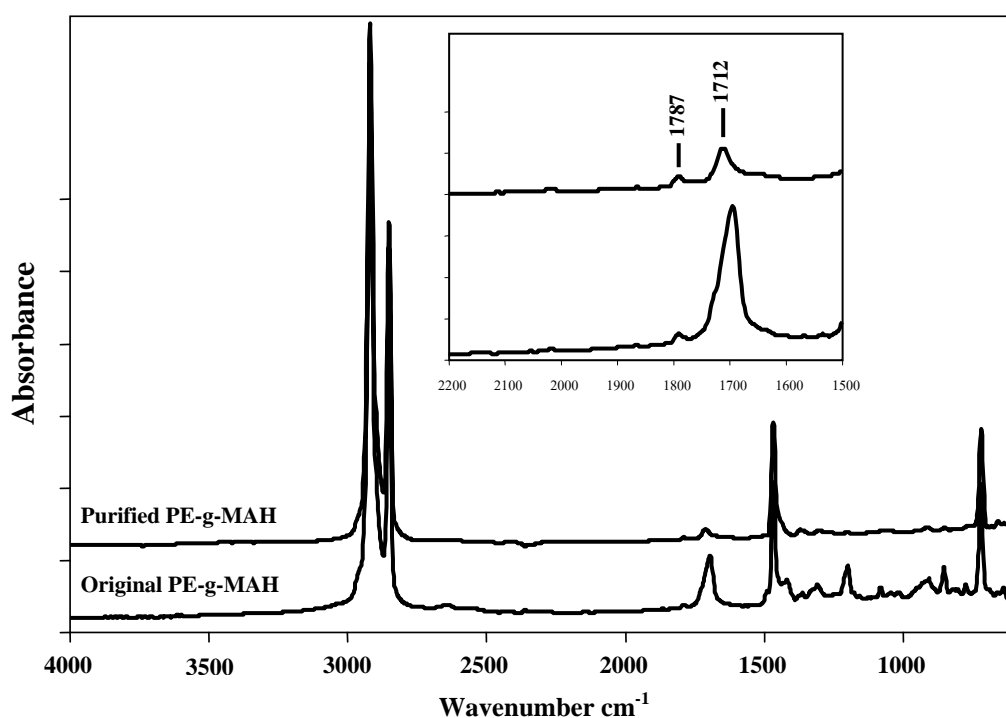


**Figure 5.4** ATR-FTIR spectra (Ge) of original and purified PE-g-MAH samples.

As can be seen in **Figure 5.4**, the amount of carboxylic group and impurity substance decreased significantly due to removal of moisture and unreactant. However, the hydrolysed anhydride groups were observed in the material.

In order to ensure the efficiency of purification, the thermal behaviors of original and purified samples were studied by using DSC and TGA instruments.

**Figure 5.5** shows the DSC melting scan curve of original and purified PE-g-MAH. The samples were heated at a heating rate of 20°C/min from room temperature to 200°C. They were then cooled to room temperature and heated again. This analysis

procedure was performed in order to ensure that the materials received comparable thermal histories.

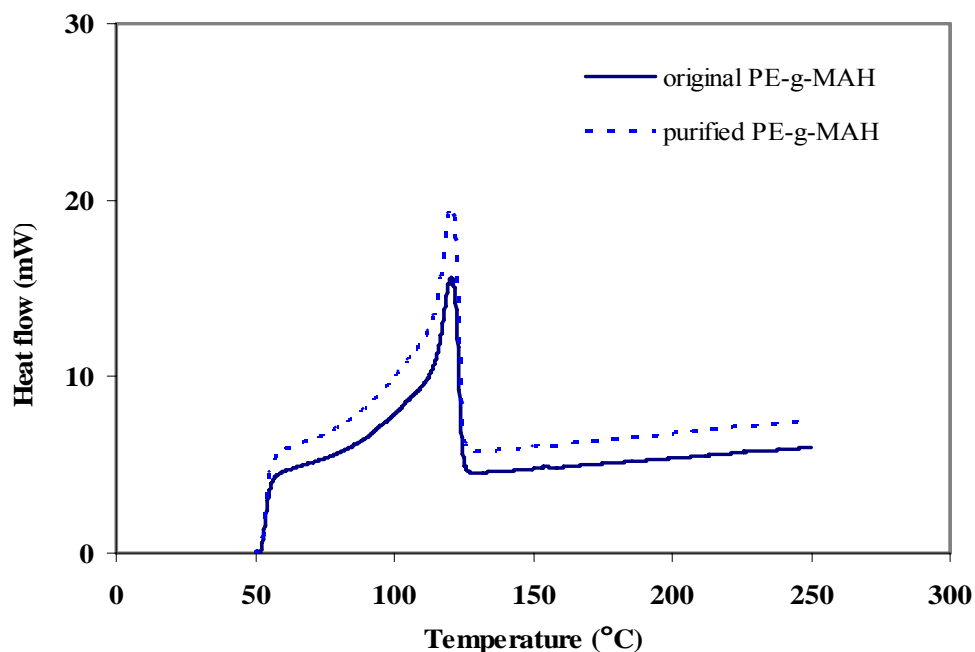


**Figure 5.5** DSC curves of original and purified PE-g-MAH.

From this figure, the melting temperature ( $T_m$ ) of original PE-g-MAH is 120.4 °C and the purification slightly decreases the temperature down to about 119.2 °C due to removal of maleic anhydride and contaminant from sample. The result observed can be explained by the assumption that the purification method had not a significant effect on the degree of crystallization of the copolymer.

Original and purified PE-g-MAH are also measured with TGA and the results are shown in **Figure 5.6**.

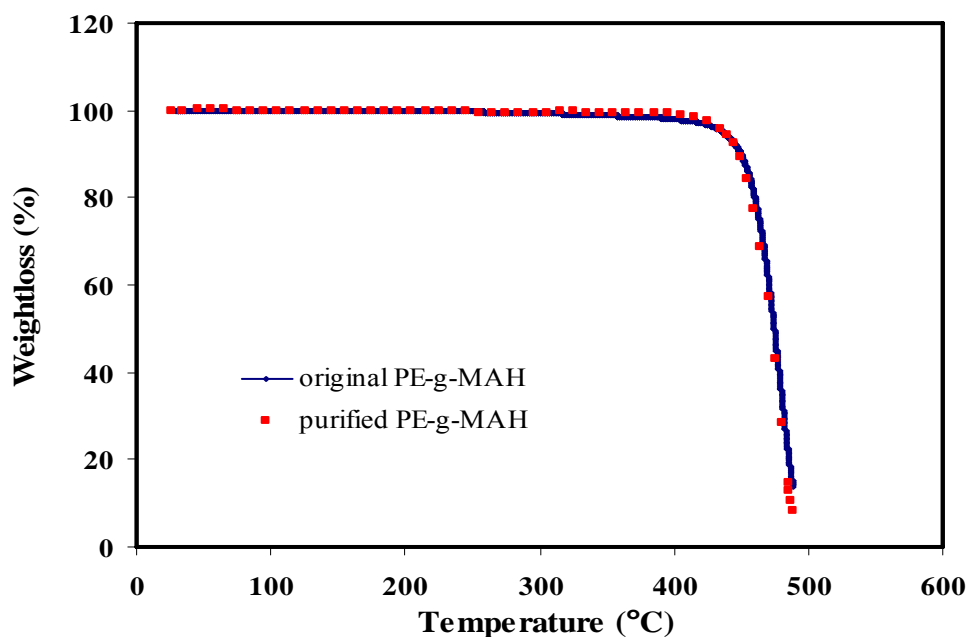


**Figure 5.6** TGA curves of original and purified PE-g-MAH.

From the results, it was noticed that both samples exhibited single-step degradation pattern with the decomposition temperature at about 450°C.

Bettini et al. [74] studied the purification of MAH copolymer which was prepared by reactive extrusion. The copolymer sample was similarly purified by dissolving in xylene and precipitation in acetone. The following stage was to verify whether the samples required heat treatment in a vacuum oven for the conversion of possible acid groups resulting from the ring opening of the anhydride. The sample with high MAH grafting contains a large amount of unreacted maleic anhydride. After purification, a significantly different percent weight loss at 202°C (bp. of MAH) of nonpurified (2.064%) and purified samples (0.022%) was observed. The purification methodology employed was efficacious in the removal of unreacted maleic anhydride. In our work, the sample having a very low degree of MAH grafting was treated in an oven. So, the change of weight loss for purified PE-g-MAH could not be detected by TGA analysis.

### (b) Compression Temperature

Compression molding was used to prepare PE-g-MAH films. Its advantages were a greatly shortened time, simplicity, and more economical. After compression, the films were analyzed by using FTIR.

**Figure 5.7** illustrates the results on the extent of maleic anhydride grafting represented in the term of intensity ratio of anhydride group ( $1787\text{ cm}^{-1}$ ) to  $\text{CH}_2$  bending of PE ( $1460\text{ cm}^{-1}$ ) as a function of compression temperature. Furthermore, it also presented the effect of purification on anhydride content under different temperatures.

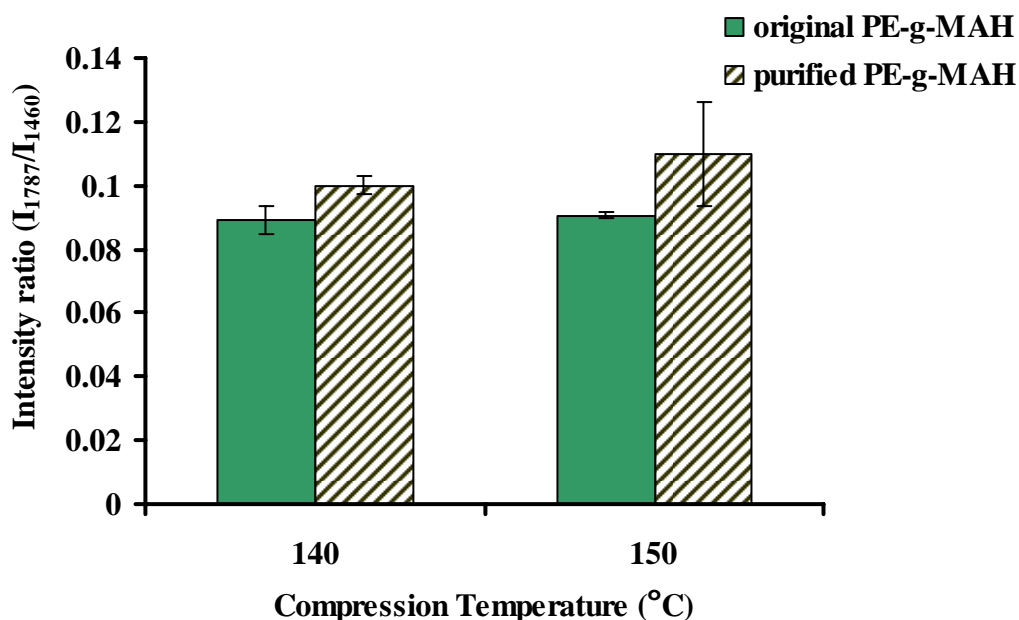


**Figure 5.7** Effect of compression temperature on intensity ratio of anhydride group.

From the figure, it is seen that the intensity ratio of purified PE-g-MAH increased with an increase in compression temperature. At a higher temperature ( $150^\circ\text{C}$ ), the film was found to change color from colorless to pale yellow and emitted a burn odor. So, the compression temperature at  $140^\circ\text{C}$  was selected for preparation of PE-g-MAH film.

### (c) Thermal Treatment

Since it is recognized that maleic acid will spontaneously form maleic anhydride at elevated temperatures, we experimented with various thermal treatments in order to decrease the acid content of PE-g-MAH.

Schmidt et al. [77] found that the annealing at temperature 120°C for 3 h of the modified maleic anhydride copolymer films induced efficient back-formation of the anhydride groups. In addition, it was reported that the most successful treatment was to heat the maleic anhydride copolymer specimen at 136°C under vacuum [102].

In general, the annealing at temperature nearly melting point of sample is suitable for annealing effect study. From DSC results, the  $T_m$  of PE-g-MAH is about 120°C. Therefore, two annealing conditions, high temperature at 120°C for 3 h and low temperature at 110°C for 24 h were chosen in this work for determining of the best condition to obtain high MAH content in the material. Although, the heat treatment in vacuum oven at temperature about 100°C has been suggested to convert the acid groups to anhydride, our samples were annealed in a common oven. It was expected that this simple method could give enough MAH content to be used for further experiments.

The transmission-FTIR spectra and the amount of carbonyl from annealing effect are presented in **Figures 5.8 and 5.9** respectively.

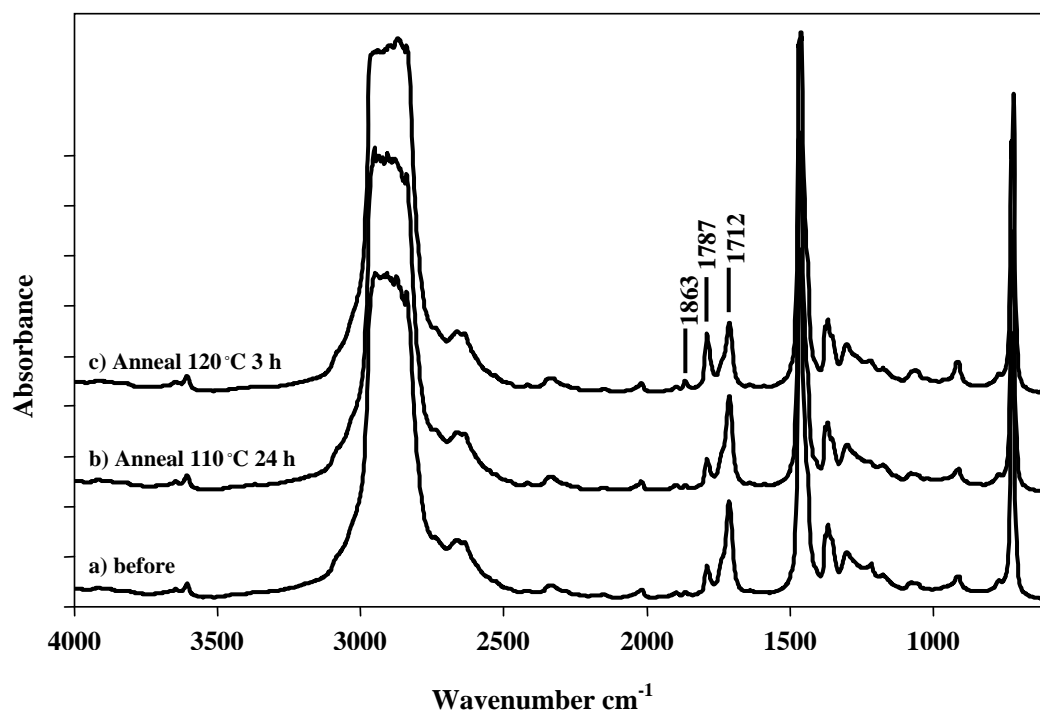


**Figure 5.8** FTIR spectra of PE-g-MAH film (a) before and after annealing at (b) 110°C, 24 h and (c) 120°C, 3 h.

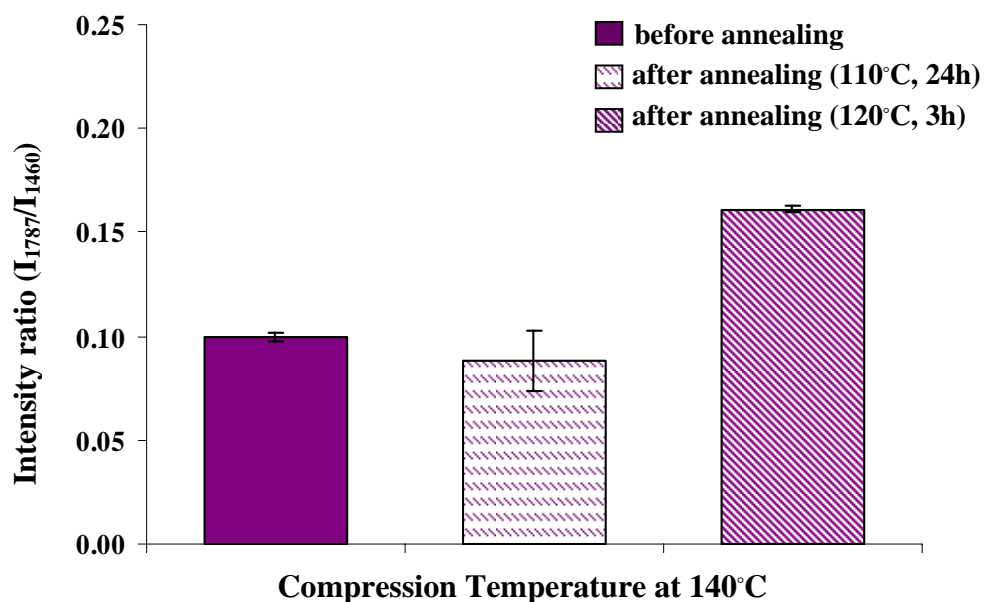


**Figure 5.9** Effect of annealing conditions on the carbonyl index of purified PE-g-MAH sample.

When the samples were submitted to heat treatment, the intensity of carbonyl bands located at 1712 and 1787  $\text{cm}^{-1}$  changed significantly (**Figure 5.8c**). This observation might be justified by the conversion of acid groups to anhydrides. The result for high temperature heating (120°C) showed the increase in the cyclic anhydride carbonyl band at 1787  $\text{cm}^{-1}$  and the reduction of the carboxylic acid carbonyl band at 1712  $\text{cm}^{-1}$ .

**Figure 5.9** shows intensity ratios of PE-g-MAH samples with and without heat treatment. The increase in anhydride groups was not affected by heating at low temperature (110°C). The intensity ratio of PE-g-MAH was raised from 0.10 to 0.16 when the annealing was carried out at 120°C 3 h. This was reported to be the results of increasing the formation of anhydride groups with annealing temperature [102].

From these results, it was concluded that the treatment which was proved as the most successful condition was to heat the specimen at 120°C for 3 h. The annealing at this condition led to high content of anhydride group in the polymer bulk.

In order to examine the surface properties of the specimen, PE-g-MAH films before and after annealing were characterized by using ATR-FTIR. The results were presented in **Figure 5.10**.

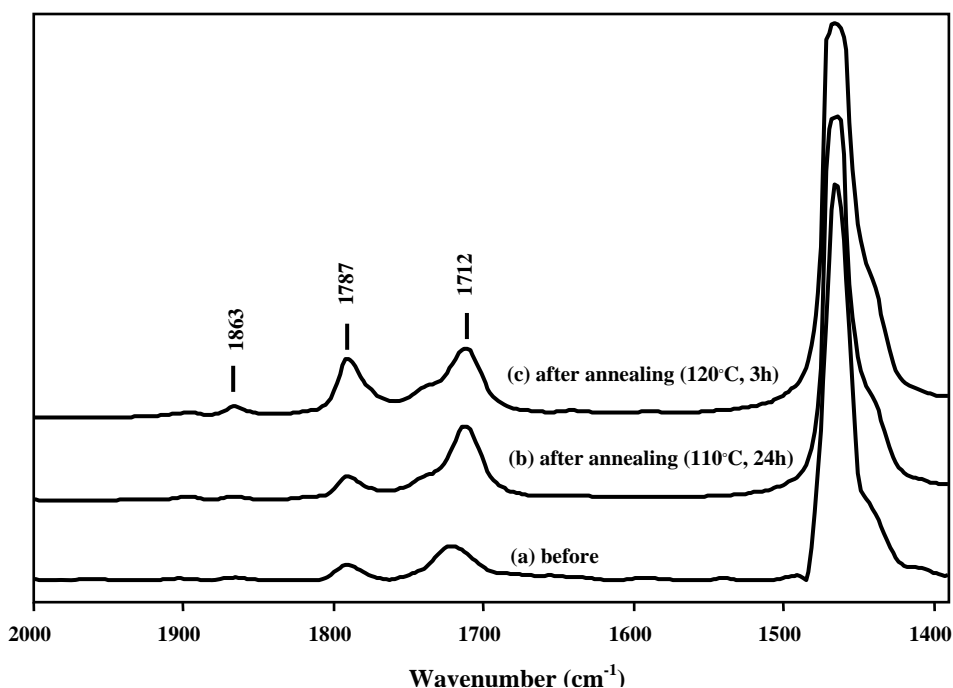


**Figure 5.10** ATR-FTIR spectra (Ge) of PE-g-MAH film (a) before and after annealing at (b) 110°C, 24 h and (c) 120°C, 3 h.

In **Figure 5.10**, it can be found that the annealing induced the converting carboxyl group into anhydride group on the film surface. This could be confirmed by the appearance of absorbance band at 1863  $\text{cm}^{-1}$  for annealing under temperature 120°C for 3 h and the decreasing of carboxylic peak (1712  $\text{cm}^{-1}$ ). Through annealing, two molecules of carboxylic groups change into an anhydride group by loss of one molecule of water. The reaction was shown in **Figure 5.11**.

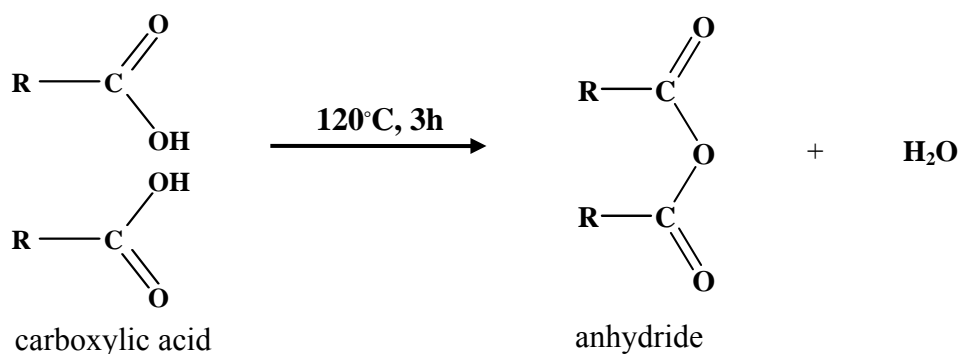


**Figure 5.11** Reaction of anhydride group conversion.

Water contact angle has been commonly used to characterize the relative hydrophilicity or hydrophobicity of film surface. Static water contact angles for the PE-g-MAH film under different annealing conditions are summarized in **Table 5.3**.

**Table 5.3** Effect of annealing on contact angle

<b>PE-g-MAH</b>	<b>Contact angle (°) (± 2)</b>
Non-annealed	83
Annealed (110°C, 24 h)	96
Annealed (120°C, 3 h)	101

It can be seen that the contact angle of non-annealed PE-g-MAH film is lower than those of annealed films. This indicated that the annealing of PE-g-MAH film increased the hydrophobicity of film surface. Changes of air-water contact angles for the annealed films were due to the increasing of anhydride group on the film surface. In addition, the annealing at temperature 120°C for 3 h gave higher contact angle than the annealing at temperature 110°C 24 h.

**Figure 5.12** shows the DSC cooling scan curves of purified PE-g-MAH before and after annealing.

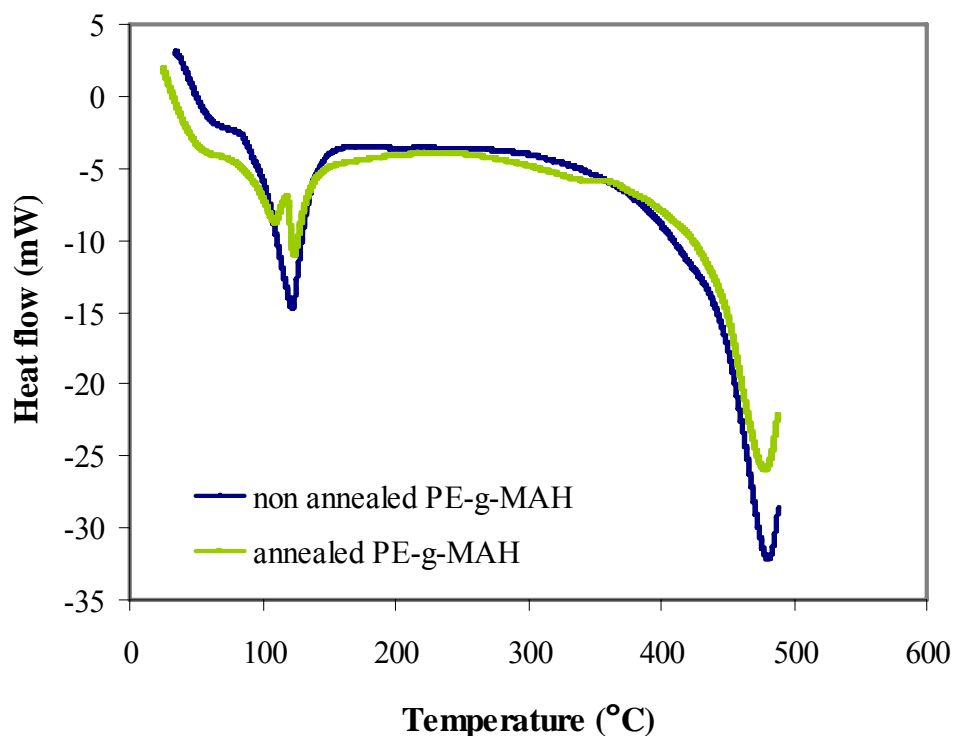


**Figure 5.12** DSC curves of purified PE-g-MAH before and after annealing.

From this figure, the annealed PE-g-MAH shows a cooling curve with two peaks at 108.3 and 123.4°C, while the non-annealed film shows only one peak at 122.9°C. It was demonstrated that after annealing, the PE-g-MAH produced two populations of crystals differing in orientation, which as shown in the DSC scan probably melt distinctly apart from each other. However, a changing of bulk properties after annealing has not effect on the amount of MAH.

In annealing effect study, the importance is focused on increasing of anhydride group and without changing on PE-g-MAH film samples which can be used to protein binding study.

## 5.2 Study of Protein Extraction from Dry Skim NR

In this work, extractable proteins from dry skim NR were selected to study protein binding ability of the PE-g-MAH film. Because skim NR contains higher protein content than dry NR. To ensure the difference of protein content, two NR samples were analyzed with FTIR technique and result obtained is demonstrated in **Figure 5.13**.

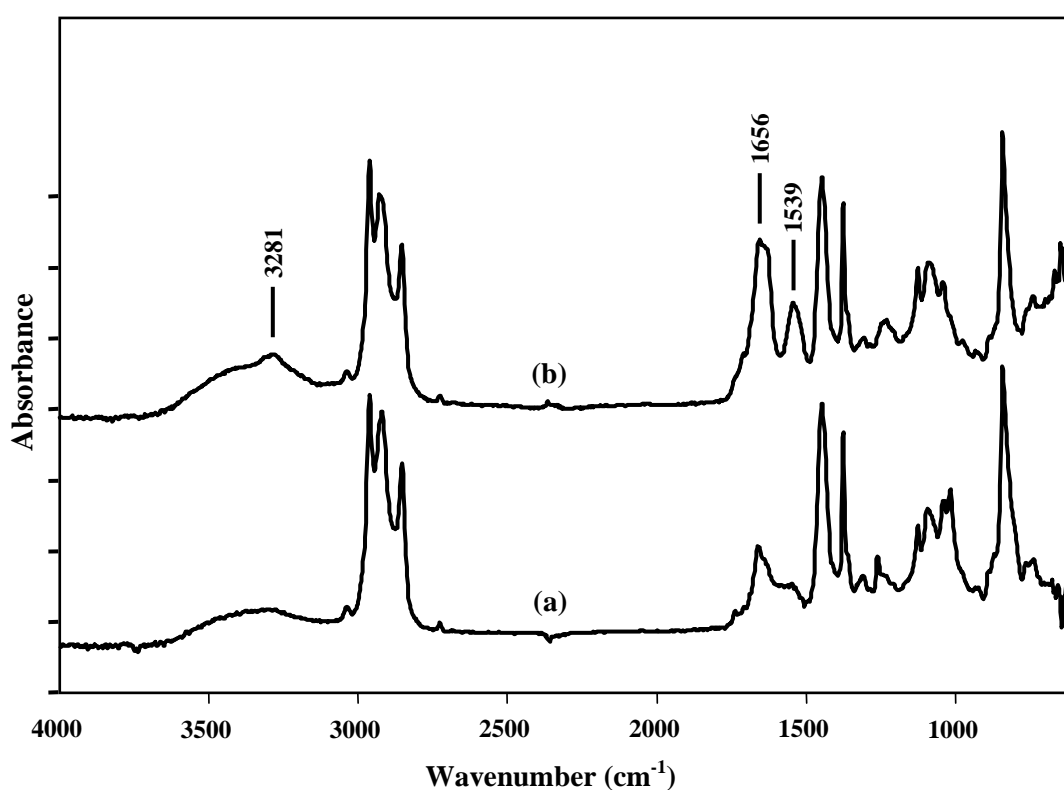


**Figure 5.13** ATR-FTIR spectra (Ge) of (a) dry NR and (b) dry skim NR.

The spectra of both NRs presented protein peaks at 3281, 1656 and 1539  $\text{cm}^{-1}$ , corresponding to N-H stretching, C=O stretching (amide I) and N-H bending (amide II) respectively. However, the significant difference in the spectra of two natural rubber samples is the much higher protein content in skim rubber.

### 5.2.1 Effect of Solution Type on Protein Extraction

The effect of solution type on protein extraction can be investigated by using FTIR technique. The spectrums of skim natural rubber before and after extraction for 12 h are shown in **Figure 5.14**. The principal peaks of proteins in skim natural rubber are observed: 3281, 1656 and 1539  $\text{cm}^{-1}$ . Their assignments are listed in **Table 5.4**. In this table, the absorption peaks are assigned to two categories: polyisoprene unit and protein.

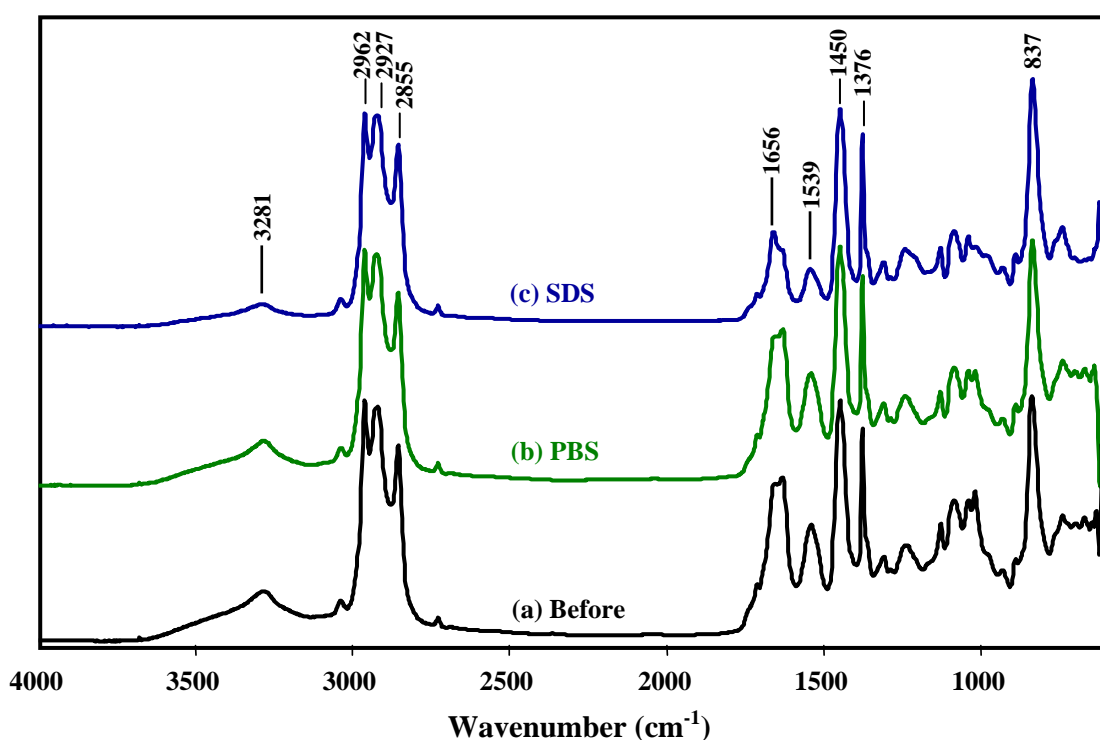


**Figure 5.14** FTIR spectra of skim natural rubber (a) before (b) after extraction with PBS and (c) after extraction with SDS.

**Table 5.4** The assignments of characteristic absorption peaks of skim natural rubber

Wavenumber (cm <sup>-1</sup> )	Description
<u>Isoprene unit</u>	
837	C = CH wagging
1376	C – H bending of CH <sub>3</sub>
1450	C – H bending of CH <sub>2</sub>
2855	C – H stretching of CH <sub>2</sub> , CH <sub>3</sub>
2927, 2962	C – H stretching of CH <sub>2</sub>
<u>Protein</u>	
1539	N – H bending (amide II)
1656	C = O stretching (amide I)
3281	N – H stretching

The efficiency of protein extraction with different solutions (PBS and SDS) could not be directly investigated from using the extractable protein yield because the protein precipitate in PBS was not produced. This may be due to the extremely dilute concentration of extractable protein in this solution. Therefore, the effect of solution type on protein extraction was analyzed from infrared results. After extraction, the decreasing of protein content in dry skim NR was observed. This result was in good agreement with that obtained by FTIR measurement (see **Figure 5.14**). A sharp decay of the protein bands was observed in the case of SDS solution. Therefore, the SDS solution was more effective than the PBS solution for protein extraction.

The efficiency of protein removal from dry skim NR was determined by two modes of infrared analysis, i.e., ATR and transmission. The results obtained were represented in terms relative intensity (RI) of N-H bending of amide group at 1539 cm<sup>-1</sup> to C-H bending of isoprene at 1375 cm<sup>-1</sup>. This reference peak is assigned to the methyl C-H bending and is insensitive to environmental change [104]. The difference between ATR and transmission mode is based upon the depth of IR beam penetrating into the sample.

In the terms of relative intensity, it can be seen that the intensity ratio of extraction with SDS are lower than that of extraction with PBS. The result indicated that SDS can remove large amount of proteins from natural rubber sample.

**Figures 5.15(a)** and **(b)** show intensity ratios of decreased proteins in the bulk sample and at the surface by transmittance mode and ATR mode respectively.

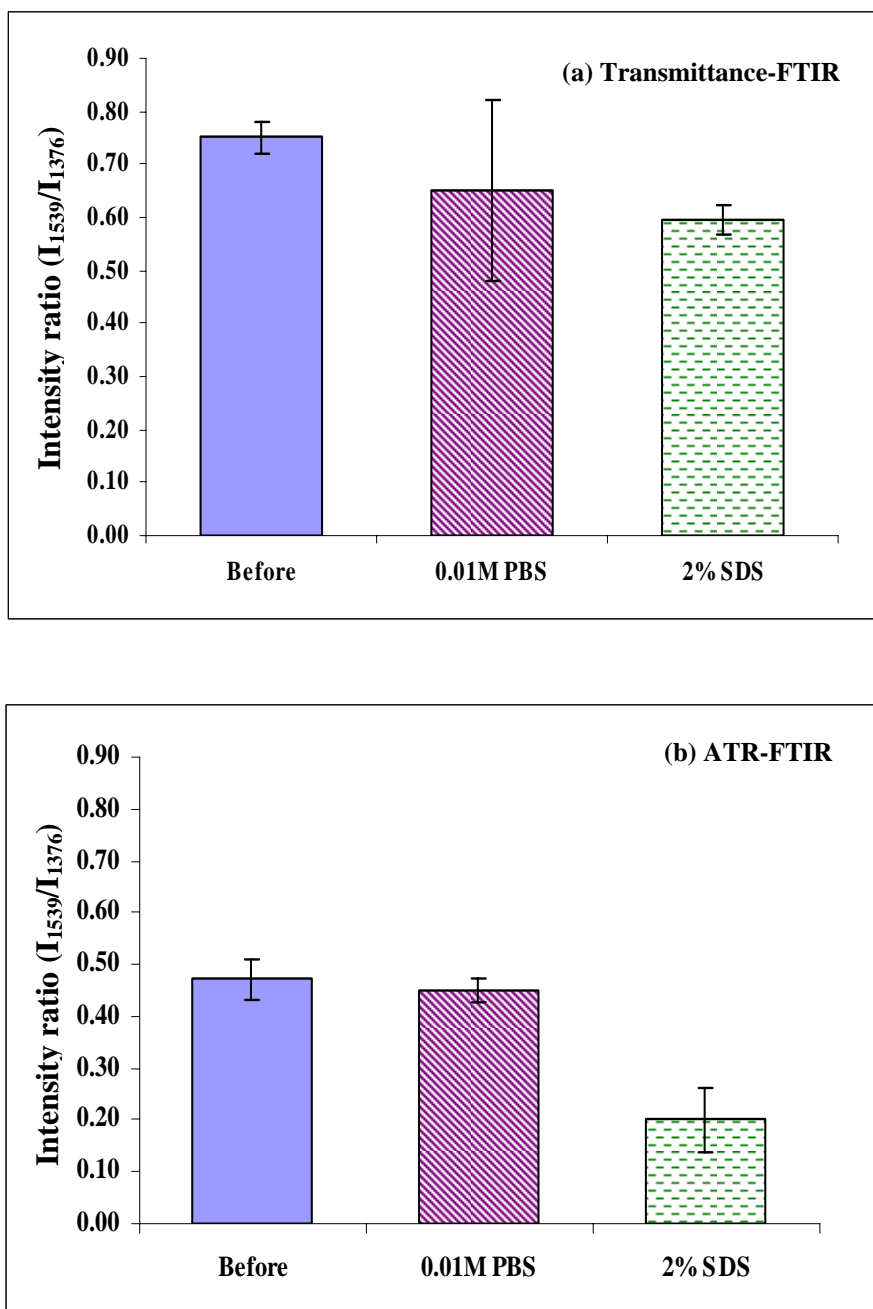


**Fig 5.15** Effect of extract solvent on intensity ratio of protein in dry skim NR: (a) transmittance mode and (b) ATR mode.

In the case of transmission mode, the protein in polymer bulk decreased after extraction in both solutions. And the extracted NR prepared using SDS shows a slightly lower residual protein in sample than that obtained using PBS. In the case of ATR mode, it clearly shows that SDS solution has a very high efficiency for protein removal from rubber surface.

In the study of Hasma et al. [82], they found that the SDS is effective detergent in solubilizing rubber particle-bound proteins.

From the results of infrared analysis, it can be concluded that the efficiency of protein removal depends on type of extract solution. Therefore, a SDS solution was selected to remove the tightly associated proteins from dry skim rubber in our following experiments.

### 5.2.2 Effect of Multiple Extractions

By repeating the extraction with fresh SDS solution, protein was continuously solubilized. Therefore, high protein content was expected to obtain by using the multiple extractions. In this work, the skim NR was cut into small pieces and the extraction with SDS was repeated three times.

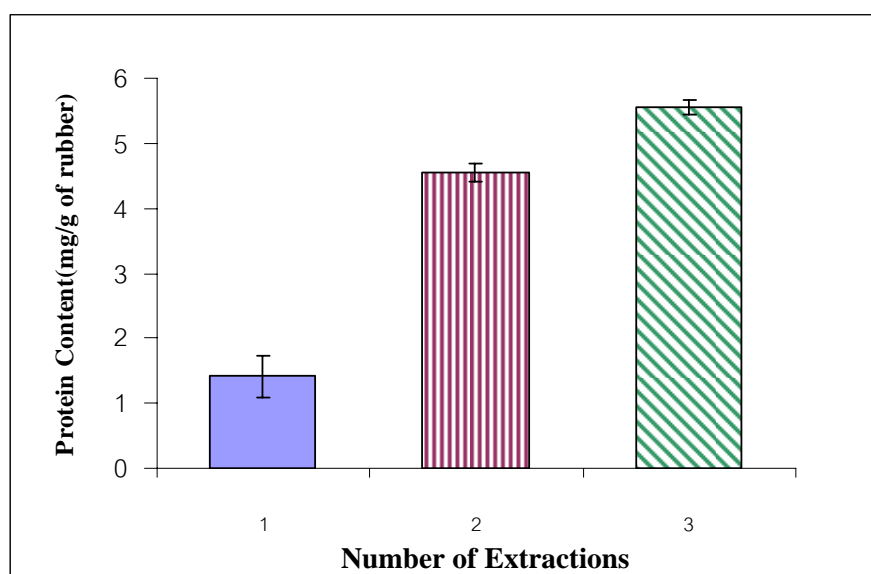


**Figure 5.16** Protein content from extraction with SDS by using multiple extractions.

**Figure 5.16** shows the extractable protein content from dry skim NR continuously increased as the extraction process was repeated. Three extractions yields the maximum protein content of 5.47 mg/g of rubber.

### 5.2.3 Effect of Sample Size

In general, a contact between surface of dry skim NR and extract solution is necessary for protein removal. Because protein on rubber surface is easily removed with extract solution. To evaluate the effect of sample size on protein removal from dry skim NR, two samples with different surface area to volume ratios were extracted by SDS solution. In this study, the rubber sheet with a thickness about 6 mm was obtained by dissolving skim NR in toluene. The samples were prepared into small sheet (0.5 x 0.5 cm<sup>2</sup>) and rubber disc of 7 cm in diameter. Protein concentration in extract solution was determined by using Bradford micro-assay. Total extractable protein is based on the sum of three SDS extractions (12 h/time) at room temperature. Data are shown in **Table 5.5**.

**Table 5.5** Effect of skim NR size on efficiency of protein extraction

Characteristic of sample	Protein contents (mg/g rubber)
Small sheet	11.16 ± 2.27
Rubber disc	2.27 ± 0.16

From this table, the sample size affects significantly the amount of protein extracted. The extractable proteins from small rubber sheets were five times higher than from NR disc. Higher protein content per gram of rubber was obtained in the extraction of smaller sample having a higher surface area. The increase of surface exposure to the extract solvent would be expected to improve extraction. And the result strongly demonstrated the important effect of surface area samples on protein extraction process.

The smaller size of the suspended sample yields a greater surface per unit sample mass that would lead to each protein extraction.

From all results, it can be concluded that the protein extraction by fresh SDS solution and repeating extraction to three times gives a high extractable protein content.

### 5.3 Characterization of Extractable Protein

The proteins obtained were subjected to the following tests:

#### 5.3.1 Molecular Weight of Extractable Protein

Protein was removed from dry skim NR by extraction with 2% SDS, precipitated with TCA, and then analysed by SDS-PAGE. From SDS-PAGE, the extractable proteins were separated and identified based primary on their molecular weight, as shown in **Figure 5.17**.

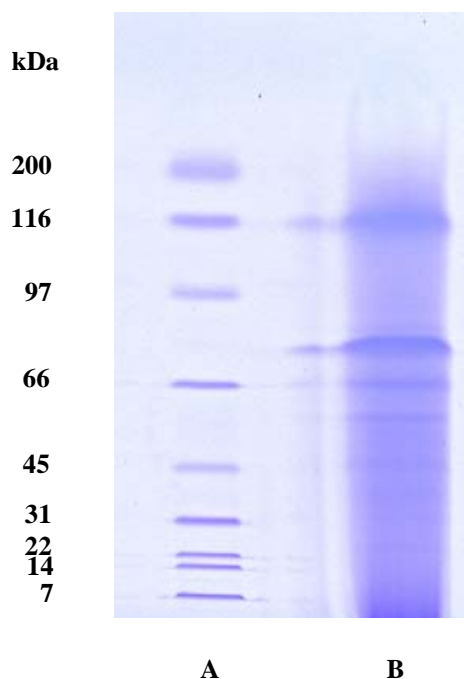


**Figure 5.17** SDS-PAGE images of standard protein (A) and extractable protein from dry skim NR (B).

**Figure 5.17** shows SDS-PAGE gel image of Standard protein (lane A) and Extractable protein (lane B). The positions of the molecular weight markers indicated at the left of the figure include many protein standards as shown in **Table 4.5** (see p. 19 section 4.6.1.2)

In this result, it was found that the extractable proteins presented three bands. The two bands had molecular weight of 66 and 116 kDa, corresponding to serum albumin and  $\beta$ -galactocidase respectively. And the unknown protein band had apparent molecular mass between 66 and 97 kDa.

### 5.3.2 Composition and Structure of Extractable Protein

After protein extraction, the extract solution was precipitated with TCA and immediately prepared into dry sample by using freeze drying process.

Protein precipitation is necessary to concentrate and eliminate interferences before protein analysis.

A freeze drying process usually consist of three stages: freezing, primary drying and secondary drying. In the first stage, freezing, the aqueous solution that has been filled into containers is frozen to a very low temperature, usually lower than  $-40\text{ }^{\circ}\text{C}$ . Then, in primary drying, the freeze dryer chamber is evacuated and the shelf temperature is elevated to sublimate ice out of the system. After all of the ice has been removed from the containers, the shelf temperature is further increased to remove unfrozen water by desorption. This stage is called secondary drying.

Freeze drying of extractable proteins yields a brownish powder material. Then, it was devided into two parts. In first part, a composition of freeze dried protein from extracts was demonstrated by elemental analysis. An accurately weighed protein powder ( $\sim 1.0\text{ mg}$ ) was burned in pure oxygen under static conditions to produce combustion products of  $\text{CO}_2$ ,  $\text{H}_2\text{O}$  and  $\text{N}_2$ . These samples were automatically analysed in a thermal conductivity analyzer. The weight percentages of nitrogen, carbon and hydrogen of the studied proteins are summarized in **Table 5.6**. The BSA standard protein was also evaluated.

**Table 5.6** CHN content of extractable proteins

Sample	%		
	C	H	N
BSA	45.39	7.55	13.51
Extractable Protein	46.84	8.05	2.75

It is well known that because the nitrogen is a main element of protein, the total nitrogen from CHN analysis can be determined to crude protein with a high degree of accuracy. Furthermore, Vemuri S. [104] reported that peptide content could be assessed by elemental analysis (CHN). This method yields highly precise values and preferable because it does not require a standard curve of reference standard. In general, the nitrogen content is multiplied by the known matrix-specific protein factors, and this provides the raw protein content.

From the result, the nitrogen content of extractable proteins is lower than that of BSA standard. This seems to suggest that with CHN analysis, BSA contains higher protein content. This is possibly due to the fact that precipitated samples prepared from extract solution of skim NR consist of protein and nonprotein components. The another reason to explain this result is the difference in amino acid composition between BSA and extractable proteins. The BSA has a high content of lysine and arginine amino acids with  $-\text{NH}_3^+$  groups in their side chains.

The structures of freeze dried protein and BSA standard protein were analyzed by using ATR-FTIR measurement. The results can be seen in **Figure 5.18**.

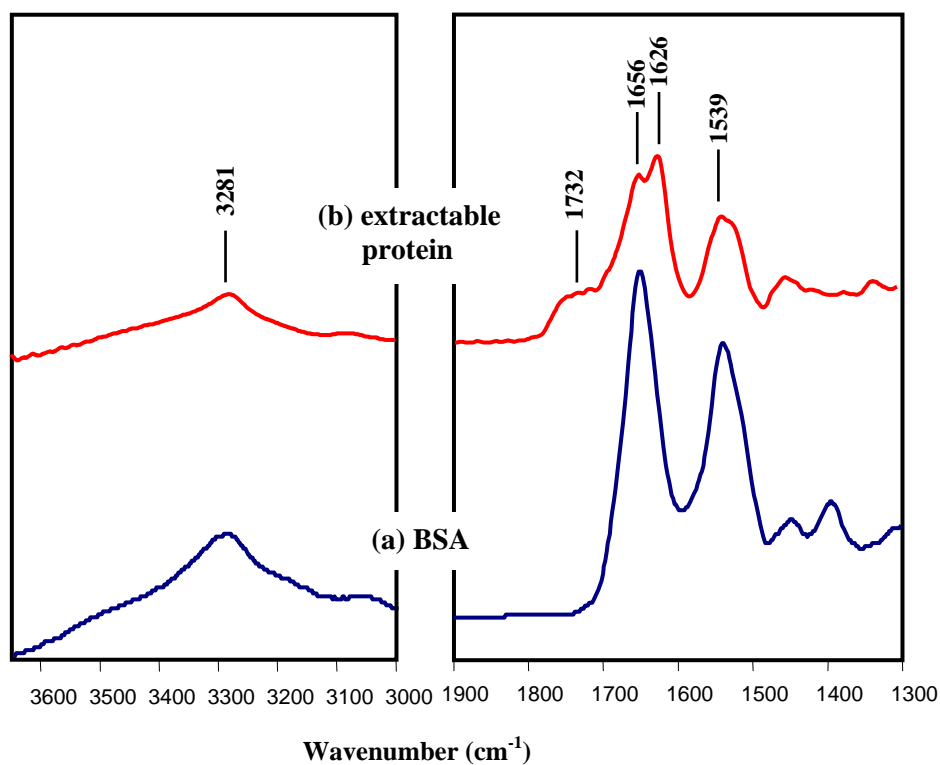


**Figure 5.18** ATR-FTIR spectra of (a) BSA standard protein and (b) extractable protein.

From this figure, although there were impurity peaks at 1732 and 1626 cm<sup>-1</sup> due to interference of nonprotein substances, the spectrum of freeze dried protein was similar to that of BSA standard protein. The protein bands observed at 3281, 1656 and 1539 cm<sup>-1</sup> were attributed to NH stretching, amide I and amide II. Therefore, it can be confirmed that the obtained sample from acid precipitation step is really extractable protein.

## 5.4 Protein Content Analysis

Several spectroscopic methods are commonly used for determination of protein content. However, the appropriate choice of method depends on five major criteria: the amount of protein available to assay, the concentration of protein, the specificity of the assay, the presence of chemicals which may interfere with the assay and the ease and reliability of performing the assay. Furthermore, to obtain accurate estimates of protein concentrations using these methods, it is important to select an appropriate standard to calibrate the method, which has a similar amino acid composition to the protein being analysed.

Ultraviolet light absorption methods are a rapid and convenient method. Generally, proteins actively absorb light in the ultraviolet region with two maxima, 280 nm and 200 nm [105]. Amino acids with aromatic rings such as tryptophan, tyrosine and phenylalanine (**Figure 5.19**) are the primary reason for the absorbance peak at 280 nm. Peptide bonds are primarily responsible for the peak at 200 nm. Although sensitive area of the protein spectrum at wavelength 280 nm is lower absorbance than those at wavelength 200 nm, this wavelength has been found to be convenient for protein estimation because fewer chemicals absorb at this wavelength than at shorter wavelength. So, the presence of protein in sample can be determined by measuring the amount of light absorbed at 280 nm.

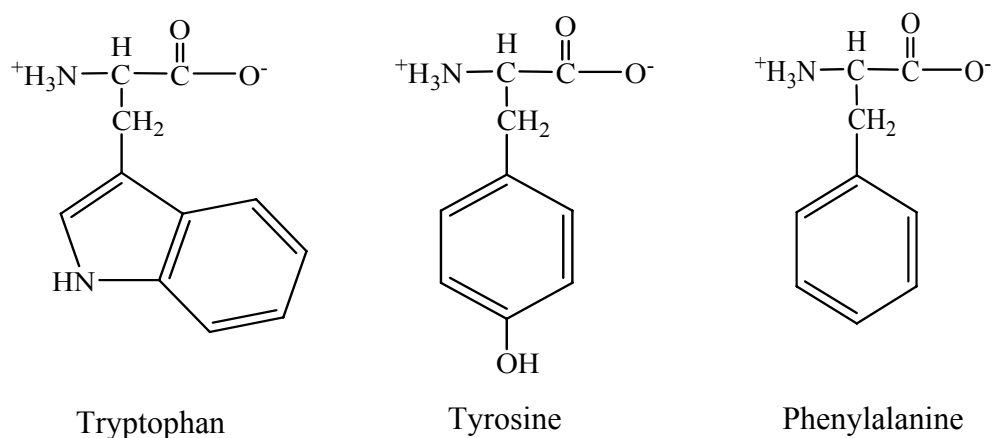


**Figure 5.19** Aromatic amino acids in proteins absorb light at 280 nm [106].

Absorbance assays at 280 nm is a widely used method to determine the protein concentration [107-108]. This is because of its simple and rapid. It can be performed directly on the sample without of any reagents and no protein standard need to be prepared. Depending on the protein, the relationship between protein concentration and absorbance is linear in a range from about 0.1-5 mg/ml.

To investigate accuracy of this method, the BSA protein standards were prepared into range of concentration 0-20  $\mu\text{g/ml}$ . Their UV-VIS spectra were recorded from 400 to 200 nm and shown in **Figure 5.20**.

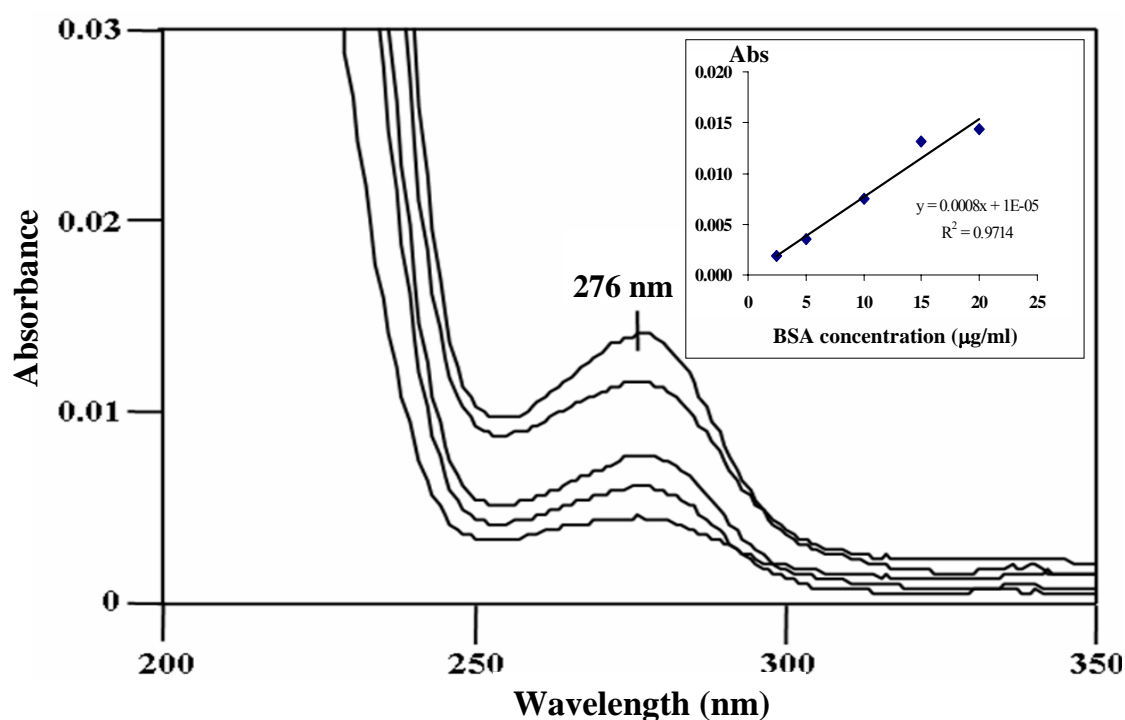


**Figure 5.20** UV-VIS spectra recorded for increasing BSA concentration in the range of 0-20  $\mu\text{g/ml}$  (pH~ 6-7) and standard curve of 276 nm, absorbance versus protein concentrations

From **Figure 5.20**, it is clearly seen that the spectra consisted of a single maximum at wavelength 276 nm. The maximum absorbance was increased when increasing of BSA concentration. The calibration curve was plotted using absorbance at 276 nm versus concentration of the standard solutions. The calibration curve showed a linear response over the range of concentrations used in the assay

procedure. Sensitivity of the assay can be described in terms of absorbance per mg/ml protein in the sample. The sensitivity at 276 nm for this albumin preparation is 0.80 absorbance units per mg/ml.

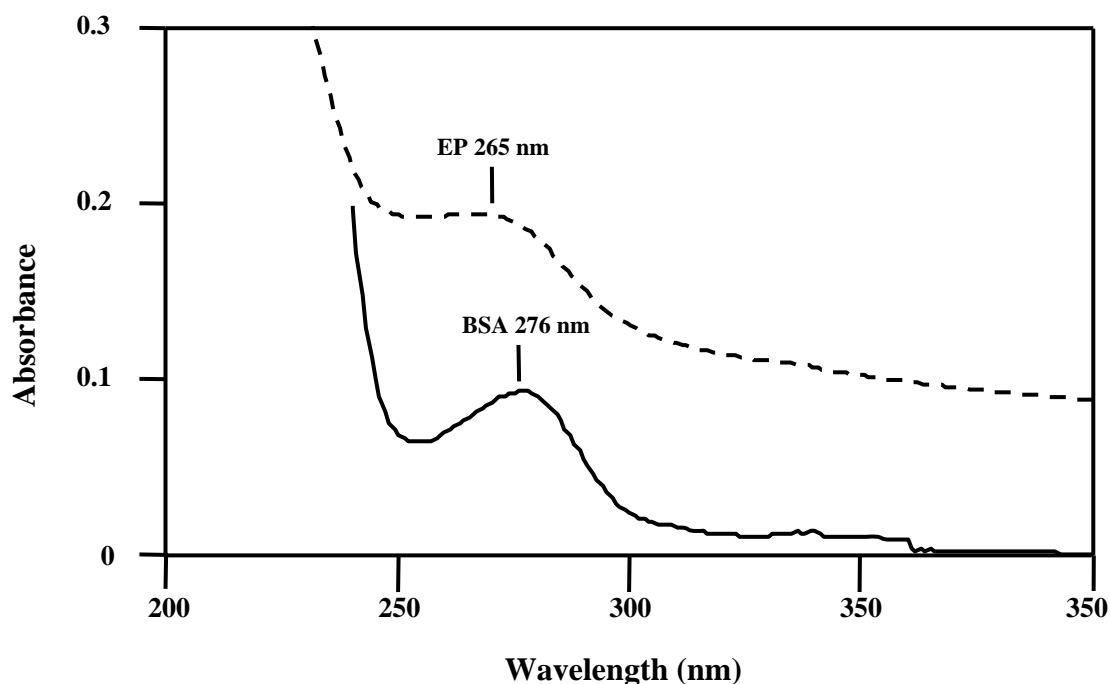


**Figure 5.21** UV absorbance spectra for BSA and extractable proteins (EP).

With the extractable proteins (**Figure 5.21**), the peak shifted to the left with a maxima at 265 nm. An absorbance of 0.088 at 276 nm indicated the presence of proteins in the sample. Although, this method can analyze directly protein, a considerable error can be occurred because different proteins have widely varying absorption characteristics, especially for unknowns or protein mixtures. Any non-protein component of the solution that absorbs ultraviolet light will interfere with the protein. In our sample, the contamination was evidenced by a higher absorbance value at 265 nm. It can be said that measurement of the UV absorbance at 276 nm is most useful for pure protein solutions.

When the direct absorbance assay at 280 nm is not efficiency for protein content analysis in this work, the assay by adding reagent was used. The Bradford assay is one of the most sensitive methods for protein analysis. It was found that the protein-

dry complex has a high maximum absorbance thus leading to great sensitivity in measurement of the protein.

The Bradford assay, known as the Coomassie brilliant blue (CBBG) protein assay [85], is widely used because of its ease of performance, rapidity, relative sensitivity and specificity for proteins. It is based on a formation of a complex between the dye (Brilliant Blue G) and protein in solution. The dye-binding was due to electrostatic attractions of the dye's sulfonic groups (in **Figure 5.22**) with protonated primary amino groups of protein (positively charged residues), such as lysine, arginine and N-terminal groups [97]. The Bradford assay is, however, protein dependant, non-linear and detergent incompatible.

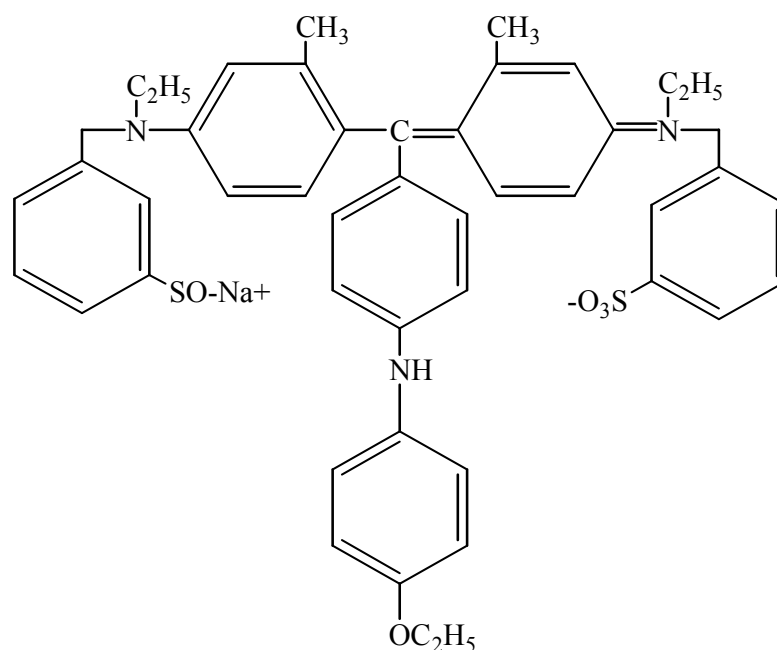
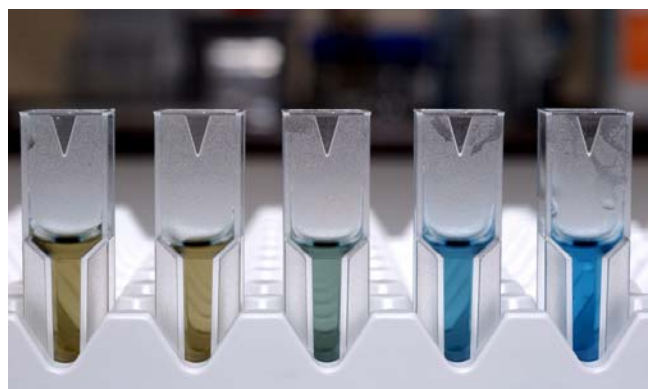


**Figure 5.22** Structure of Coomassie brilliant blue (CBBG) G-250 dye [87].

When the protein solution was reacted with Bradford reagent, the dye binds to protein to form a dye-protein complex. This process results in a shift in absorbance, which corresponds to a color change, and the complex has a maximum wavelength at 595 nm. **Figure 5.23** shows the color changes after the formation of the CBBG-protein complex of BSA at different total protein concentrations. Solution without protein still

is reddish brown. Solutions with protein turn blue: the more concentrated the protein, the more blue solution is obtained.



Blank      low       $\longrightarrow$       high concentration

**Figure 5.23** Colors of a typical standard curve.

Addition of the dye reagent to protein results in a change of maximum wavelength, as seen in **Figure 5.24**.

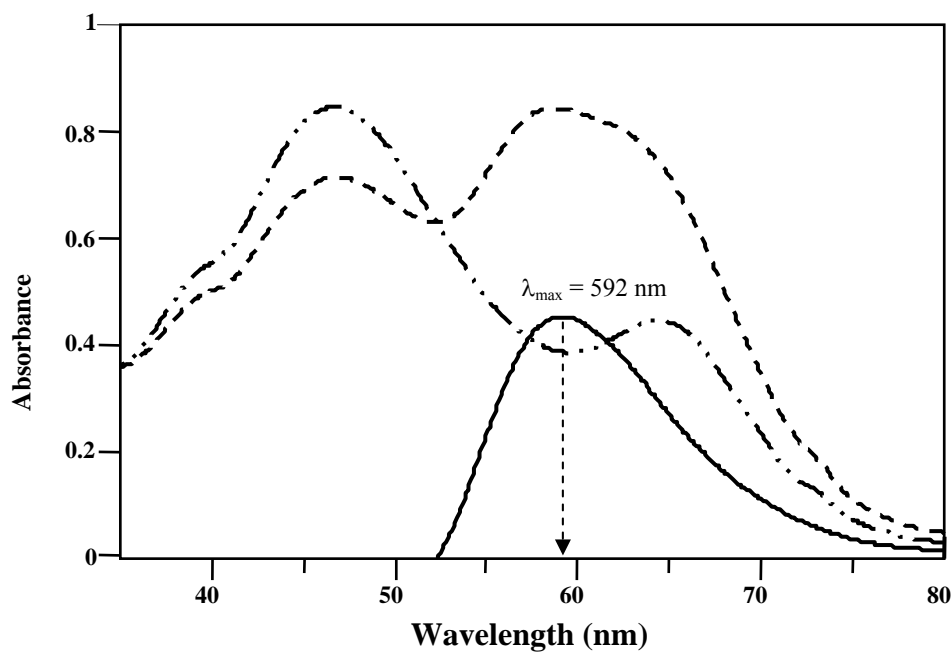


**Figure 5.24** UV-VIS spectra of CBBG without protein (— · ·), with 20 µg/ml BSA (pH 0.4) (— — —) and blank subtraction (——).

The absorbance spectrum of dye reagent shows maxima at 470 nm (red dye form) and 650 nm (green dye form). Addition of protein to the dye reagent results in a marked decrease of the 470 nm absorption, a new shoulder at 592 nm, and little change at 650 nm. Subtraction of the dye blank results in a single absorption maximum at 592 nm. Under this subtraction, there are practically no free dye molecules, as demonstrated by the complete disappearance of the red dye form that absorbs at 470 nm. The similar results were reported by Compton and Jones [87] in which the dye-protein complex had an absorbance maximum at 595 nm as well as negative minima at 470 and 650 nm.

Fazekas de st. Groth et al. [97] reported that a reduction in the number of protein primary amino groups should result in reduced dye response. This observation was found that the color development is essentially completed within 2 min, and remains stable for a period of 1 h. A fading of the color after this period of time was occurred by the physical removal of the protein-dye complex from solution.

Chial and coworkers [94], found that the calibration curve of Bradford method depends on assay procedure. When the pH was raised, a reddish ionic form of the dye ( $\lambda$  max = 470 nm) is replaced by a greenish dye form ( $\lambda$  max = 650 nm) in the vicinity of pH 1. The aim of this following study was to find the optimum condition (with respect to high sensitivity and accuracy) for determining residue protein in solution. The reagent volumes used in two experiments are shown in **Table 5.7**.

**Table 5.7** Preparation of calibration curve in different assays

Assays	pH	BSA stock concentration (mg/ml)	Bradford reagent ( $\mu$ l)	Phosphate buffer ( $\mu$ l)	Total volume ( $\mu$ l)
I	0.2-0.4	1	1000	80-100	1100
II	0.4-1.0	0.02	200	0	1000

When all reagents were mixed, the mixtures were analysed by UV-VIS spectrophotometer. The spectra recorded in the range 350-800 nm of the dye-protein complex at different conditions are presented in **Figure 5.25**.

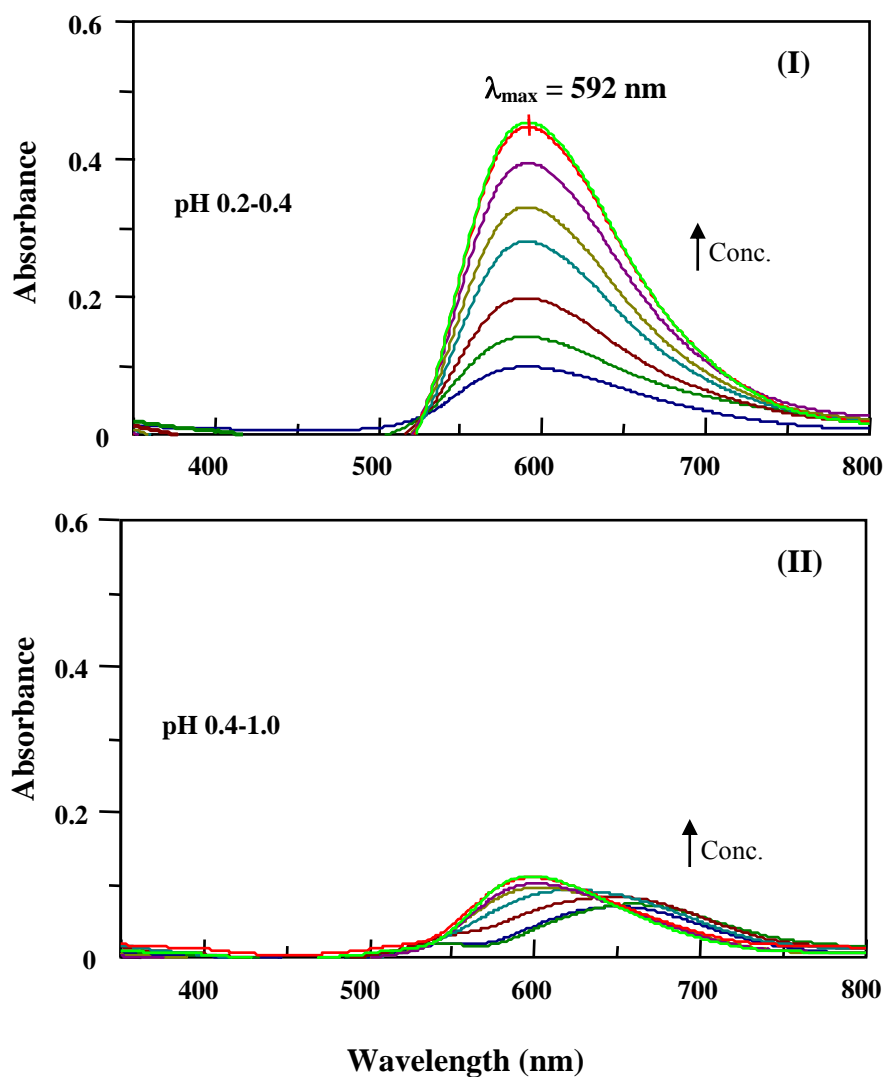


**Figure 5.25** Spectra of CBBG-protein complex of BSA under two different conditions Assay I) BSA 0-20  $\mu\text{g/ml}$ , pH 0.2-0.4, Bradford concentration = 90.9%v/v Assay II) BSA 0-12  $\mu\text{g/ml}$ , pH 0.4-1.0, Bradford concentration = 20.0%v/v.

In general, Coomassie Brilliant Blue G interacts with protein and stain blue under acidic conditions. **Table 5.7** shows that all standard solutions had pH values in the range from 0.2 to 1.0.

From **Figure 5.26**, a different characteristic of absorption spectra was observed. In the case of assay I, the dye-protein solution absorbed light at a wavelength of 592 nm. Furthermore, the maximum absorption increased with increasing BSA concentration. While assay II gave a shift in maximum absorption from 645 nm at pH 0.4 to 598 at pH 1. The change in the spectral shape might be due to the change of pH in protein solution. A variation in pH values is believed to involve absence of phosphate buffer in solution. The phosphate buffer is used when working with proteins to resist changes in the hydrogen ion concentration (pH) of protein solution. It helps to maintain in native conformation of protein. So the shift of maximum absorption was not observed in assay I which had pHs of 0.2-0.4.

Comparison of the intensity peak, it was found that the assay I was more sensitive than the assay II. It seems that the higher concentration of Bradford reagent in assay I is prone in promoting the formation of dye-protein complex, leading to an increase in absorbance. Thus, altering a sample to reagent ratio increased the sensitivity of the test. In addition, assay linearity may be improved by increasing the amount of dye in the system.

From the results, it was concluded that the assay I is suitable for calibration curve preparation in Bradford method because of high sensitivity and accuracy. These lead to a good linearity of standard curve.

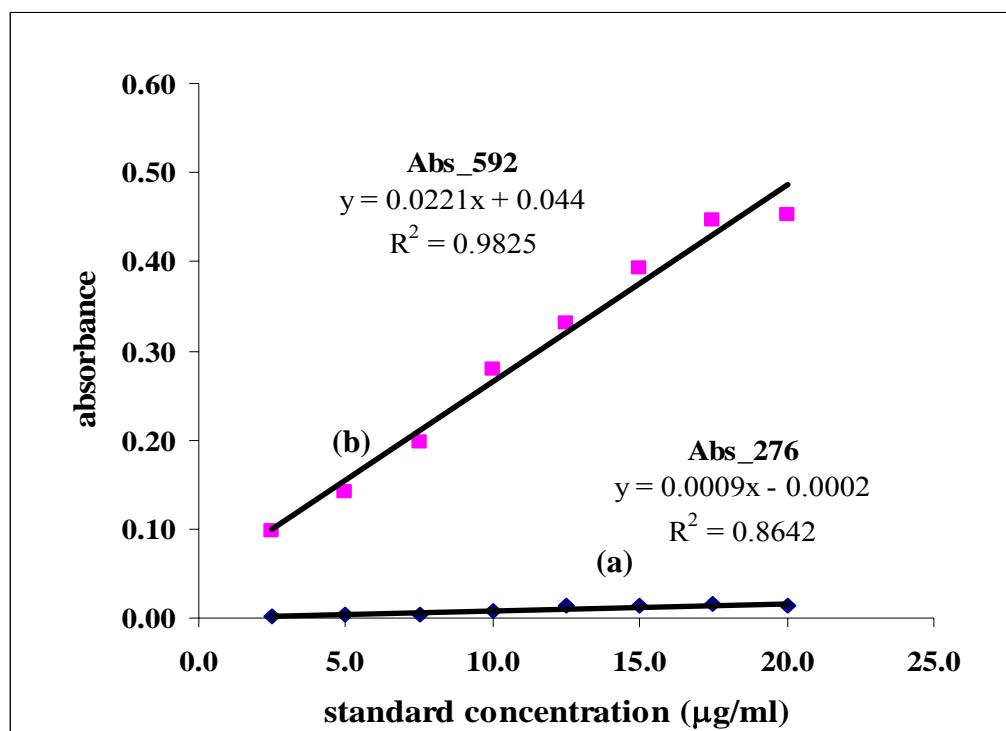


**Figure 5.26** Calibration curves of BSA standard for  
(a) the spectrophotometric assay ( $\lambda_{\max} = 276$  nm)  
(b) the Bradford assay ( $\lambda_{\max} = 592$  nm).

**Figure 5.26** shows calibration curves of BSA obtained using the spectrophotometric assay ( $\lambda_{\max} = 276$  nm) and the Bradford assay ( $\lambda_{\max} = 592$  nm). The linearity of both calibration curves was observed under standard analytical conditions.

Sensitivity of the assay can be described in terms of absorbance per mg/ml protein in the sample. The sensitivity at 276 nm for this albumin preparation is 0.90 absorbance units per mg/ml. A sensitivity of 22 absorbance units at 592 nm was observed for the mixture of same sample and Coomassie Brilliant Blue. This indicated that the “Bradford” assay approximately twenty-two times more sensitive than the spectrophotometric assay.

It was known that an important drawback of the Bradford method stems from its variation in response to different proteins. For any given proteins, however, overestimation of protein will occur when a non-protein produces a 595 nm absorption that is not compensated for by the solvent-dye blank. Since the assay

system is based on the interaction of hydrophobic sites of protein, detergents severely interfere with micro assay.

**Table 5.8** shows the maximum non-interfering concentrations of materials, which were used to dissolve extractable proteins prior to mixing with Bradford reagent (urea, triton x-100 and 2-mercaptoethanol) and dilute protein solution (PBS).

**Table 5.8** Compatible concentrations of possible interfering materials with Bradford assay

Chemical	Compatible concentration	Concentration in our samples
Urea	3.0 M	$1.85 \times 10^{-2}$ M
Triton® X-100	0.125 %	$9.27 \times 10^{-3}$ %
2-mercaptoethanol	1.3 M	$2.3 \times 10^{-5}$ M
PBS	No interference	-

In order to make sure there are no interference of these substance present in the protein solution, the concentrations of each material were evaluated. It was found that their concentrations in the sample were too dilute to affect the protein assay.

From all these results, the Bradford assay was selected to be used in our following experiments because it is fairly rapid, very sensitive and relatively resistant to interference by other compounds present in the protein solution.

## 5.5 Study of Protein Binding on PE-g-MAH Film

The use of two PE-g-MAH films, prepared UV photografting and compression of commercial granule, for protein binding was investigated in this part. In preliminary study, milk was selected as a sample solution because it has high protein content and lower interference than other materials. The Bovine Serum Albumin (BSA) was used as a model protein to study optimum immersion time for protein binding. After binding, the changes of chemical structure on the film surface and the amount of immobilized protein were analysed.

### 5.5.1 Possibility of Protein Immobilization on the PE-g-MAH

In this part, the protein binding was studied in milk by using PE-g-MAH granule as a solid support. The protein components of milk could be divided into two groups, the casein function and the whey proteins. They are shown in **Table 5.9**.

**Table 5.9** The components of protein in milk

Protein	Content (%)
<u>Caseins:</u>	
$\alpha_{s1}$ - casein	32
$\alpha_{s2}$ - casein	8
$\beta$ - casein	32
$\kappa$ - casein	8
Total	80
<u>Whey proteins:</u>	
$\beta$ - lactoglobulin	12
$\beta$ - lactalbumin	4
Immunoglobulins	3
Serum albumin	1
Total	20

From this table, it can be seen that casein is one of the most nutritive milk proteins in that it contains all of the common amino acids and tends not to have a particularly compact globular structure. It forms complexes called micelles that are dispersed in the water phase of milk. The casein micelles consist of subunits of the different caseins ( $\alpha_{s1}$ ,  $\alpha_{s2}$  and  $\beta$ ) held together by calcium phosphate bridges on the inside surrounded by a layer of  $\kappa$ -casein which helps to stabilize the micelle in solution, as shown in **Figure 5.27**.

Molecular Formula of Casein:  $C_{47}H_{48}N_3NaO_7S_2$

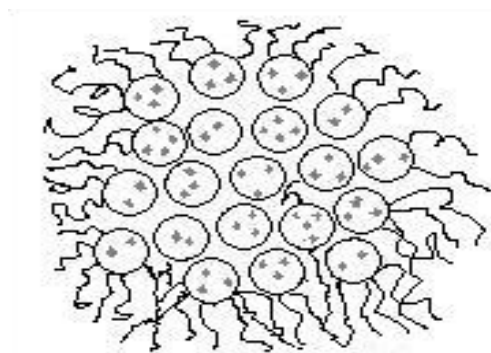


**Figure 5.27** Casein Micelle

- submicelle
- ◆ Calcium phosphate
- ~  $\kappa$ -casein peptide chain

The covalent coupling of protein molecules to PE-g-MAH resin involves mild reaction. The reaction mixture was stirred in varied times from 5 to 9 h at temperature about 10°C to maintain a stability of protein and its coupling reaction mostly occurred on the surface. After binding, the ATR-FTIR technique was used to analyze a change of the chemical structure on the surface. The result is shown in **Figure 5.28**.

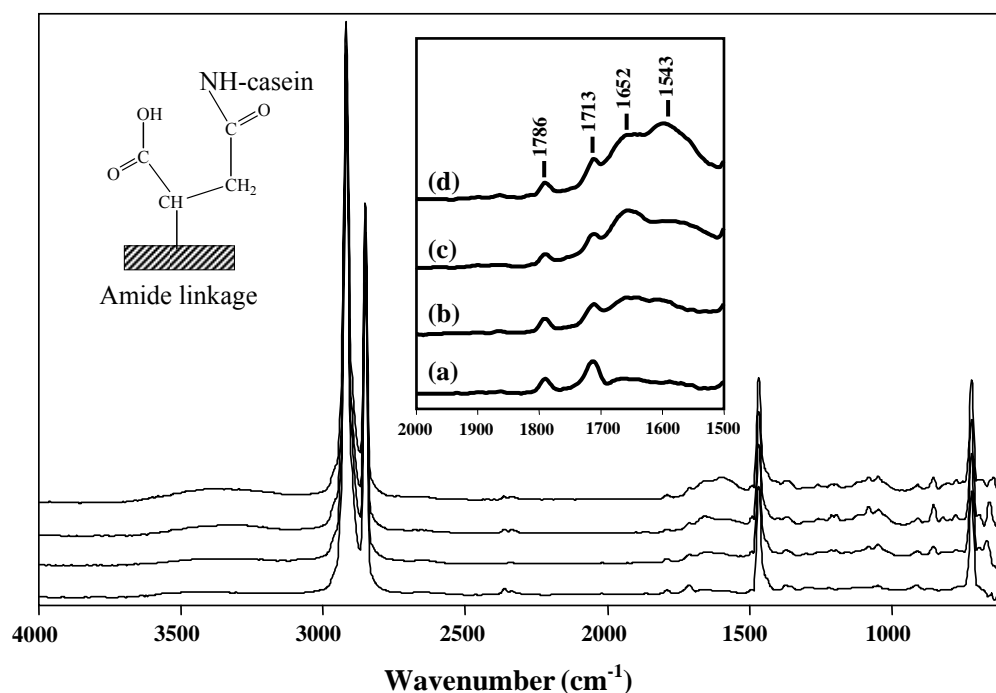


**Figure 5.28** ATR-FTIR spectra of resin before (a) and after binding protein in milk (b) 5 h, (c) 7 h, (d) 9 h.

ATR spectra in **Figure 5.28** present the evidence of the protein immobilization onto the polymeric substrate. Two characteristic peaks, 1652 cm<sup>-1</sup>(amide I) and 1543 cm<sup>-1</sup>(amide II), are inspected as proof of the presence of protein on the surface. The amide I band originates predominantly from the C=O stretching vibration of the peptide groups. Furthermore, it was found that ability of protein binding increased with increasing time to 9 h of binding reaction. From the obtained result, it is possible that the protein could be immobilized onto PE-g-MAH under mild condition.

### 5.5.2 Determination of Optimum Immersion Time

It was reported that the amount of immobilized protein on the substrate is upon a change in immersion time for protein binding [8-9, 109-111].

To determine the suitable time for protein immobilization, the commercial PE-g-MAH film having approximately 2x2 cm<sup>2</sup> was used for BSA binding. The reaction temperature was kept at room temperature and the immersion time was varied from 2 to 8 h. **Figure 5.29** shows the kinetics of protein binding on PE-g-MAH film.

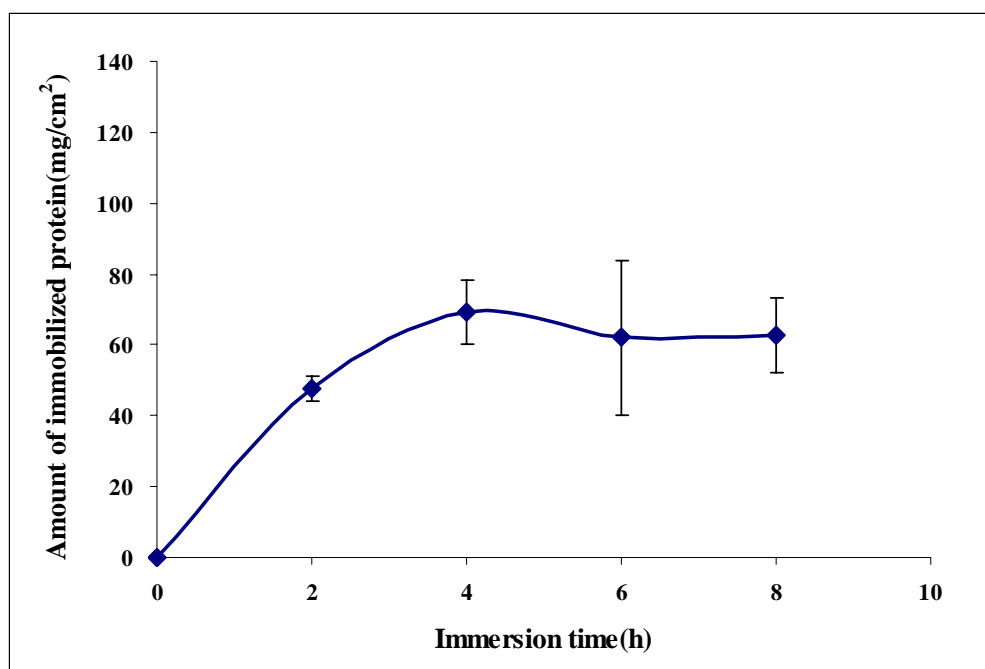


**Figure 5.29** Effect of binding time on the amount of immobilized protein (BSA) on commercial PE-g-MAH film.

It was found that as the immersion time increased, the amount of immobilized protein increased in the first 4 h of protein binding. After this time, the protein immobilization on polymeric surfaces is completed. This may be because the binding reaction is controlled by a steric effect. When a longer immersion time was used, the residue amino groups of protein are difficultly immobilized onto PE-g-MAH film. So, the optimum immersion time at 4 h was selected for protein binding study. A similar result was found earlier by Avramescu et al. [8] for BSA-coupling on ethylene vinyl alcohol copolymer (EVAL) membranes activated by CO<sub>2</sub>-plasma treatment. The amount of protein bound onto the EVAL membranes was presented as a function of the reaction time. The curve of binding time shows high-protein binding rate at the initial time and constant rate in the next time, in which the amount of immobilized BSA is completed after 8 h. Furthermore, a similar results was also found by Can and Güner [110]. They explained that the constant binding rate at the longer time may be because of the decrease in BSA concentration in the container with time due to protein binding.

### 5.5.3 Study of Protein Binding with Extractable Protein.

#### 5.5.3.1 Determination of Coupling Condition

On the basis of results obtained in a previous study on bovine serum albumin, the immobilizing of protein onto PE-g-MAH film was tested in aqueous buffer. The result showed that the immersion time at 4 h gives the highest amount of immobilized protein. This time was applied for extractable protein binding study.

We designed a similar strategy as that used for protein binding study. The first step of this strategy was to develop a methodology to bind proteins onto polymer in solution under limited volume of extracted protein and apply many samples for testing in the same time. So, in this work, a small size of PE-g-MAH film was used in this experiment and the protein solution was contained in microtube (~ 1.5 ml) for occurring coupling reaction. The setup of protein binding testing is shown in **Figure 5.30**.

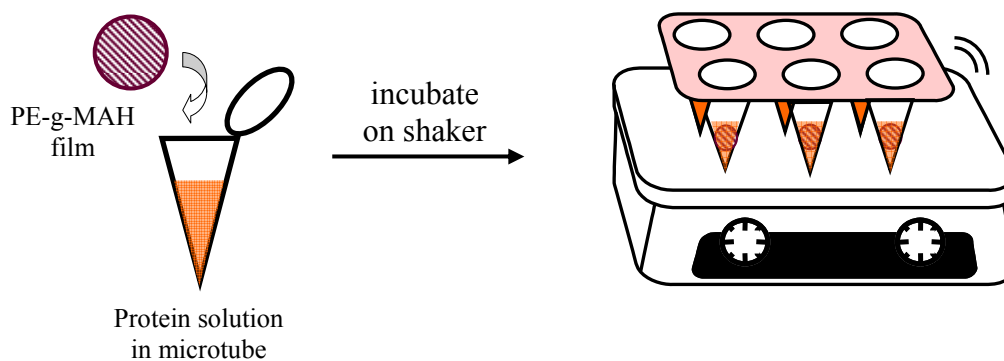


**Figure 5.30** The setup of protein binding testing.

Ladavière et al. [9] reported that the reproducibility was quite satisfactory for experiments run on the same day with identical reactant solutions. But, when differing reagent stock solutions were used, the day to day reproducibility was only fair. It is probably occurred because a slight variation in the preparation of the stock solutions had a greater impact on the course of the reaction. In this work, to avoid an error in protein binding process, a fresh stock solution of protein was prepared in all

experiment and the reproducibility of experiment runs with the same protein solution on the same day.

The immobilization reaction onto the PE-g-MAH occurs by nucleophilic attack of the reactive anhydride moieties by the primary amine groups of the proteins, as depicted in **Figure 5.31**. The immobilization of protein onto maleic anhydride was described by Brissova et al. [114]. Since the reaction takes place in a mostly aqueous medium, the hydrolysis of the anhydride functions is very likely to occur. The hydrolysis by water was reported in the work of Ladiavière et al. [109]. They studied the covalent immobilization of protein onto (Maleic Anhydride-alt-methyl Vinyl Ether) copolymer under aqueous condition.

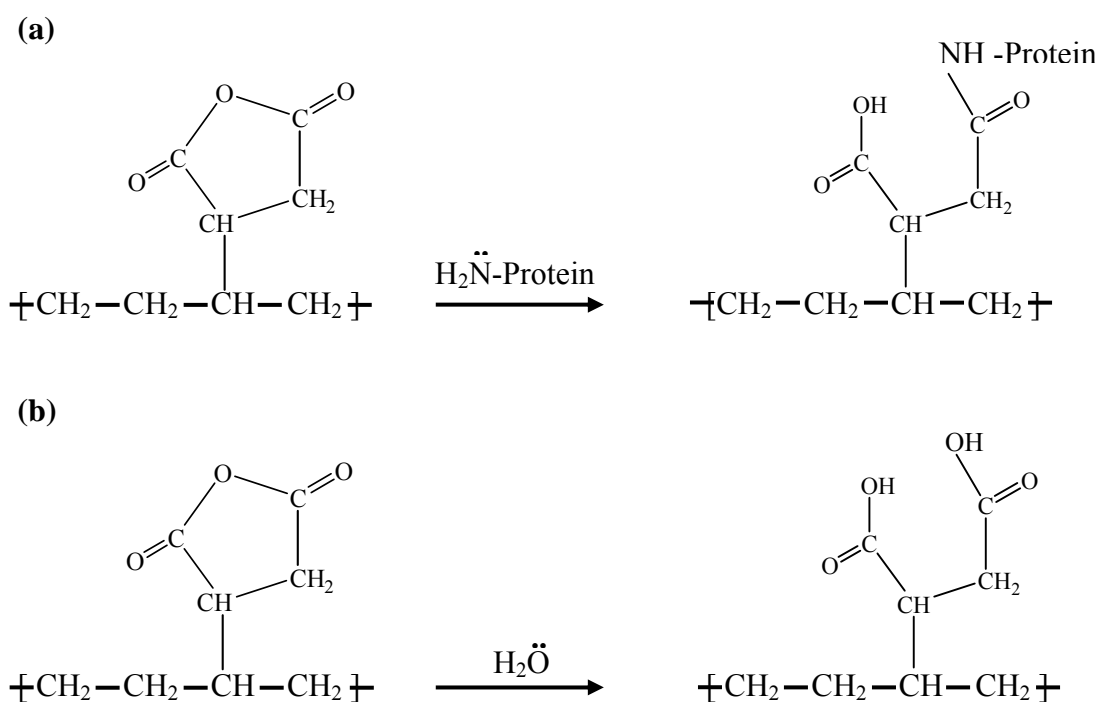


**Figure 5.31** Coupling reaction between the protein molecule and the PE-g-MAH film (a) and the hydrolysis reaction of polymer (b).

From **Figure 5.31**, it can be seen that the formation of carboxylate groups was obtained from the coupling reaction between anhydride moieties and primary amine of protein (**Figure 5.31(a)**) and the reaction of anhydride with water molecule (**Figure 5.31(b)**).

Generally, the hydrolysis with water molecule can be difficultly occurred under mild condition. To study the occurrence of hydrolysis reaction, the PE-g-MAH film was immersed in boiling water for 1 h. The change of carboxylic content, which was occurred from hydrolysis reaction and protein coupling, was investigated by using ATR-FTIR. It is presented in **Figure 5.32**.

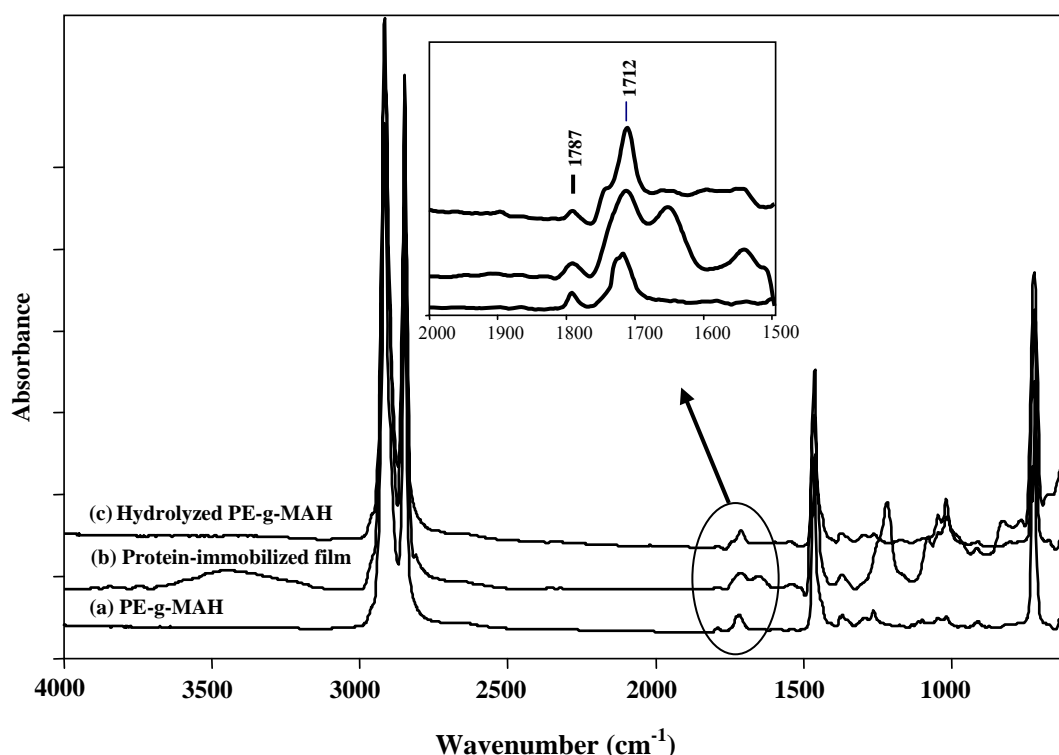


**Figure 5.32** ATR-FTIR spectra of PE-g-MAH (a) before (b) after protein binding and (c) after hydrolysis reaction.

The spectrum of PE-g-MAH after hydrolysis presented an enhance of C=O stretching of carboxylic acid peak at about 1712 cm<sup>-1</sup>. This significant evidence indicated the performance of hydrolysis reaction on PE-g-MAH surface. However, such hydrolysis reaction could not completely occur under conditions used. This was confirmed by the observation of residual anhydride peak at 1787 cm<sup>-1</sup> in the spectrum of hydrolyzed sample. From this result, it can be concluded that the side reaction from hydrolysis by water rarely occurred under mild condition of protein binding process.

Therefore, the majority of carboxylic acid content on protein-immobilized film was obtained from protein coupling reaction.

Further evidence supporting the occurrence of carboxylic acid group onto the hydrolyzed film and BSA-coupling film was obtained by studying the change of hydrophilic properties. The contact angle measurement was selected for this study.

**Table 5.10** presents contact angles of annealed PE-g-MAH film, BSA-coupling film (4 h of coupling time) and hydrolyzed film. The annealed film showed the highest contact angle of 101°. While the contact angle of BSA-coupling film and hydrolyzed film was significantly decreased into 63° and 68° respectively. The reduction of contact angle was reported to be the result of the formation of carboxylic acid groups on PE-g-MAH surface.

**Table 5.10** Contact angles of annealed PE-g-MAH before and after BSA coupling and hydrolysis reaction

Sample	Contact angle (°) (± 2)
Annealed PE-g-MAH	101
BSA-coupling film	63
Hydrolyzed film	68

In the latter case, the buffer solution was used to give the most efficient medium for the covalent grafting of protein. It was found that the hydrolysis of the reactive anhydride moieties in phosphate buffer was slower than in any other more basic medium such as carbonate and borate buffer [9].

Ladavière et al. [9] studied kinetics of the BSA-coupling reaction in phosphate buffer. They found that an occurrence of the maximum coupling yield in 0.1M buffer concentration is faster than that in 0.01M buffer concentration. The maximum coupling yield was obtained within 20 min for 0.1M phosphate buffer and within 40 min for 0.01M phosphate buffer. And the coupling reaction occurred at a pH close

to neutrality in order to limit the competing hydrolysis reaction. A neutral pH of phosphate buffer saline (PBS) is usually used because it is isotonic and no destroys to protein structure. Therefore, in this work, we selected 0.1M phosphate buffer saline at pH 7 to dissolve and dilute protein.

### 5.5.3.2 Effect of MAH Content

In this study, two MAH grafted PE films, having anhydride content on the surface, have been used to evaluate comparatively the effectiveness of protein binding. They are the commercial MAH-grafted PE (0.90 %wt MAH) and the PE-g-MAH sample by UV photografting. Maleic anhydride concentration on the surface was examined by using ATR-FTIR measurement. The anhydride content on the film surface could be quantitatively analyzed from the intensity ratio of C=O stretching of anhydride group ( $1786\text{ cm}^{-1}$ ) to  $\text{CH}_2$  bending of PE ( $1460\text{ cm}^{-1}$ ). The extent of anhydride group reported in term of intensity ratio is summarized in **Table 5.11**.

**Table 5.11** Intensity ratio of anhydride group on different PE-g-MAH films

Sample	Intensity ratio (C=O stretching / $\text{CH}_2$ bending)
Commercial film	0.03
UV photografted film	0.11

**Table 5.11** shows that the intensity ratio of commercial PE-g-MAH is lower than that of UV photografted film. Although the two sides of commercial sample contains anhydride group, it is believed that the photografted film has higher MAH content at the surface. To investigate the effect of the MAH content on the amount of immobilized protein, both PE-g-MAH films were used in this work.

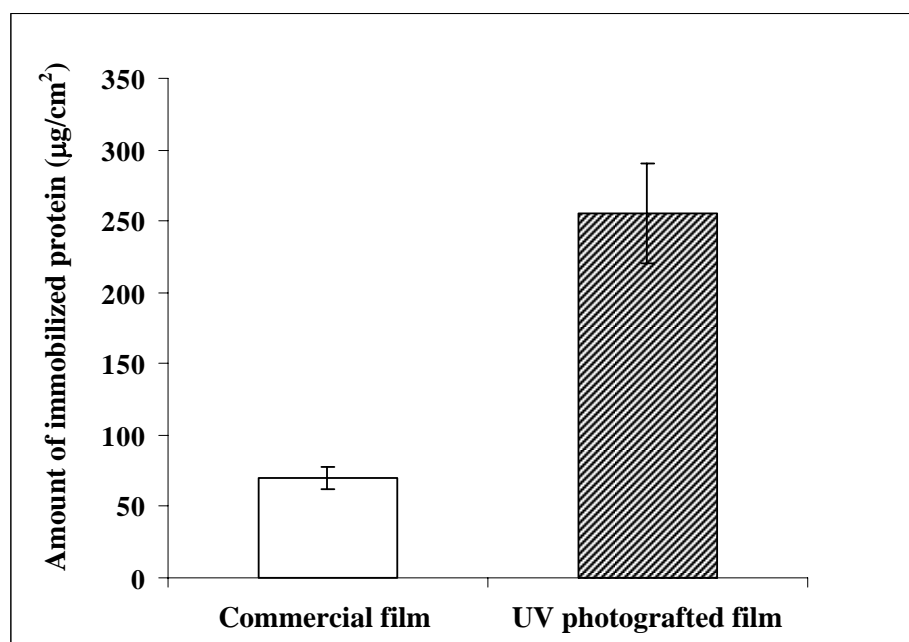


**Figure 5.33** Immobilization of extractable protein on commercial PE-g-MAH film (□) and UV photografted PE-g-MAH film (▨)

As can be seen in **Figure 5.33**, there is a significant difference between commercial and UV photografted films for protein immobilization. This result indicated that the large amount of anhydride groups on surface obtained from UV photografting technique led to the increase in protein binding.

An effect of reactive group content on amount of immobilized protein was similarly found by Qiu et al [70]. They reported that an increase of reactive surface-anhydride groups, led to an increasing in amount of enzyme per gram of  $\text{Fe}_3\text{O}_4$  / poly (styrene-co-maleic anhydride) magnetic composite microspheres. Yoon et coworkers studied the BSA adsorption under electrostatic condition and found that the maximal content of reactive groups on surface resulted in a highest adsorption of protein amount [71-73].

Chen et al. [113] investigated the lysozyme adsorption of macroporous chitosan (CS) / carboxymethylcellulose (CMC) blend membranes. The lysozyme adsorption capacity increased with an increase in the CMC concentration and maximized when the CMC concentration was 20 mol%. When the CMC content exceeded 20 mol%, the adsorption properties became worse. This phenomenon may be due to the high

carboxymethyl group density on the surface of the membranes, which caused large steric hindrance when the CMC content increased.

To confirm the binding of protein on PE-g-MAH film, the surface of film was investigated by ATR-FTIR spectroscopy. The binding reaction occurred through covalent linkage between anhydride group of MAH and amino group of protein which led to amide linkage on the surface. It can be seen in **Figure 5.34**.

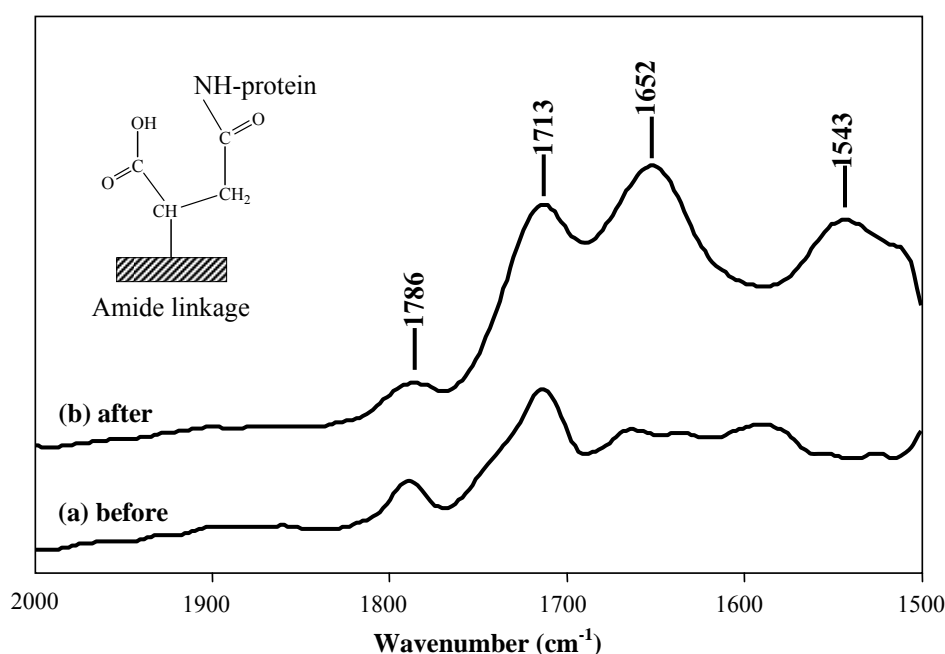


**Figure 5.34** ATR-FTIR spectra of PE-g-MAH film (a) before and (b) after immersion in protein solution.

From **Figure 5.34**, it is clearly seen that the intensity of anhydride peak (1786 cm<sup>-1</sup>) decreased after protein binding experiment. Furthermore, the appearance of bands at 1652 cm<sup>-1</sup> (amide I mode) and 1543 cm<sup>-1</sup> (amide II mode) confirms the protein binding of the PE-g-MAH film via covalent bond. The similar result was found by Belfer et al. [114]. They investigated the albumin adsorption of modified polyethersulfone (PES) ultrafiltration membranes. The modified membrane surfaces were characterized by ATR-FTIR spectroscopy. It was shown that two characteristic bands at 1650 cm<sup>-1</sup> and 1540 cm<sup>-1</sup> were inspected as proof of the presence of albumin on solid surfaces.

### 5.5.3.3 Effect of Protein Concentration

The concentration of protein is factor that can have effect on the course of the binding reaction. For this study, the extractable protein was prepared into two different concentrations at 0.6 mg/ml and 1.0 mg/ml. The use of low concentration was found in many studies of protein adsorption and protein immobilization [41, 114].

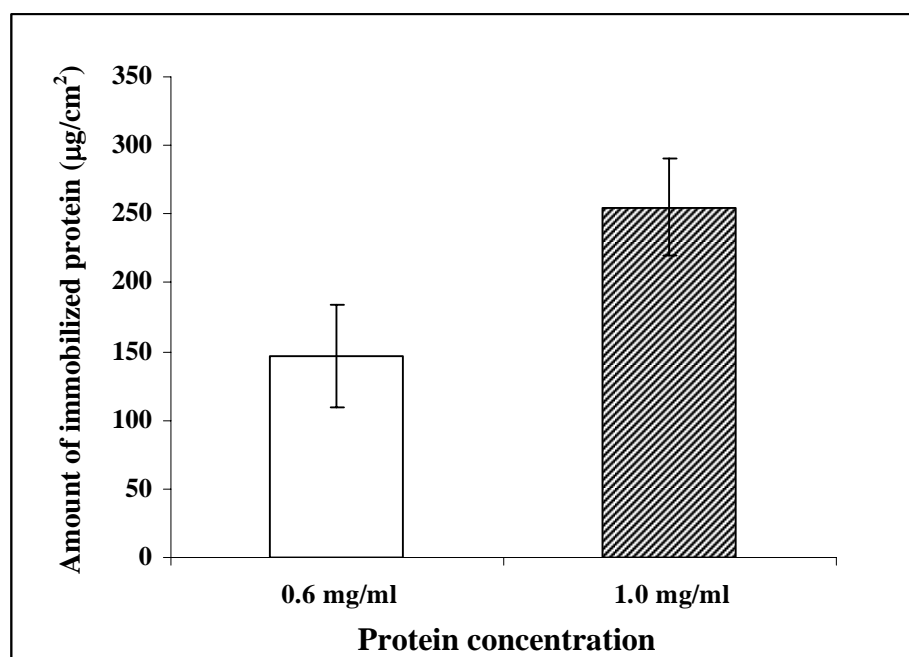


**Figure 5.35** Effect of extractable protein concentration on amount of protein immobilization.

From **Figure 5.35**, it can be seen that increasing protein concentration in solution results in an increase in the protein amount immobilized on the film surface. This observation was similar to the results obtained by other workers [70, 110-111, 113, 115-116]. These results were reported that with higher protein concentration more protein molecule could be grafted onto the film surface.

### 5.5.3.4 Efficiency of Protein Immobilization

In the study of protein immobilization onto PE-g-MAH film, the results showed that PE film containing anhydride reactive group can greatly improve the protein

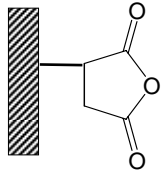
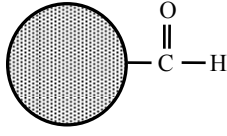
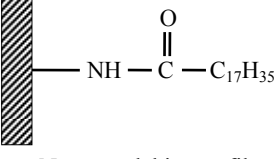
binding ability of the film under optimized conditions. It was also found that the protein immobilization appeared to be sensitive for immersion time, reactive surface content and protein concentration. Moreover, the pH condition played obviously an important role in the immobilization. Some other functionalized materials were selected to consider the efficiency of protein immobilization by MAH-grafted PE under similar binding process, as presented in **Table 5.12**.

**Table 5.12** The used conditions for BSA immobilization onto various supports

Material	Condition of protein immobilization			Reference
	BSA concentration (mg/ml)	Immersion time (h)	pH	
PE-g-MAH	1.0	4	7.0	This work
Formylated PS	10.0	4	4.5	[117]
N-stearoylchitosan	0.1	3	7.4	[118]

It should be noted that the variation in conditions for BSA immobilization has substantially influenced on the amount of immobilized protein. The maximum amount of immobilized proteins on the different functionalized supports is compared in **Table 5.13**.

**Table 5.13** Comparison of the maximum binding capacities of the BSA protein onto various supports

Structure of materials	Type of immobilization	Maximum binding capacity ( $\mu\text{g}/\text{cm}^2$ )
 <p>PE-g-MAH film</p>	covalent binding (PE-CO-NH-Protein)	72.3
 <p>Formylated PS bead</p>	covalent binding (PS-CH = N-protein)	49.0
 <p>N-stearoylchitosan film</p>	hydrophobic adsorption	4.86

From **Table 5.13**, it was obviously seen that the functional group on the supports reacted with protein though different types of immobilization (covalent interaction and hydrophobic adsorption). Type of immobilization mainly depended upon reactive functional group on the surface support. For our work, the immobilization of protein can be performed via covalent binding of their amino group by anhydride group on the PE surface. It was shown that the protein could be immobilized more on the anhydride group of PE-g-MAH ( $72.3 \mu\text{g}/\text{cm}^2$ ) than on formylated PS support ( $49.0 \mu\text{g}/\text{cm}^2$ ). This might be to the difference in the amount of reactive groups on the surface and the reactivity of functional groups with protein. While hydrophobic adsorption of surface modified chitosan film shows a lower amount of immobilized protein ( $4.86 \mu\text{g}/\text{cm}^2$ ).

From these results, it was concluded that the anhydride group of PE-g-MAH film showed a high efficiency of protein immobilization. Furthermore, the selection of suitable condition with functionalized supports will be able to enhance the ability of protein immobilization on surface supports in all case.

#### **5.5.4 Modification of PE-g-MAH Film with 1,4-Butanediamine**

The anhydride content of polyethylene grafted with maleic anhydride was found to play a significant role in occurring covalent immobilization of protein. It was found that when the anhydride group on the surface increases, the amount of immobilized protein increases. For that aim, a strategy was developed and applied to enhance anhydride content on the PE-g-MAH surface by introducing a second layer of a more hydrophilic maleic anhydride copolymer through the using a crosslinking reagent, as can be seen in **Figure 5.36**. This chemical modification of polymeric surface was studied by Schmidt and coworkers [77]. Thin film of poly(octadecene-alt-maleic anhydride), POMA was dipped in aqueous solution of 1,4-butadiazine (BDA), followed by the crosslinking with maleic anhydride copolymer.

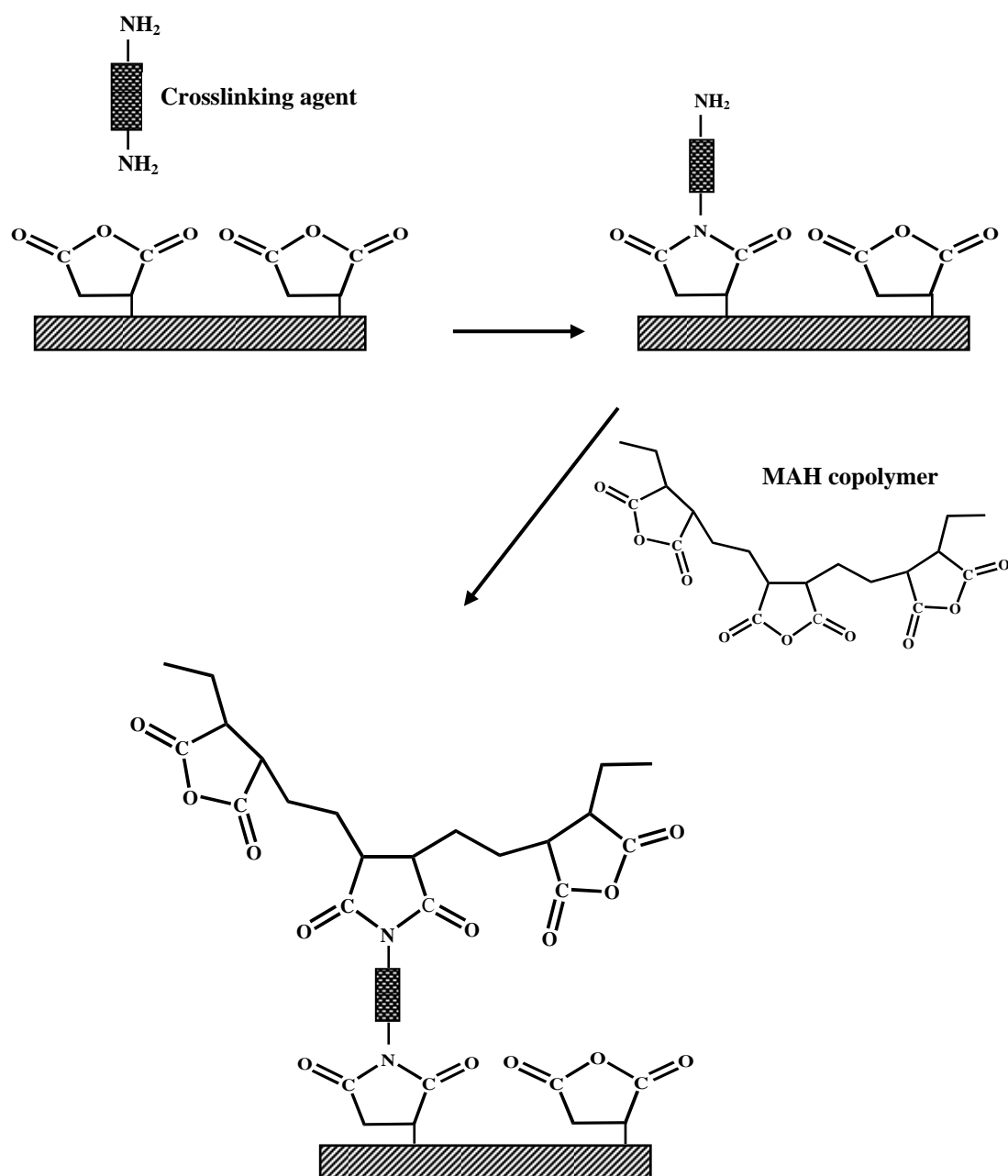


**Figure 5.36** Principle of the modification.

From this figure, it is anticipated that the surfaces with flexible bound maleic anhydride copolymers have advantages for protein immobilization because a high number of anhydride groups are available for a covalent coupling in a highly adaptable interfacial structure.

In our work, BDA (diamine) was used as a crosslinking reagent between PE-g-MAH film and a second copolymer. The preparation of advanced film with high anhydride content could be separated into two steps: firstly, modification of PE-g-MAH film with BDA. and secondly, crosslinking reaction between amino groups on modified film and anhydride groups of second copolymer.

In first step, the annealed PE-g-MAH films were dipped for 2 h in 2%BDA under stirring at room temperature. Next the modified films were rinsed with deionized water, 0.5M HCl solution and deionized water again. Finally, the samples were tempered for 2 h at 120°C for imidization. Through the choice of adequate conditions, this reaction can be restricted to apart of the anhydride groups that permit subsequent covalent protein immobilization via the remaining moieties (see **Figure 5.37**).

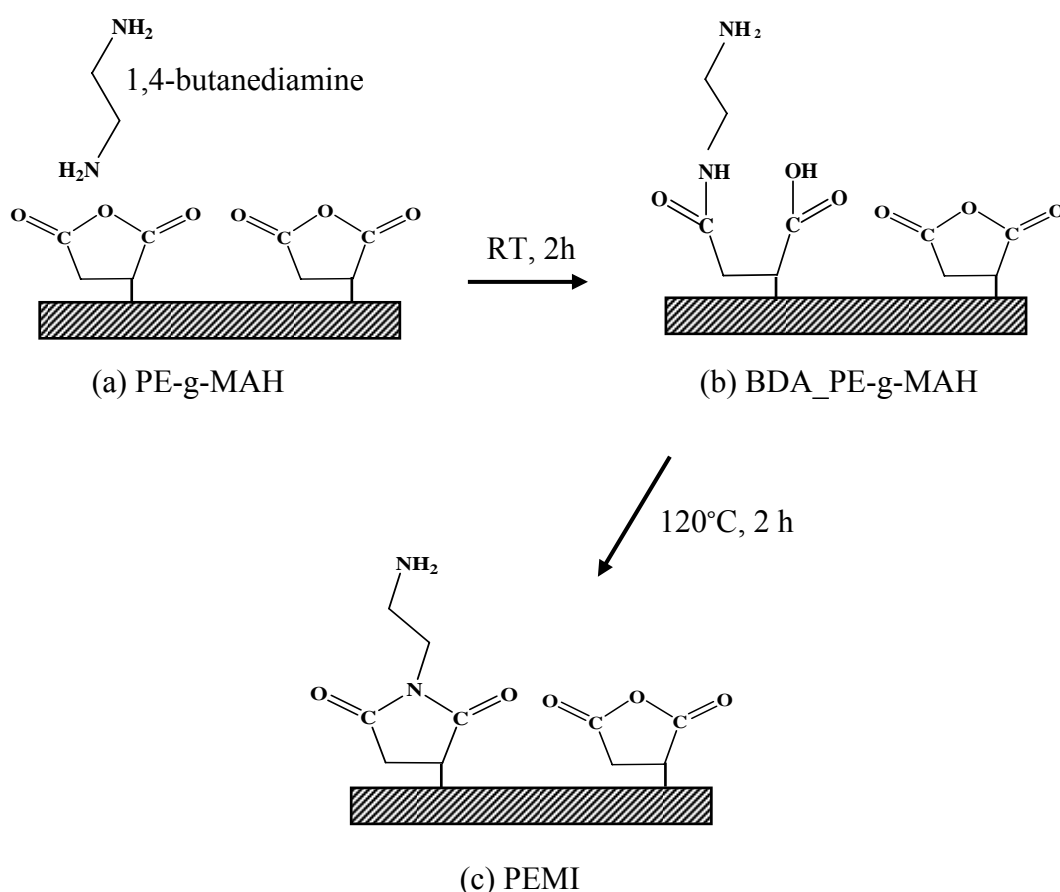


**Figure 5.37** Preparation of polymer film bearing reactive amino groups.

It is well known that the formation of amic acids proceeds quickly at low temperatures, but the imidization requires high temperatures. **Figure 5.37** shows that the modification of the PE-g-MAH films was achieved through the two step formation; firstly, an amic acid (BDA\_PE-g-MAH) was obtained from immersion reaction in functional amine solution and then it was thermally converted into the desired product of a cyclic imide (PEMI), which was very stable in aqueous solution. Imides are distinguished from amides by a substantially increased stability to hydrolysis. Because the films were prepared here for subsequent protein immobilization in aqueous buffer solutions, imide formation was considered to be necessary for sufficient film stability.

The modification reactions were monitored by ATR-FTIR measurement, as can be seen in **Figure 5.38**.

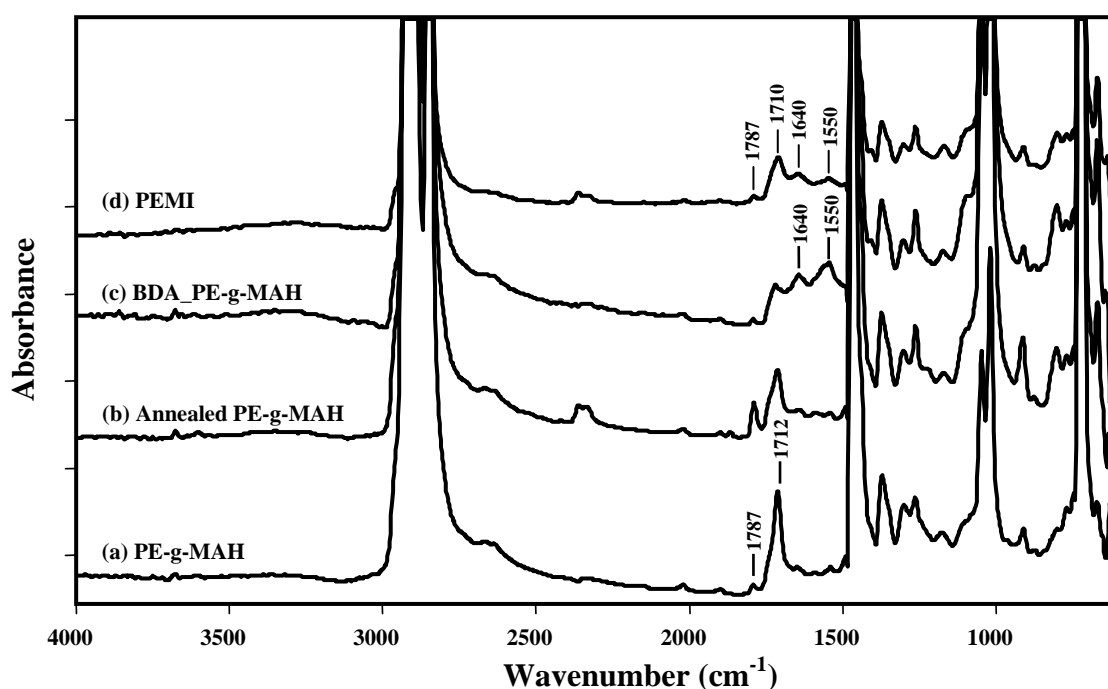


**Figure 5.38** ATR-FTIR spectra of

- |                   |                       |
|-------------------|-----------------------|
| (a) PE-g-MAH      | (b) Annealed PE-g-MAH |
| (c) BDA _PE-g-MAH | (d) PEMI              |

From **Figure 5.38**, the PE-g-MAH film modified with BDA shows broad bands at 1550 and 1640 cm<sup>-1</sup> indicating the presence of amic acid.

For the imidised PEMI, a sharp decay of the amide bands ( $1550$  and  $1640\text{ cm}^{-1}$ ) occurred, which was associated with the appearance of the imide band at  $1710\text{ cm}^{-1}$ . Furthermore, a small anhydride band at  $1787\text{ cm}^{-1}$  can be observed. The remaining anhydride groups were considered to permit subsequent protein coupling. From the results obtained, it was denoted that the partially modified film could be prepared by the reaction with functional amine.

The next step is the formation of a secondary polyanhydride layer. In previous work [78], the POMA films containing reactive amine groups were then modified with poly(styrene-alt-maleic anhydride) and poly(propene-alt-maleic anhydride) in THF. However, this process was not explained in detail.

The further work will focus on an ongoing experiment which has been set up to find suitable conditions (solvent, time and temperature of reaction) for binding secondary polyanhydride layer on the imidised PEMI film.

## **CHAPTER 6**

### **CONCLUSIONS**

This research focused on the protein binding ability of MAH copolymer via covalent linkage under optimum condition. The MAH copolymers used were a home made PE-g-MAH obtained from photografting technique and commercial PE-g-MAH. The extraction of protein from skim natural rubber was studied and the suitable time for protein binding was determined. In addition, the effects of MAH content and protein concentration were investigated under optimal immersion time. After binding, the change of chemical structure on the film surface and the amount of immobilized protein were analyzed. The following conclusions could be drawn.

#### **1. Optimum Conditions for Preparation of PE-g-MAH**

1.1 The optimum condition for the MAH photografting on LDPE film was at the distance between lamp and sample of 25 cm and under irradiation for 5 min. The purification of commercial PE-g-MAH granule is necessary to obtain a uniform material before compression. The compression temperature at 140°C was selected for preparation of PE-g-MAH film.

1.2 The annealing condition at 120°C for 3 h was proved as the most successful condition to increase the content of anhydride group in both polymer bulk and polymer surface.

## **2. Study of Protein Extraction from Dry Skim NR**

2.1 The extraction with SDS showed higher extractable proteins than that with PBS because SDS solution could remove the lightly associated protein from dry skim rubber. The protein extraction by fresh SDS solution and repeating extraction to three times (12 h /time) gave a high extractable protein content.

2.2 SDS-PAGE indicated that the extractable proteins had molecular weight of 66 and 116 kDa, corresponding to serum albumin and  $\beta$ -galactocidase respectively. CHN elemental analysis and ATR-FTIR confirmed that the obtained sample from acid precipitation step was really extractable protein.

## **3. Study of Protein Binding on PE-g-MAH film**

3.1 The coupling reaction occurred in phosphate buffer saline (PBS) at a pH close to neutral can limit the competing hydrolysis reaction. The optimum immersion time for protein binding was 4 h.

3.2 The PE-g-MAH film showed a high efficiency of protein immobilization ( $72.3 \mu\text{g}/\text{cm}^2$ ). The amount of anhydride groups on the surface had a significant influence on the protein binding ability of the film.

Our results demonstrate the feasibility of using PE-g-MAH for binding the proteins. The efficient surface modification method on the PE-g-MAH surface will be developed in future studies to increase the protein binding ability in NR latex under optimized condition. This will be very useful in improving the NR product.

## REFERENCES

1. Ghazaly HM. Factory production of examination glove from low protein latex. *J Nat Rubb Res* 1994; 9: 96-108.
2. Ng KP, Yip E and Mok KL. Production of natural rubber latex gloves with low extractable protein content: some practical recommendations. *J Nat Rubb Res* 1994; 9: 87-95.
3. Klinklai W, Saito T, Kawahara S, Tashiro K, Suzuki Y, Sakdapipanich J and Isono Y. Hyperdeproteinized natural rubber prepared with urea. *J Appl Polm Sci*. 2004; 93: 555-559.
4. Thiangchanya A, Siri-upathum C, Naranong N and Sonsuk M. Improvement of RVNRL film properties by adding fumed silica and hydroxyl apatite. *Songklanakarin J Sci Technol*. 2003; 25: 53-61.
5. Rogero SO, Lugao AB, Yoshii F and Makuuchi K. Extractable proteins from irradiated field natural rubber latex. *Radiation Physics and Chemistry* 2003; 67: 501-503.
6. Nita LE, Chiriac AP, and Vasile C. Possibilities of collagen adsorption on some polymeric matrices based on styrene copolymer. *J Appl Polm Sci* 2006; 100: 3554-3561.
7. Burnham MR, Szarowski D, Martin DL and Turner JN. Direct characterization of protein diffusion and retention in polyacrylamide hydrogels using fluorescence confocal microscopy. *Microsc Microanal* 2005; 11: 1264-1265.
8. Avramescu ME, Sager WFC, Wessling M. Functionalised ethylene vinyl alcohol copolymer (EVAL) membranes for affinity protein separation. *J Membr Sci*. 2003; 216: 177-193.
9. Ladevière C, Delair T, Domard A, Pichot C, and Mandrand B. Covalent immobilization of Bovine Serum Albumin onto (Maleic Anhydride-alt-Methyl Vinyl Ether) copolymers. *J Appl Polym Sci* 1999; 72: 1565-1572.

10. Liu S, Vareiro MMLM, Fraser S, and Jenkins ATA. Control of attachment of bovine serum albumin to pulse plasma-polymerized maleic anhydride by variation of pulse conditions. *Langmuir* 2005; 21: 8572-8575.
11. Yang W and Ranby B. Bulk surface photografting process and its applications: II. Principal factors affecting surface photografting. *J Appl Polym Sci* 1996; 62: 545-555.
12. Chan CM. *Polymer Surface Modification and Characterization: Surface Grafting*. Hanser Publisher. New York; 1994.
13. Deng JP, Yang WT and Ranby B. Melt-photografting polymerization of maleic anhydride onto LDPE film. *Eur Polym J* 2002; 38: 1449-1455.
14. Subramaniam A. The chemistry of natural rubber latex. *Latex Allergy* 1995; 15: 1-21.
15. Tata SJ, Moir GFJ. The proteins of *Hevea brasiliensis* latex. Part 5. Starch gel electrophoresis of C serum proteins. *J Rubb Res Inst Malaysia*. 1964; 18: 97.
16. Archer BL. The proteins of *Hevea brasiliensis* latex: 4. Isolation and characterization of crystalline hevein. *Biochem J* 1960; 75: 236-240.
17. Bristow GM. Composition and cure behaviour of skim block Natural Rubber. *J nat Rubb Res* 1990; 5: 114-134.
18. Blackley DC. *High polymer lattices*. Maclaren and Sons. London; 1996.
19. Blackley DC. *Encyclopedia of polymer science and engineering*. 2<sup>nd</sup> ed. John Wiley & sons. Canada; 1987.
20. Lau CM, Subramaniam A, and Tajima Y. Recovery and Application of Waste Solid from Natural Rubber Latex Serum. *Proc Rubb Res Inst Malasia Rubb Grow Conf Malacca*. 1989: 525-530.
21. Archer BL and McMullen AI. In: *International Rubber Conference 1960 Proceedings Kuala Lumpur, Kuala Lumpur, Rubber Research Institute of Malaya* 1961; 787-795.
22. Archer BL, Barnard D, Cockbain EG, Dickenson PB, McMullen AI. In: Bateman L(Ed). *The Chemistry and physics of rubber-like substances*. Maclaren and Sons/Wiley. London/New York; 1963.

23. Tata SJ. Distribution of proteins between the fractions of hevea latex separated by ultracentrifugation. *J Rubb Res Inst Malaysia* 1980; 28: 77-85.
24. Moir GFJ. *Nature (London)* 1959; 184: 1926-1928.
25. Cook AS, Sekhar BC. *J Rubb Res Inst Malaysia* 1953; 14: 163-168.
26. Hamzah S, Gomez JB. *J Rubb Res Inst Malaysia* 1983; 31: 117-129
27. Hsia RCH. *Trans Inst Rubb Ind* 1958; 34: 267-290
28. Fay MF. Hand dermatitis. *AORN Journal* 1991; 54: 451-467.
29. Leynadier F, and Dry J. Allergy to Latex. *Clinical Review in Allergy* 1991; 9; 371-377.
30. Hamann CP. Natural Rubber Latex Protein Sensitivity in Review. *Am J Contact Dermatitis* 1993; 4: 4-21.
31. Klinklai W, Saito T, Kawahara S, Tashiro K, Suzuki Y, Sakdapipanich J and Isono Y. Hyperdeproteinized Natural Rubber Prepared with Urea. *J Appl Polm Sci* 2004; 93: 555-559.
32. Citation: Dalrymple Audley 1992 Rubber Developments.
33. Rogero SO, Lugao AB, Yoshii F and Makuuchi K. Extractable proteins from irradiated field natural rubber latex. *Radiation Physics and Chemistry* 2003; 67: 501-503.
34. Parra DF, Martins CFP, Collantes HDC and Lugao AB. Extractable proteins from field radiation vulcanized natural rubber latex. *Nuclear Instruments and Methods in Physics Research B* 2005; 236: 508-512.
35. Decher G, Hong JD and Schmitt J. Buildup of ultrathin multilayer films by a self-assembly process: III. Consequitively alternating adsorption of anionic and cationic polyelectrolytes on charged surfaces. *Thin Solid Films* 1992; 210/211: 831-835.
36. Lvov Y, Decher G and Mohwald H. Assembly, structural characterization and thermal behavior of layer-by-layer deposited ultrathin films of poly(vinyl sulfate) and poly(allylamine). *Langmuir* 1993; 9: 481-486.
37. Kajiya Y, Sugai H, Iwakura C and Yoneyama H. Glucose sensitivity of polypyrrole films containing immobilized glucose oxidase and hydroquinonesulfonate ions. *Anal Chem* 1991; 63: 49-54.

38. Leggett GJ, Roberts CJ, Williams PM, Davies MC, Jackson DE and Tendler SJB. Approaches to the immobilization of proteins at surfaces for analysis by scanning tunneling microscopy. *Langmuir* 1993; 9: 2356-2362.
39. McMorn P, and Hutchings GJ. Heterogeneous enantioselective catalysts: strategies for the immobilization of homogeneous catalysts. *Chem Soc Rev* 2004; 33: 108-122.
40. Hudson S, Magner G, Cooney J and Hodnett K. Methodology for the Immobilization of enzymes onto mesoporous materials. *J Phy Chem B* 2005; 109: 19496-19506.
41. Greene G, Radhakrishna H and Tannenbaum R. Protein binding properties of surface-modified porous polyethylene membranes. *Biomaterials* 2005; 26: 5972-5982.
42. Blin JL, Gérardin C, Carteret C, Rodehüser L, Sevre C and Stébé MJ. Direct one-step immobilization of glucose oxidase in well-ordered mesostructured silica using a nonionic fluorinated surfactant. *Chem Mater* 2005; 17: 1479-1486.
43. Hoffmann AS. Biologically functional materials. In: Ratner BD, Hoffman AS, Schoen FJ and Lemons JE. *Biomaterial science: an introduction to materials in medicine* 1996. Academic Press. New York; 1996.
44. Karlstrom G, Johansson H-O. Lattice model calculations of interactions between proteins and surface grafted polymers with tethered affinity ligands. *Coll Surf B* 2001; 20: 245-256.
45. Stabel TJ, Casale ES, Swaisgood HE and Horton HR. Anti-IgG immobilized controlled-pore glass. Thionyl chloride-activated succinamidopropyl-glass as a covalent immobilization matrix. *Appl Biochem Biotechnol* 1992; 36: 87-96.
46. Varavinit S, Chaokasem N and Shobsngob S. Covalent immobilization of glucoamylase to bagasse dialdehyde cellulose. *World J Microbiol & Biotechnol* 2001; 17: 721-725.
47. Horák D, Rittich B, and Španová A. Effect of reaction parameters on properties of dispersion-polymerized hydrophilic microspheres as supports for immobilization of proteins. *Progr Colloid Polym Sci* 2004; 124: 77-81.

48. Iyengar L, Rao AVSP. Urease bound to chitin with glutaraldehyde. *Biotechnol Bioeng* 1979; 21: 1333-1343.
49. Amiji MM. Platelet adhesion and activation on an amphoteric chitosan derivative bearing sulfonate groups. *Colloids and Surfaces B: Biointerfaces* 1998; 10: 263-271.
50. Coulet PR, Godinot C and Gautheron DC. Surface-bound aspartate aminotransferase on collagen films: Compared properties with native enzyme. *Biochim Biophys Acta* 1975; 391: 272-281.
51. Kennedy JF, Kalogerakis B and Cabral JMS. Immobilization of enzymes on cross-linked gelatin particles activated with various forms and complexes of titanium (IV) species. *Enzyme Microb Technol* 1984; 6: 68-72.
52. Bajpai AK and Sharma M. Preparation and characterization of Novel pH-Sensitive Binary Grafted-Polymeric Blends of Gelatin and Poly(vinyl alcohol): Water Sorption and Blood Compatibility Study. *J Appl Polym Sci* 2006; 100: 599-617.
53. Mikos AG, Lyman MD, Freed LE, Langer RL. Wetting of poly(L-lactic acid) and poly(DL-lactic-co-glycolic acid) foams for tissue culture. *Biomaterials* 1994; 15: 55-58.
54. Grisser HJ, Chatelier RC, Gengenbach TR, Johnson GJ and Steele JG. Growth of human cells on plasma polymers: putative role of amine and amide groups. *J Biomater Sci Polym Ed* 1994; 5(6): 531-554.
55. Epailard FP, Chevet B, Bross JC. Modification of isotactic polypropylene by a cold plasma or an electron beam and grafting of the acrylic acid onto these activated polymers. *J Appl Polym Sci* 1994; 53: 1291-1306.
56. Ajayaghosh A and Das S. Photografting of acrylic monomers on polystyrene support. *J Appl Polym Sci* 1992; 45: 1617-1622.
57. Suh H, Hwang YS, Lee JE, Han CD and Park JC. Behavior of osteoblasts on a type I atelocollagen grafted ozone oxidized poly L-lactic acid membrane. *Biomaterials* 2001; 22: 219-230.
58. Valuev IL, Chupov VV, Valuev LI. Chemical Modification of polymer with physiologically active species using water-soluble carbodiimides. *Biomaterials* 1998; 19: 41-43.

59. Nakajams K, Hirano Y, Iida T, Nakanima A. Adsorption of plasma proteins on Arg-Gly-Asp-Ser peptide-immobilized poly(vinyl alcohol) and ethylene-acrylic acid copolymer films. *Polm J* 1990; 22: 985-990.
60. Ma Z, Gao C and Jiacong Shen JJ. Protein immobilization on the surface of poly-L-lactic acid films for improvement of cellular interactions. *Eur Polm J* 2002; 38: 2279-2284.
61. Beitz J, Schellenberger A, Lasch J and Fischer J. Catalytic properties and electrostatic potential of charged immobilized enzyme derivatives: Pyruvate decarboxylase attached to cationic polystyrene beads of different charge densities. *Biochim Biophys Acta* 1980; 612: 451-454.
62. Nita LE, Chiriac AP, and Vasile C. Possibilities of Collagen Adsorption on Some Polymeric Matrices Based on Styrene Copolymer. *J Appl Polm Sci* 2006; 100: 3554-3561.
63. Priola A, Bongiovanni R and Gozzelino G. Solvent influence on the radical grafting of maleic anhydride on low density polyethylene. *Eur Polym J* 1994; 9: 1047-1050.
64. Machado AV, Covas JA and Van Duin M. Effect of polyolefin structure on maleic anhydride grafting. *Polymer* 2001; 42: 3649-3655.
65. Gayload NG, Mehta R, Kumar V and tazi M. Maleation of linear low-density polyethylene by reactive processing. *J Appl Polym Sci* 1992; 44: 1941-1949.
66. EL Kholdi O, Lecamp L, Lebaudy P, Bunel C and Alexandre S. Modification of adhesive properties of a polyethylene film by photografting. *J Appl Polym Sci* 2004; 92: 2803-2811.
67. Deng JP, Yang WT and Ranby B. Surface Photografting Polymerization of Vinyl Acetate (VAc), Maleic anhydride, and Their Charge Transfer Complex. II. VAc(2). *J Appl Polym Sci* 2000; 77: 1522-1531.
68. Chiang WY and Ku YA. The effect of Maleic Anhydride grafting on the flame retardation of plasma pretreated polyethylene. *Polym Degrad stab* 2002; 76: 281-290.
69. Deng JP, Yang WT and Ranby B. Surface Photografting Polymerization of Vinyl Acetate (VAc), Maleic anhydride, and Their Charge Transfer Complex. I. VAc(1). *J Appl Polym Sci* 2000; 77:1513-1521.

70. Qiu GM, Zhu BK and Xu YY.  $\alpha$ - Amylase immobilized by Fe<sub>3</sub>O<sub>4</sub>/poly (styrene-co-maleic anhydride) magnetic composite microspheres: Preparation and Characterization. *J Appl Polym Sci* 2005; 95: 328-2284.
71. Yoon JY, Kim JH and Kim WS. The relation ship of interaction forces in the protein adsorption onto polymeric microspheres. *Coll Surf A* 1999; 153: 413-419.
72. Yoon JY, Kim JH and Kim WS. Interpretation of protein adsorption phenomena onto functional microspheres. *Coll Surf B* 1998; 12(1): 15-22.
73. Yoon JY, Park HY, Kim JH and Kim WS. Adsorption of BSA on highly carboxylated microsphere-quantitative effect of surface functional groups and interaction forces . *J Coll Interf Sci* 1996; 177(2): 613-320.
74. Bettini SHP, Agnelli JAM. Evaluation of methods used for analyzing maleic anhydride grafted onto polypropylene by reactive processing. *Polymer testing* 2000; 19: 3-15.
75. Callais PA and Kazmierczak RT. ANTEC, Dallas. TX, 7-11 May 1990.
76. Sathe SN, Rao GSS, and Devi S. Grafting of maleic anhydride onto polypropylene: synthesis and characterization. *J Appl Polym Sci* 1994; 53: 239-245.
77. Schmidt U, Zschoche S, and Werner C. Modification of poly(octadecene-alt-maleic anhydride) films by reaction with functional amines. *J Appl Polym Sci* 2003; 87: 1255-1266.
78. Levin Y, Pecht M, Goldstein L and Katchalski E. A water-insoluble polyanionic derivative of Trypsin: I. Preparation and properties. *Biochemistry* 1964; 3: 1905-1913.
79. Piatigorsky J, Horowitz J, and Simpson T. Partial dissociation and renaturation of embryonic chick d-crystalline Characterization by ultracentrifugation and circular dichroism. *Biochim Biophys Acta* 1977; 490: 279-289.
80. Ryden L, Deutsch HF. Preparation and Properties of the Major Copper-binding Component in Human Fetal Liver. *J Biol Chem* 1978; 253: 519-524.
81. Alenius H, Makinen-kiljunen S, Turjanmaa K, Palosuo T, Reunala T. Allergen and protein content of latex gloves. *Ann Allergy* 1994; 73: 315-320.

82. Hasma H. Proteins of Natural Rubber Latex Concentrate. *J nat Rubb Res* 1992; 7(2): 102-112.
83. Rogero SO, Lugao AB, Yoshii F, and Makuuchi K. Extractable proteins from irradiated field natural rubber latex. *Radiation Physics and Chem* 2003; 67: 501-503.
84. Lowry OH, Rosebrough NR, Farr AL, and Randall RJ. Protein measurement with the Folin phenol reagent. *J Biol Chem* 1951; 196: 265-275.
85. Bradford MM. A rapid and sensitive method for the quantitation of microgram quantities of protein utilizing the principle of protein-dye binding. *Anal Biochem* 1976; 72: 248-254.
86. Peterson GL. Review of the Folin phenol protein quantitation method of Lowry, Rosebrough, Farr and Randall. *Anal Biochem* 1979; 100: 201-220.
87. Compton SJ, and Jones CG. Mechanism of dye response and interference in the Bradford protein assay. *Anal Biochem* 1985; 151: 369-374.
88. Krimm S and Bandeker J. Vibrational spectroscopy and conformation of peptides, polypeptides and proteins. *J Adv Protein Chem* 1986; 38: 181-364.
89. Dong A, Prestralski SD and Allison JF. Infrared spectroscopy studies of lyophilization- and temperature-induced protein aggregation. *J Pharm Sci* 1995; 84: 415-424.
90. Bollag DM, Rozycki MD, and Edelstein SJ. *Protein Method*. 2<sup>nd</sup> ed. Wiley Liss. Newyork; 1956.
91. Holme DJ and Pack H. *Analytical biochemistry*. Longman group. Newyork; 1983.
92. Smith PK, Krohn RI, Hermanson GT, Mallia AK, Gartner FH and Provenzano MD. Measurement of protein using Biocinchoninic acid. *Anal Biochem* 1985; 150: 76-85.
93. London GM. *Organic Chemistry*, 2<sup>nd</sup> ed., Benjamin-Cummings. Menlo Park. carifornia; 1985.
94. Chial HJ, Thompson HB, and Splittgerber AG. A spectral study of the charge forms of Coomassie Blue G. *Anal Biochem* 1993; 209: 258-266.
95. Sedmak JJ and Grossberg SE. A rapid sensitive and versatile assay for protein using Coomassie brilliant blue G250. *Anal Biochem* 1977; 79: 544-552.

96. Read SM and Northcote DH. Minimization of variation in the response to different proteins of the Coomassie blue G dye-binding assay for protein. *Anal Biochem* 1981; 116: 53-64.
97. Fazekas de St Groth S, Webster RG and Datyem A. Two new staining procedures for quantitative estimation of protein on electrophoretic strips. *Biochim Biophys Acta* 1963; 71: 377-391.
98. Righetti PG and Chillemi F. *J Chromatography* 1978; 157: 243-251.
99. Saleemuddin M, Ahmad H, and Husain A. A rapid, simple and highly sensitive calorimetric assay for the endoproteases using Coomassie Brilliant Blue G-250. *Ind J Biochem Biophys (Suppl)* 1980; 17: 69.
100. Pierce J and Suelter CH. An evaluation of the Coomassie brilliant blue G-250 dye-binding method for quantitative protein determination. *Anal Biochem* 1977; 81: 478-480.
101. Spector T. Refinement of the Coomassie blue method of protein quantitation: A simple and linear spectrophotometric assay for  $\leq 0.5$  to 50  $\mu\text{g}$  of protein. *Anal Biochem* 1978; 86:142-146.
102. Rim PB. A DSC and DMA Study of polymers with crystallizable side chains: Poly( $\alpha$ -olefin-co-maleic anhydride). *J Macromol Sci Phys* 1984-85; B23: 549-573.
103. Nor HM and Ebdon JR. Ozonolysis of natural rubber in chloroform solution part I: A study by GPC and FTIR spectroscopy. *Polymer* 2000; 4: 2359-2365.
104. Vemuri S. Comparison of assays for determination of peptide content for lyophilized thymalfasin. *J Peptide Res* 2005; 65: 433-439.
105. Stoscheck C.M. Quantitation of Protein. *Methods in Enzymology* 1990; 182: 50-69.
106. [http://www2.truman.edu/~mnagan/pdf/protein\\_conc.pdf](http://www2.truman.edu/~mnagan/pdf/protein_conc.pdf); Internet; accessed 25 May 2007.
107. Layne E. Spectrophotometric and Turbidimetric Methods for Measuring Proteins. *Methods in Enzymology* 1957; 3: 445-455.
108. Brewer Jr H, Schlueter R and Aldred J. *J Biol chem* 1970; 245: 4232-4240.
109. Ladavière C, Delair T, Domard A, Rousseau AN, Mondrand B and Mallet F. Covalent Immobilization of proteins onto (Maleic Anhydride-alt-Methyl Vinyl

- Ether) Copolymers: Enhanced Immobilization of Recombinant Protein. *Bioconjugate Chem* 1998; 9: 655-661.
110. Can HK, Güner A. Investigation of Adsorption –Desorption Cynamism of Bovine Serum Albumin on crosslinked N,N'-Diethylaminoethyl Dextran Microbeads: Solution Phase. *J Appl Polym Sci* 2006; 99: 2288-2299.
111. Li W and Li S. A study on the Adsorption of Bovine Serum Albumin onto electrostatic microspheres: Role of surface groups. *Colloid and Surfaces A: Physicochem Eng Aspects* 2007; 295: 159-164.
112. Briššová M, Augustin J and Staudner E. Reaction of maleic anhydride copolymers with albumin in water system. *Macromol. Rapid. Commun* 1994; 15: 211-216.
113. Chen X, Liu J, Feng Z, Shao Z. Macroporous chitosan/ carboxymethylcellulose blend membranes and their application for lysozyme adsorption. *J Appl Polym Sci* 2005; 96: 1267-1274.
114. Belfer S, Fainchtain, Purinson Y and Kedem O. Surface characterization by FTIR-ATR spectroscopy of polyethersulfone membranes-unmodified and modified and protein fouled. *J Memb Sci* 2000; 172: 113-124.
115. Yang C, Guan Y, Xing J, Jia G and Liu H. Synthesis and protein immobilization of monodisperse magnetic spheres with multifunctional groups. *Reactive & Functional Polymers* 2006; 66: 267-273.
116. Wan LS, Xu ZK Wang ZG and Wang JL. Copolymerization of acrylonitrile with N-vinyl-2-pyrrolidone to improve the hemocompatibility of polyacrylonitrile. *Polymer* 2005; 46: 7715-7723.
117. Shmanai VV and Bylina. Protein immobilization on formylated polystyrene supports. *Reactive & Functional Polymers* 2000; 43: 243-251.
118. Tangpasuthadol V, Pongchaisirikul N, and Hoven VP. Surface modification of chitosan films: effects of hydrophobicity on protein adsorption. *Carbohydrate Research* 2003; 338: 937-942.

## **APPENDIX**

## Appendix A

### Carboxyl index of anhydride group obtained from commercial film

**Table A1** Intensity ratio of anhydride group under different compression temperatures

Compression Temperature (°C)	Intensity ratio ( $I_{1787/1460}$ )	
	Original PE-g-MAH	Purified PE-g-MAH
140	$0.089 \pm 0.004$	$0.100 \pm 0.003$
150	$0.091 \pm 0.001$	$0.104 \pm 0.016$

**Table A2** Intensity ratio of purified PE-g-MAH sample under different annealing conditions

PE-g-MAH film	Intensity ratio ( $I_{1787/1460}$ )
Before	$0.100 \pm 0.002$
Anneal 110°C, 24 h	$0.088 \pm 0.014$
Anneal 120°C, 3 h	$0.161 \pm 0.002$

## Appendix B

### Extraction of protein from dry skim NR

**Table B1** Intensity ratio of decreased proteins in the bulk sample and at the surface (Extraction time = 12 h)

Extract solvent	Intensity ratio ( $I_{1539/1376}$ )	
	Transmittance-FTIR	ATR-FTIR
<b>Before</b>	$0.752 \pm 0.030$	$0.455 \pm 0.015$
<b>0.01 M PBS</b>	$0.650 \pm 0.171$	$0.442 \pm 0.011$
<b>2% SDS</b>	$0.595 \pm 0.025$	$0.200 \pm 0.061$

**Table B2** Protein content from multiple extractions with SDS (Extraction time = 12 h / times)

Number of extraction	Protein content (mg/g of rubber)
1	$1.414 \pm 0.312$
2	$4.554 \pm 0.140$
3	$5.551 \pm 0.117$

## Appendix C

### Protein binding efficiency of PE-g-MAH film

**Table C1** Amount of immobilized BSA on annealed commercial PE-g-MAH film for different durations (BSA concentration = 1.0 mg/ml)

Binding time (h)	Amount of immobilized BSA ( $\mu\text{g}/\text{cm}^2$ )						
	1	2	3	4	5	AVG	STDEV
2	46.22	40.39	34.56	50.88	52.25	44.86	7.40
4	65.31	61.19	80.44	87.31	67.44	72.34	11.04
6	96.25	56.38	47.44	56.38	49.50	61.19	20.01
8	81.12	57.75	66.69	-	-	68.52	11.79

**Table C2** Extracted protein binding efficiency with different MAH contents (Protein concentration = 1.0 mg/ml)

Volume of protein solution for analysis ( $\mu\text{l}$ )	Amount of immobilized proteins ( $\mu\text{g}/\text{cm}^2$ )	
	Annealed commercial film	Annealed UV photografted film
10	$66.68 \pm 10.10$	$259.24 \pm 54.33$
15	$72.41 \pm 6.66$	$250.79 \pm 17.21$
AVG	$69.87 \pm 7.90$	$255.01 \pm 35.15$

**Table C3** Extracted protein binding efficiency of UV-grafted film under different protein concentrations

Volume of protein solution for analysis ( $\mu\text{l}$ )	Amount of immobilized proteins ( $\mu\text{g}/\text{cm}^2$ )	
	0.6 mg/ml of protein concentration	1.0 mg/ml of protein concentration
10	$165.98 \pm 28.94$	$259.24 \pm 54.33$
15	$121.64 \pm 40.85$	$250.79 \pm 17.21$
AVG	$146.28 \pm 37.60$	$255.01 \pm 35.15$



*WORLD RUBBER SUMMIT*



**การประชุมสุดยอดยางโลก ครั้งที่ 1**  
**1<sup>st</sup> World Rubber Summit**

**26-29 July 2006**  
**Bangkok Thailand**

## USE OF MALEIC ANHYDRIDE COPOLYMER FILM FOR BINDING EXTRACTABLE PROTEINS FROM NATURAL RUBBER

Ladawan Watthanachote<sup>1</sup>, Dr. Thirawan Nipithakul<sup>2</sup>

<sup>1</sup>Polymer Science and Technology Programme, Faculty of Science, Mahidol University, Salaya Center, Nakhon Pathom 73170.

<sup>2</sup>Department of Chemistry, Faculty of Science, Mahidol University, Phayathai, Bangkok 10400.

### ABSTRACT

A copolymeric membrane material containing maleic anhydride group for protein binding was carried out by compression of commercial polyethylene-maleic anhydride copolymer resin. Annealing the PE-MAH film induced efficient back formation of the anhydride groups. The surface properties of the copolymer were analyzed by Attenuated Total Reflection Fourier Transforms Infrared Spectroscopy (ATR-FTIR) and water contact angle measurement. In this work, extractable proteins from dry skim natural rubber (NR) were selected to study protein-binding ability of the PE-MAH film. Two solutions, phosphate buffered saline (PBS) and sodium dodecyl sulfate (SDS), have been used for protein extraction. The extractable proteins were examined by Sodium Dodecyl Sulfate-Polyacrylamide Gel Electrophoresis (SDS-PAGE) method. Quantitative analysis of the protein binding was investigated by the dye-binding assay of Bradford. The spectroscopic results show that proteins can be successfully immobilized onto the film surface via covalent linkage.

**Introduction:** Maleic anhydride (MAH) has properties that make them of particular interest for surface modification. It can be form in such a way that anhydride group functionality is retained for subsequent chemical modification. The anhydride group very reactive to primary amine group and slightly less reactive to alcohol. Therefore, the covalent binding of proteins onto polymeric film containing maleic anhydride group can be occurred. The chemical reaction is illustrated in Figure 1. The amide and carboxylic acid groups are formed by cleavage of anhydride ring.

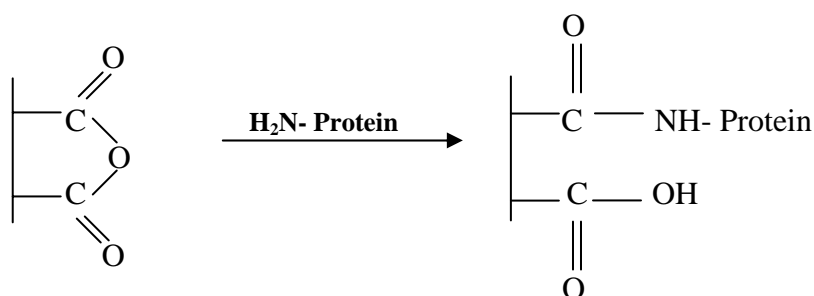


Figure 1. Coupling reaction between maleic anhydride and protein

### Experimental:

The film of polyethylene-maleic anhydride copolymer was prepared by compression at 130°C for 5 min. Then the PE-MAH sample was annealed under defined conditions in order to obtain high content of anhydride groups on the surface.

Dry skim NR was cut into small pieces and then immersed in extract solution at room temperature for 12 h. For a comparative test, two kinds of extract solution were chosen in this study. They are 0.01M phosphate buffered saline (PBS) at pH 7 and 2% sodium dodecyl sulfate (SDS). Sodium Dodecyl Sulfate–Polyacrylamide Gel Electrophoresis (SDS-PAGE) was used to identify the extractable proteins from NR.

The annealed PE-MAH film was immersed in extractable protein solution and bovine serum albumin (BSA) solution used as a model protein. The protein concentration was fixed at 1 mg/ml. The mixtures were stirred at room temperature for 2 h. Finally, the films were washed three times with deionized water and dried. The film surface was characterized by ATR-FTIR technique. The protein concentration was detected by using the colorimetric analysis. After adding a Bradford reagent, the color of protein solution was developed into violet. The change of color intensity was quantified by UV-VIS spectrophotometer.

### Results, discussion and conclusion:

By SDS-PAGE technique, the extractable proteins were separated and identified based primarily on their molecular weights (Figure 2). It was found that the protein content obtained with SDS was higher than that with PBS. This result was in good agreement with that obtained by FTIR measurement (Figure 3). A sharp decay of the protein bands was observed at 3281, 1656 and 1539  $\text{cm}^{-1}$ .

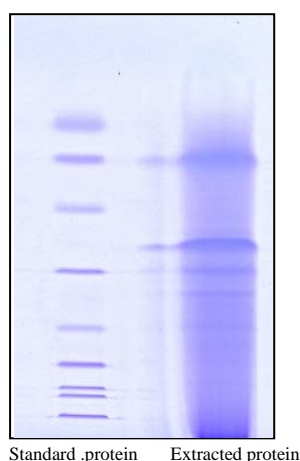


Figure 2. Identification of extracted proteins by SDS-PAGE method

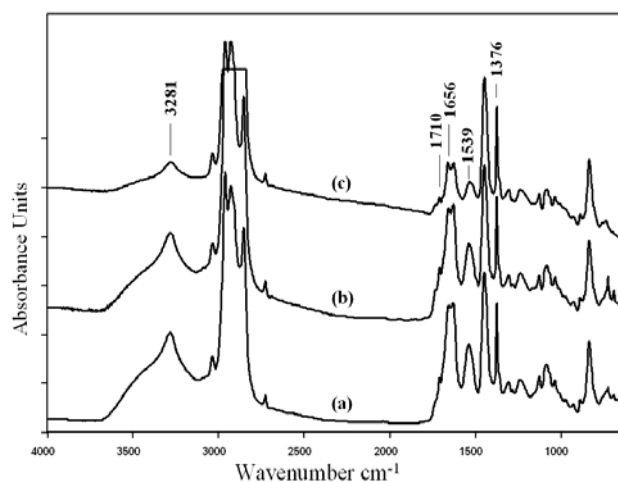


Figure 3. FTIR spectra (Transmission) of dry skim NR before (a) and after extracted with PBS (b) and SDS (c)

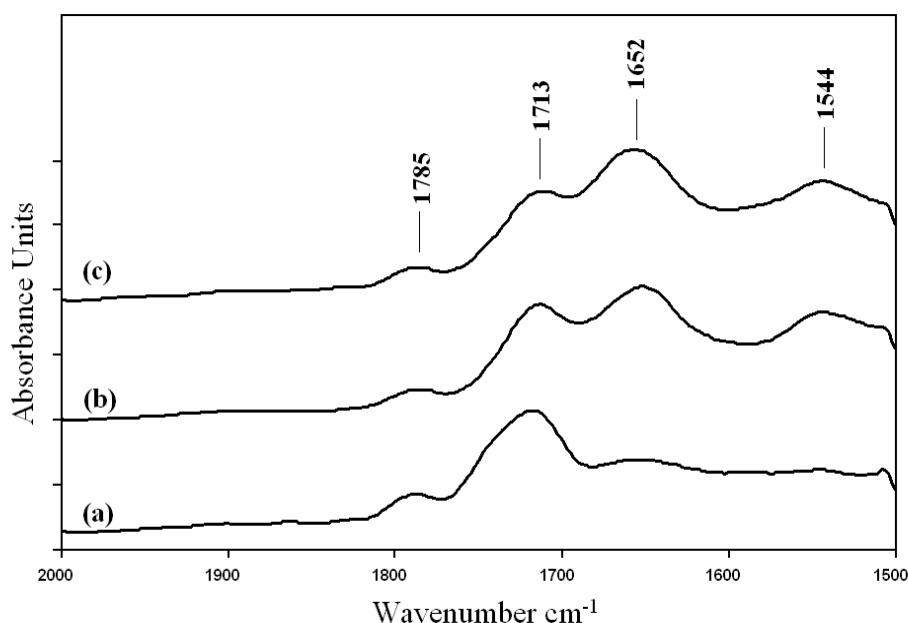


Figure 4. ATR-FTIR spectra of PE-MAH film before(a) and after binding extractable protein (b) and BSA(c)

In Figure 4, the spectrum of PE-MAH film shows specific peaks at  $1785\text{ cm}^{-1}$ , corresponding to the characteristic absorption of the carbonyl stretching in cyclic anhydride groups of MAH. Additionally, the sample also presented strong absorption peak at  $1713\text{ cm}^{-1}$ , which was assigned to carbonyl stretching of carboxylic acid.

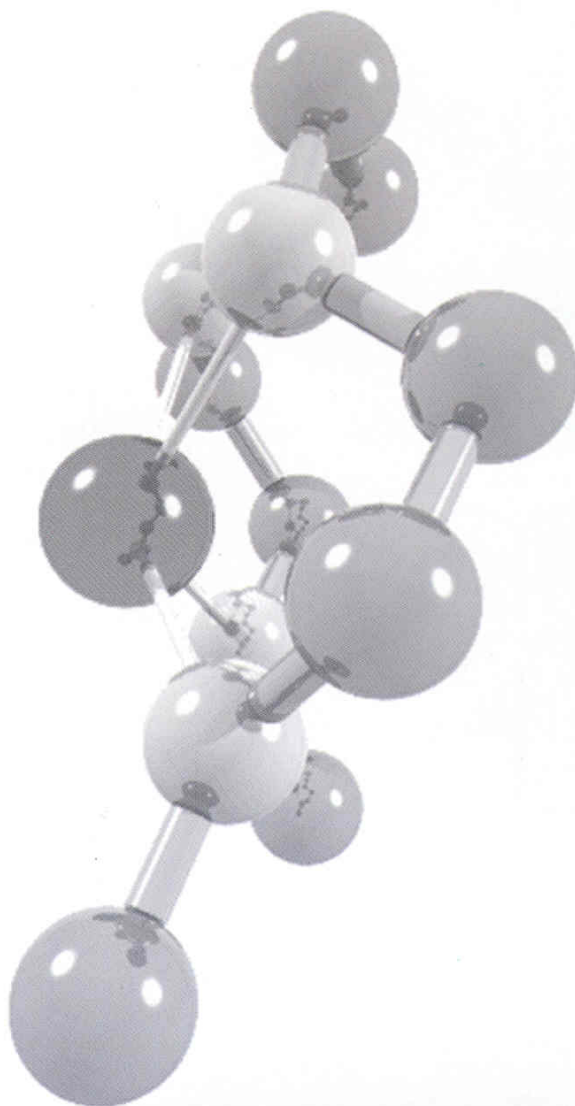
It is clearly seen that the intensity of anhydride peak decreases after protein binding experiment. Furthermore, the appearance of bands at  $1652\text{ cm}^{-1}$  (amide I mode) and  $1544\text{ cm}^{-1}$  (amide II mode) confirms the protein binding of the PE-MAH film.

In conclusion, our results demonstrate the feasibility of using PE-MAH for binding the proteins in natural rubber. The efficient surface modification method on the PE-MAH surface will be developed in future studies to increase the protein binding ability in NR latex under optimized conditions. This will be very useful in improving the NR product.

- References:**
1. Greene, G., Radhakrishna, H., Tannenbaum, R., *Biomaterials*. 2005, 26, 5972-5982.
  2. Bayer, T., Eichhorn, K.J., Jacobasch, H.J., *Macromol. Chem. Phys.* 1999, 200, 852-857.

1<sup>st</sup>

# Polymer Graduate Conference of Thailand



Organized by

May 10-11, 2007  
Mahidol University  
Salaya Nakhonpathom



## Preparation of Polyethylene Graft Maleic Anhydride Film for Binding Extractable Proteins from Natural Rubber

Ladawan Watthanachote<sup>1</sup> and Thirawan Nipithakul<sup>2</sup>

<sup>1</sup>Polymer Science and Technology Programme, Faculty of Science, Mahidol University, Salaya, Nakhon Pathom 73170. Email: g4736232@student.mahidol.ac.th

<sup>2</sup>Department of Chemistry, Faculty of Science, Mahidol University, Phayathai, Bangkok 10400. Email: sctnp@mahidol.ac.th

### Abstract

A membrane material containing maleic anhydride (MAH) group for protein binding was carried out by two different techniques; MAH photografting on LDPE film and compression of commercial PE-g-MAH granule into sheet form. The surface properties of the film were analyzed by Attenuated Total Reflection Fourier Transforms Infrared Spectroscopy (ATR-FTIR) and water contact angle measurement. In this work, Bovine Serum Albumin (BSA) as a model protein and extractable proteins (EP) from dry skim natural rubber (NR) were selected to study protein binding ability of the PE-g-MAH film. Sodium dodecyl sulfate (SDS) has been used to extract proteins from NR. Quantitative analysis of the protein binding was investigated by the dye-binding assay of Bradford. The spectroscopic results show that proteins can be successfully immobilized onto the film surface via covalent linkage.

**Keywords :** Polyethylene graft maleic anhydride, Natural rubber, Protein binding

### 1. Introduction

Maleic anhydride (MAH) has properties that make it of particular interest for surface modification. It can be formed in such a way that anhydride group functionality is retained for subsequent chemical modification. The anhydride group is very reactive to primary amine group and slightly less reactive to alcohol. Therefore, the covalent binding of proteins onto polymeric film containing maleic anhydride group can be occurred.

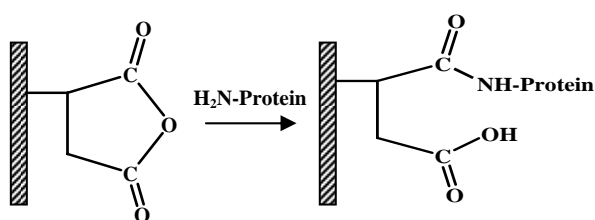


**Figure 1.** Coupling reaction between maleic

*anhydride and protein*

The chemical reaction is illustrated in Figure 1 The amide and carboxylic acid groups are formed by cleavage of anhydride ring.

### 2. Experimental

#### 2.1. Preparation of PE-g-MAH Film

##### 2.1.1) MAH Photografting by UV Irradiation Technique

Low density polyethylene (LDPE) film was cut into circular samples and then subjected to extraction in soxhlet with acetone to get rid of the additives and impurities before use.

Maleic anhydride (MAH) was grafted onto LDPE film by UV irradiation (UV lamp: high-pressure mercury lamp, 1000 w). The films containing

MAH and photoinitiator were laid on the holder of the irradiation equipment, as shown in Figure 2. The distance between the film and the UV lamp was fixed at 25 cm. The optimum condition was decided under the irradiation time of 5 min.

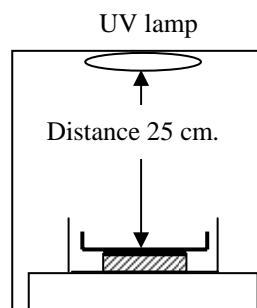


**Figure 2.** Schematic diagram for grafting polymerization

#### 2.1.2) Compression of Commercial PE-g-MAH

PE-g-MAH resin was purified by dissolving in xylene. Then, the temperature was lowered to 45°C with continuous stirring. The precipitate was vacuum filtered, washed several times with acetone and left in an oven for solvent removal.

The purified PE-g-MAH was prepared into a sheet sample by using a hydraulic hot press at 15 ton and under constant temperature of 140°C for 5 min.

In order to obtain high content of anhydride groups on the surface, PE-g-MAH film was annealed in an oven under temperature at 120°C for 3 h.

#### 2.2 Extraction of protein from NR

About 5 g of small NR pieces was immersed in 2% SDS solution and then shaken at room temperature for 12 h in 3 times. The extract solution was then immediately subjected to protein precipitation by Trichloroacetic acid (TCA). Finally, the precipitated proteins were redissolved in Lysis buffer solution.

#### 2.3 Protein Binding Studies on the Films

Bovine Serum Albumin (BSA) and extractable proteins (EP) were used to study the protein binding on the film. The protein concentration was fixed at 1

mg/ml.

Circular samples having a diameter of 0.6 cm were immersed in 0.1M PBS at pH 7 for 2 h before binding.

The films were then placed into individual 1.5 ml microtube to which 0.5 ml of protein solution was added. The mixture was incubated at room temperature for defined time on shaker. After that, the films were removed from the protein solution and rinsed with 0.1M PBS. Finally, they were sonicated in 2 ml of 1% SDS for 15 min to remove noncovalently bound protein and dried in vacuum at room temperature.

Protein solution was pipetted into microtube. The 0.1 M phosphate buffer and Bradford reagent (brown solution) were added respectively. The sample was mixed (Solution color is developed into violet). Then, the absorbance at 592 nm was measured by UV-Vis spectrophotometer.

### 3. Results and discussion

#### 3.1 Surface Analysis of PE-g-MAH film

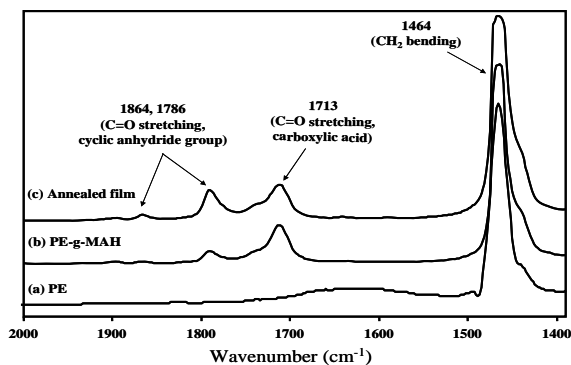


**Figure 3.** ATR-FTIR spectra of (a) PE (b) PE-g-MAH (c) annealed film

It is clearly seen that the IR spectra of grafted films from both preparation methods show specific peaks at 1864 and 1786  $\text{cm}^{-1}$ , corresponding to the characteristic absorption of the carbonyl stretching in cyclic anhydride groups of MAH. Additionally, the sample also presented strong absorption peak at 1712  $\text{cm}^{-1}$ , which was assigned to C=O stretching of

carboxylic acid.

After annealing, the results showed the increase in the cyclic anhydride carbonyl band at  $1786\text{ cm}^{-1}$  and the reduction of the carboxylic acid carbonyl band at  $1712\text{ cm}^{-1}$ . The IR result was supported by contact angle values which increased from  $83^\circ$  to  $100^\circ$  for annealed sample.

From ATR-FTIR results, the anhydride content on the film surface could be quantitatively analyzed by using the ratio of peak intensity of C=O stretching of anhydride group to  $\text{CH}_2$  bending of PE. The extent of anhydride group reported in term of intensity ratio is summarized in Table 1.

**Table 1.** Intensity ratio of anhydride group on different PE-g-MAH films

Sample	Intensity ratio (C=O stretching / $\text{CH}_2$ bending)
Commercial film	0.03
UV photografted film	0.11

It is seen that the intensity ratio of commercial PE-g-MAH is lower than that of UV photografted film. This means that the UV photografted sample contains higher anhydride content at the surface. To investigate the effect of the initial MAH concentration on the amount of immobilized protein, both PE-g-MAH films were used in this work.

### 3.2 Effect of immersion time

To determine the suitable time for protein immobilization, the commercial PE-g-MAH film having approximately  $2 \times 2\text{ cm}^2$  was used for BSA binding. The reaction temperature was kept at room temperature and the immersion time was varied from 2 to 8 h. Figure 4 shows the kinetics of protein binding on PE-g-MAH film.

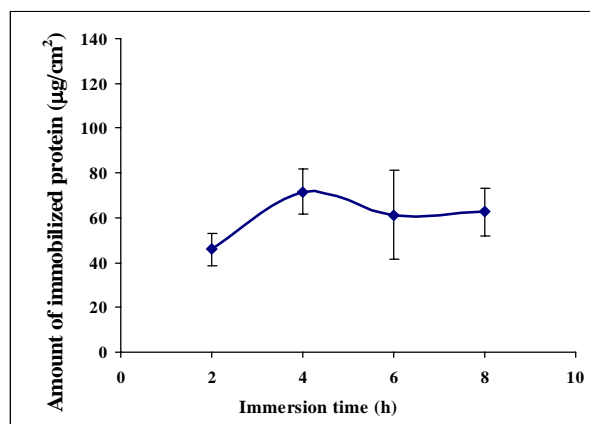


**Figure 4.** Effect of binding time on the amount of immobilized protein on commercial PE-g-MAH film

It was found that as the immersion time increased, the amount of immobilized protein increased in the first 4 h of protein binding. After this time, the protein immobilization on polymeric surfaces is completed. This may be because the binding reaction is controlled by a steric effect. When a longer immersion time was used, the residue amino groups of protein are difficultly immobilized onto PE-g-MAH film. So, the optimum immersion time at 4 h was selected for protein binding study.

### 3.3 Effect of anhydride group on protein binding

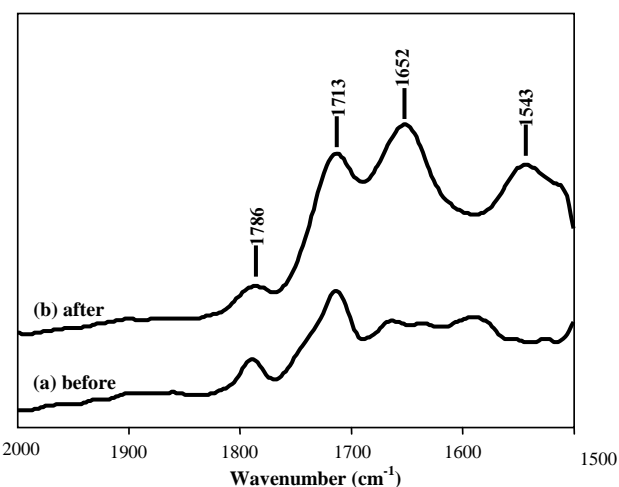


**Figure 5.** ATR-FTIR spectra of PE-g-MAH film (a) before and (b) after immersion in protein solution

Figure 5 shows that the intensity of anhydride peak ( $1786\text{ cm}^{-1}$ ) decreased after protein binding experiment. Furthermore, the appearance of bands at  $1652\text{ cm}^{-1}$  (amide I) and  $1543\text{ cm}^{-1}$  (amide II) confirms the protein binding of the PE-g-MAH film via covalent linkage.

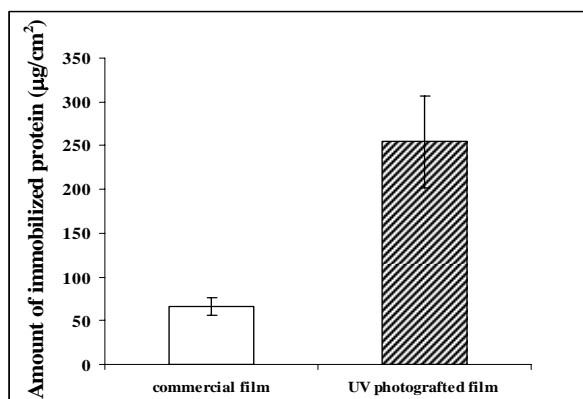


**Figure 6.** Protein content after extractable protein binding studies on commercial PE-g-MAH film ( $\square$ ) and UV photografted PE-g-MAH film ( $\text{▨}$ )

As can be seen in Figure 6, there is a significant difference between commercial and UV photografted films for protein content. This result

indicated that the large amount of anhydride groups on surface obtained from UV photografting technique led to the increase in protein binding.

#### 4. Conclusion

Our results demonstrate the feasibility of using PE-g-MAH for binding the proteins. The efficient surface modification method on the PE-g-MAH surface will be developed in future studies to increase the protein binding ability in NR latex under optimized conditions. This will be very useful in improving the NR product.

#### References

- [1] Greene, G., Radhakrishna, H., Tannenbaum, R., *Biomaterials*, **26**, 5972, (2005).
- [2] Jian, P.D., Wan T.Y., Bengt R., *Eur Polym J.*, **38**, 1449, (2002).
- [3] Belfer S., Fainchtein R., Purinson Y., O.Kedem. *J. Membr. Sci.*, **172**, 113, (2000).

## **BIOGRAPHY**

**NAME:** Miss Ladawan Watthanachote

**DATE OF BIRTH:** October 17, 1978

**PLACE OF BIRTH:** Nakornsawan, Thailand

**INSTITUTIONS ATTENDED:** Prince of Songkla University, 1996-1999:  
Bachelor of Science (Chemistry)  
Mahidol University, 2004-2007:  
Master of Science  
(Polymer Science and Technology)

**EXPERIENCES:** Centaco Co., Ltd., 2000-2001:  
Analyst (feed laboratory)  
Pan Cosmetic International Co., Ltd.,  
2001-2004:  
Scientist (Medical Research and  
Development Center)  
Faculty of Science, Mahidol University,  
2004-2007: Teaching Assistance

**HOME ADDRESS:** 149 Sue-thong Townhouse  
Soi Phahonyothin 52,  
Phahonyothin Rd., Saimai,  
Bangkok 10220 Thailand  
Email: jumrd2@hotmail.com